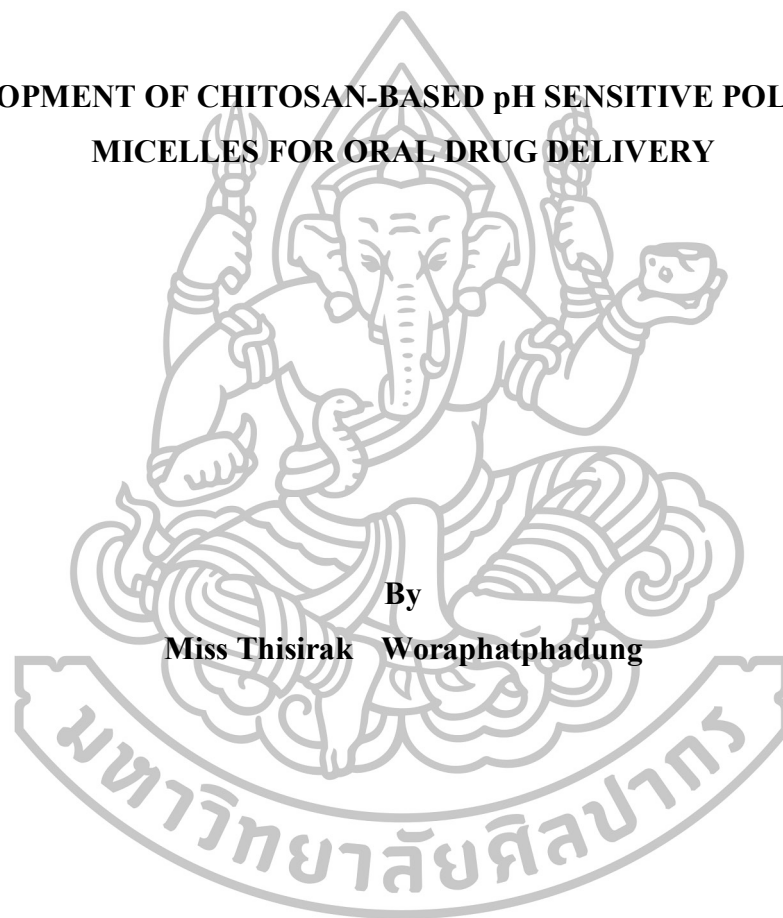




**DEVELOPMENT OF CHITOSAN-BASED pH SENSITIVE POLYMERIC
MICELLES FOR ORAL DRUG DELIVERY**



**A Thesis Submitted in Partial Fulfillment of the Requirements for the Degree
Doctor of Philosophy Program in Pharmaceutical Technology
Graduate School, Silpakorn University
Academic Year 2016
Copyright of Graduate School, Silpakorn University**

**DEVELOPMENT OF CHITOSAN-BASED pH SENSITIVE POLYMERIC
MICELLES FOR ORAL DRUG DELIVERY**



**By
Miss Thisirak Woraphatphadung**

**A Thesis Submitted in Partial Fulfillment of the Requirements for the Degree
Doctor of Philosophy Program in Pharmaceutical Technology
Graduate School, Silpakorn University
Academic Year 2016
Copyright of Graduate School, Silpakorn University**

การพัฒนาพอลิเมอร์ไมเซลล์ที่ไวต่อการเปลี่ยนแปลงพีเอชจากโคโคซานเพื่อนำส่งยาโดยการ
รับประทาน



วิทยานิพนธ์นี้เป็นส่วนหนึ่งของการศึกษาตามหลักสูตรปริญญาปรัชญาดุษฎีบัณฑิต
สาขาวิชาเทคโนโลยีสารสนเทศ
ภาควิชาเทคโนโลยีสารสนเทศ
บัณฑิตวิทยาลัย มหาวิทยาลัยศิลปากร
ปีการศึกษา 2559
ลิขสิทธิ์ของบัณฑิตวิทยาลัย มหาวิทยาลัยศิลปากร

The Graduate School, Silpakorn University has approved and accredited the Thesis title of “Development of chitosan-based pH sensitive polymeric micelles for oral drug delivery” submitted by MISS Thisirak Woraphatphadung as a partial fulfillment of the requirements for the degree of Doctor of Philosophy in Pharmaceutical Technology.

.....
(Associate Professor Panjai Tantatsanawong, Ph.D.)
Dean of Graduate School
...../...../.....

The Thesis Advisor

1. Associate Professor Praneet Opanasopit, Ph.D.
2. Associate Professor Theerasak Rojanarata, Ph.D.
3. Warayuth Sajomsang, Ph.D.

The Thesis Examination Committee

..... Chairman
(Associate Professor Tanasait Ngawhirunpat, Ph.D.)
...../...../.....

..... Member
(Professor Masayuki Yokoyama, Ph.D.)
...../...../.....

..... Member
(Associate Professor Praneet Opanasopit, Ph.D.)
...../...../.....

..... Member
(Associate Professor Theerasak Rojanarata, Ph.D.)
...../...../.....

..... Member
(Warayuth Sajomsang, Ph.D.)
...../...../.....

56354801 :MAJOR : PHARMACEUTICAL TECHNOLOGY

KEY WORDS : ORAL DRUG DELIVERY / pH SENSITIVE POLYMERIC MICELLES /
CHITOSAN DERIVATIVES / MELOXICAM / CURCUMIN

THISIRAK WORAPHATPHADUNG : DEVELOPMENT OF CHITOSAN-BASED pH
SENSITIVE POLYMERIC MICELLES FOR ORAL DRUG DELIVERY. THESIS ADVISORS :
ASSOC. PROF. PRANEET OPANASOPIT, Ph.D. ASSOC. PROF. THEERASAK ROJANARATA,
Ph.D. AND WARAYUTH SAJOMSANG, Ph.D. 116 pp.

The objectives of this study were to synthesize pH sensitive amphiphilic chitosan derivatives, i.e. *N*-naphthyl-*N,O*-succinyl chitosan (NSCS), *N*-octyl-*N,O*-succinyl chitosan (OSCS) and *N*-benzyl-*N,O*-succinyl chitosan (BSCS) and to formulate polymeric micelles (PMs) for oral drug delivery. The critical micelle concentration (CMC) and *in vitro* cytotoxicity of NSCS, OSCS and BSCS PMs were studied. Meloxicam (MX) and curcumin (CUR) were selected as model drugs. Drug-loaded pH sensitive PMs were prepared by the physical entrapment methods (dialysis, O/W emulsion, dropping and evaporation). The influence of entrapment methods, hydrophobic moieties of copolymers and initial amount of drug (5-40% w/w to polymer) on entrapment efficiency (EE) and loading capacity (LC) were investigated. Moreover, the particle size, morphology, micelles structure stability, drug release, intestinal permeation and cytotoxicity of the drug-loaded PMs were investigated. The NSCS, OSCS and BSCS were successfully synthesized via reductive *N*-amination and *N,O*-succinylation, and characterized by ¹H NMR, ATR-FTIR, GPC and elemental analysis. The amphiphilic chitosan derivatives formed PMs at a low CMC in aqueous media. *In vitro* cytotoxicity of NSCS, OSCS and BSCS PMs had low cytotoxicity on Caco-2 cells and HT-29 cells. For MX-loaded PMs, the evaporation method gave PMs with the highest loading capacity and OSCS showed the higher loading capacity than other chitosan derivatives. In addition, increasing initial amount of MX from 5 to 40% w/w to polymer increased the loading capacity of PMs. The particle sizes of all MX-loaded PMs were in the range of 84-382 nm and showed spherical shape in deionized water. PMs exhibited the morphological changes under different pH medium, confirming the responsiveness to pH. *In vitro* release studies of MX from all MX-loaded PMs and MX free drug were conducted for 8 h to mimic the conditions of the GI tract. In acidic medium (pH 1.2) as the simulated gastric fluid (SGF), the percent cumulative release of MX from MX-loaded PMs was approximately 10-20%. When the pH was shifted to 6.8 as simulated intestinal fluid (SIF), the MX release from all MX-loaded PMs significantly increased (approximately 100 %), compared with free MX (approximately 60%), due to the ionization of the succinic acid moiety. Moreover, there were no significant differences in the intestinal permeation of MX from MX-loaded PMs and MX free drug. These results suggest that MX was successfully loaded into the PMs to increase solubility with high efficiency and MX release behaviors depending on the pH. For oral colon-targeted drug delivery, CUR-loaded NSCS PMs prepared by the dialysis method presented the highest loading capacity. An increasing initial amount of CUR from 5% to 40% w/w to polymer resulted in the increase of loading capacity of PMs. Among the hydrophobic cores, there were no significant differences in loading capacity of CUR-loaded PMs. The particle sizes of all CUR-loaded PMs were in range of 120-338 nm. The PMs from NSCS with 5% initial CUR, showed the highest structure stability. *In vitro* release behaviors of CUR from all CUR-loaded PMs were pH-dependent. In SGF, the percent cumulative release of CUR from all CUR-loaded PMs was about 20%. Afterward, the amount of CUR released from CUR-loaded PMs significantly increased (SIF; 50-55%) and (SCF; 60-70%), compared with free CUR (approximately 20%) (*p*<0.05). CUR-loaded NSCS exhibited the highest anti-cancer activity against HT-29 colorectal cancer cells with IC₅₀ of 6.18 ± 0.18 µg/mL. The stability studies indicated that all CUR-loaded PMs were stable for at least 3 months. In summary, pH-responsive amphiphilic chitosan derivatives (NSCS, OSCS, and BSCS) were successfully synthesized and used for the preparation of PMs. These PMs had the potential to improve the solubility of MX and CUR, and to control the drug release at targeted sites by oral administration. OSCS PMs could be used as desirable for MX oral drug delivery, whereas NSCS PMs was suitable for CUR oral colon-targeted drug delivery.

Program of Pharmaceutical Technology

Graduate School, Silpakorn University

Student's signature.....

Academic Year 2016

Thesis Advisors' signature 1.....2.3.

56354801: สาขาวิชาเทคโนโลยีเภสัชกรรม

คำสำคัญ : ระบบนำส่งยาในรูปแบบรับประทาน/พอลิเมอร์ไมเซลล์ที่ไวต่อการเปลี่ยนแปลงพีเอช/อนุพันธ์โคโคซาน/เมลลอคซิแคม/เคอร์คูมิน

วิทยากร วรวัฒน์ผลุง : การพัฒนาพอลิเมอร์ไมเซลล์ที่ไวต่อการเปลี่ยนแปลงพีเอชจากโคโคซานเพื่อนำส่งยาโดยการรับประทาน. อาจารย์ที่ปรึกษาวิทยานิพนธ์ : ญญ.รศ.ดร.ปราณีต โอปนยะโสภิต ภก.รศ.ดร.ธีรศักดิ์ วิจารณ์ราช และ ดร.วราวุธ ทะโจมแสง. 116 หน้า.

การศึกษานี้มีวัตถุประสงค์เพื่อสังเคราะห์อนุพันธ์โคโคซานที่ไวต่อการเปลี่ยนแปลงพีเอช *N*-naphthyl-*N,O*-succinyl chitosan (เอ็นเอสซีเอส), *N*-octyl-*N,O*-succinyl chitosan (โอเอสซีเอส) and *N*-benzyl-*N,O*-succinyl chitosan (บีเอสซีเอส) และเตรียมพอลิเมอร์ไมเซลล์สำหรับนำส่งยา โดยการรับประทาน ศึกษาหาความเข้มข้นวิกฤตของการเกิดไมเซลล์และการทดสอบความเป็นพิษต่อเซลล์ในหลอดทดลอง ในการศึกษานี้ได้เลือกยา เมลลอคซิแคมและเคอร์คูมินเป็นยาต้นแบบ โดยบรรจุยาในพอลิเมอร์ไมเซลล์ด้วยวิธีทางกายภาพ (วิธีแยกสารผ่านเยื่อ วิธีอิมัลชันชนิดน้ำมันในน้ำ วิธีการหยด และวิธีระเหยแห้ง) ศึกษาผลของวิธีการเตรียมพอลิเมอร์ไมเซลล์ ชนิดของพอลิเมอร์และปริมาณตัวยาเริ่มต้น (ร้อยละ 5-40 โดยน้ำหนักต่อพอลิเมอร์) ต่อประสิทธิภาพในการบรรจุและความสามารถในการบรรจุ นอกจากนี้ศึกษาขนาดอนุภาค รูปร่าง ความคงสภาพของโครงสร้างไมเซลล์ การปลดปล่อยยา การดูดซึมผ่านผนังลำไส้และความเป็นพิษต่อเซลล์ของพอลิเมอร์ไมเซลล์ที่บรรจุยา ผลการทดลองพบว่าประสบความสำเร็จในการสังเคราะห์ เอ็นเอสซีเอส โอเอสซีเอสและบีเอสซีเอส ด้วยวิธี reductive *N*-amination และ *N,O*-succinylation และการประเมินสมบัติทางเคมีฟิสิกส์ด้วยเทคนิค เอนเอ็มอาร์ เอฟทีไออาร์ จีพีซีและการวิเคราะห์ธาตุเคมีอนุพันธ์โคโคซานที่สังเคราะห์ได้นี้สามารถก่อตัวเป็นไมเซลล์ในตัวกลางที่เป็นน้ำด้วยค่าความเข้มข้นวิกฤตของการเกิดไมเซลล์ต่ำ การทดสอบความเป็นพิษต่อเซลล์คาร์โก-2 และเซลล์เอชที-29 ในหลอดทดลองของอนุพันธ์โคโคซาน เอ็นเอสซีเอส โอเอสซีเอส และบีเอสซีเอส มีค่าความเป็นพิษต่อเซลล์ต่ำ สำหรับการเตรียมพอลิเมอร์ไมเซลล์บรรจุยาเมลลอคซิแคมด้วยวิธีทางกายภาพ พบว่าวิธีระเหยแห้งสามารถบรรจุยาได้มากกว่าวิธีอื่น และพอลิเมอร์ไมเซลล์ที่เตรียมจากโอเอสซีเอสมีความสามารถในการบรรจุยาสูงกว่าการใช้ อนุพันธ์ชนิดอื่น นอกจากนี้การเพิ่มปริมาณตัวยาเริ่มต้นต่อพอลิเมอร์จากร้อยละ 5 ถึงร้อยละ 40 โดยน้ำหนัก มีผลเพิ่มความสามารถในการบรรจุยา ขนาดอนุภาคของไมเซลล์อยู่ในช่วง 84-382 นาโนเมตร และมีรูปร่างกลม พอลิเมอร์ไมเซลล์มีการเปลี่ยนแปลงทางรูปลักษณะภายใต้สภาวะละลายที่มีพีเอชแตกต่างกันซึ่งแสดงถึงความไวต่อการเปลี่ยนแปลงพีเอชของพอลิเมอร์ที่สังเคราะห์ได้ การศึกษาการปลดปล่อยยาเมลลอคซิแคมจากยาที่บรรจุในพอลิเมอร์ไมเซลล์ และเมลลอคซิแคมในรูปแบบอิสระในตัวกลางที่จำลองสภาวะทางเดินอาหารเป็นเวลา 8 ชั่วโมง พบว่าการปลดปล่อยเมลลอคซิแคมที่บรรจุในพอลิเมอร์ไมเซลล์ในสภาวะจำลองกระเพาะอาหารพีเอช 1.2 ประมาณร้อยละ 10-20 และเมื่อปรับพีเอชของตัวกลางให้จำลองสภาวะลำไส้เล็กพีเอช 6.8 พบว่าการปลดปล่อยเมลลอคซิแคมจากไมเซลล์เพิ่มขึ้นอย่างมีนัยสำคัญทางสถิติ (ประมาณร้อยละ 100) เมื่อเปรียบเทียบกับรูปแบบอิสระ (ประมาณร้อยละ 60) ทั้งนี้เนื่องจากผลของการแตกตัวเป็นไอออนของส่วนหมู่กรดซัลโฟนิก นอกจากนี้พบว่าความสามารถในการดูดซึมผ่านผนังลำไส้หนูของยาเมลลอคซิแคมที่บรรจุในพอลิเมอร์ไมเซลล์และยาในรูปแบบอิสระไม่แตกต่างกัน จากผลการทดลองแสดงว่าประสบความสำเร็จในการเตรียมพอลิเมอร์ไมเซลล์บรรจุยาเมลลอคซิแคมเพื่อเพิ่มการละลายและควบคุมการปลดปล่อยยาโดยการปรับเปลี่ยนพีเอช สำหรับการนำส่งยาสู่ลำไส้ใหญ่โดยการรับประทานนั้น พบว่าพอลิเมอร์ไมเซลล์ที่เตรียมจากเอ็นเอสซีเอสบรรจุเคอร์คูมินด้วยวิธีแยกสารผ่านเยื่อจะบรรจุยาได้มากที่สุด การเพิ่มปริมาณตัวยาเริ่มต้นต่อพอลิเมอร์จากร้อยละ 5 ถึงร้อยละ 40 โดยน้ำหนัก มีผลเพิ่มความสามารถในการบรรจุยาการใช้พอลิเมอร์ต่างชนิดกันเพื่อเตรียมพอลิเมอร์ไมเซลล์สำหรับบรรจุเคอร์คูมิน พบว่ามีความสามารถในการบรรจุไม่แตกต่างกัน โดยมีขนาดอนุภาคอยู่ในช่วง 120-338 นาโนเมตร พอลิเมอร์ไมเซลล์ที่เตรียมจากเอ็นเอสซีเอสบรรจุเคอร์คูมินเริ่มต้นร้อยละ 5 มีความคงสภาพของโครงสร้างไมเซลล์ดีที่สุด การปลดปล่อยเคอร์คูมินออกจากพอลิเมอร์ไมเซลล์ขึ้นอยู่กับการเปลี่ยนแปลงพีเอช โดยพบว่าในสภาวะจำลองกระเพาะอาหารพีเอช 1.2 มีการปลดปล่อยยาประมาณร้อยละ 20 และการปลดปล่อยยาเพิ่มขึ้นอย่างมีนัยสำคัญทางสถิติ เมื่อปรับพีเอชเป็น 6.8 เพื่อจำลองสภาวะลำไส้เล็ก (ปลดปล่อยยาร้อยละ 50-55) และปรับพีเอชเป็น 7.4 จำลองสภาวะลำไส้ใหญ่ (ปลดปล่อยยาร้อยละ 60-70) เมื่อเทียบกับยาในรูปแบบอิสระปลดปล่อยยาร้อยละ 20 ($p < 0.05$) เคอร์คูมินบรรจุในพอลิเมอร์ไมเซลล์ที่เตรียมจากเอ็นเอสซีเอสมีฤทธิ์ยับยั้งการเจริญของเซลล์มะเร็งลำไส้ใหญ่เอชที-29 สูงสุด ค่า IC_{50} เท่ากับ 6.18 ± 0.18 ไมโครกรัม/มิลลิลิตร การทดสอบเสถียรภาพ พบว่าเคอร์คูมินบรรจุในพอลิเมอร์ไมเซลล์ทั้งหมดมีเสถียรสภาพอย่างน้อย 3 เดือน สรุปได้ว่าประสบความสำเร็จในการสังเคราะห์อนุพันธ์โคโคซานที่สามารถก่อตัวเป็นพอลิเมอร์ไมเซลล์ได้ซึ่งไมเซลล์เหล่านี้มีศักยภาพในการเพิ่มการละลายยา และควบคุมการปลดปล่อยยาเมลลอคซิแคมและเคอร์คูมินไปบริเวณเป้าหมายได้ในรูปแบบรับประทาน พอลิเมอร์ไมเซลล์ที่เตรียมจากโอเอสซีเอสเหมาะสำหรับการใช้เพื่อนำส่งยาเมลลอคซิแคม ในขณะที่ไมเซลล์ที่เตรียมจากเอ็นเอสซีเอสเหมาะสำหรับการนำส่งเคอร์คูมินสู่ลำไส้ใหญ่โดยการรับประทาน

สาขาวิชาเทคโนโลยีเภสัชกรรม

ลายมือชื่อผู้ศึกษา.....

ลายมือชื่ออาจารย์ที่ปรึกษาวิทยานิพนธ์ 1..... 2..... 3.....

บัณฑิตวิทยาลัย มหาวิทยาลัยศิลปากร

ปีการศึกษา 2559

ACKNOWLEDGEMENTS

I wish to express sincere appreciation to every person who contributed in diverse ways to a success of my research. First of all, I would like to express the deepest appreciation to my thesis advisor, Assoc. Prof. Dr. Praneet Opanasopit for her excellent guidance, encouragement, patience, and providing me with an excellent atmosphere for doing research and my thesis co-advisors, Assoc. Prof. Dr. Theerasak Rojanarata and Dr. Warayuth Sajomsang for valuable advice, support and kindness. I wish to thank my thesis committees Assoc. Prof. Dr. Tanasait Ngawhirunpat for valuable time, insightful comments and suggestion, Ms. Areerut Sripattanaporn for cell culture helps.

I would like to express my gratitude to Prof. Dr. Masayuki Yokoyama for giving me a great opportunity to research at Medical Engineering Laboratory, Research Center for Medical Science, The Jikei University School of Medicine, Tokyo, Japan. He gave excellent ideas, warm encouragement and supported me everything in Japan. I also wish to thank Dr. Koichi Shiraishi for his precious suggestions, patience, helpful support and care during my living in Japan.

My next gratitude and appreciation goes to the Commission of Higher Education (Thailand), the Thailand Research Funds through the Golden Jubilee Ph.D. Program (Grant No.PHD/0027/2556) and the graduate school of Silpakorn University for financial support. The Silpakorn University Research and Development Institute and National Nanotechnology Center (NANOTEC) for facility support. I also would like to pass my heartfelt thanks to all my friends and members of the Pharmaceutical Development of Green Innovation Group (PDGIG) for caring, friendship and generous support.

Finally, I would like to express the deepest gratefulness to my parent and my family for their encouragement and believing in me.

TABLE OF CONTENTS

	Page
English Abstract.....	iv
Thai Abstract.....	v
Acknowledgements.....	vi
List of Tables.....	viii
List of Figures.....	xi
List of Abbreviations.....	xv
Chapter	
1 Introduction.....	1
2 Literature Reviews.....	7
3 Materials and Methods.....	33
4 Results and Discussion.....	45
5 Conclusions.....	75
References.....	78
Appendix.....	92
Biography.....	113

LIST OF TABLES

Table	Page
2.1 BCS drug classification.....	10
2.2 <i>In vitro</i> cytotoxicity.....	22
2.3 pH sensitive polymer typically used to prepare polymeric micelles for oral drug delivery.....	27
2.4 Physicochemical properties of the drugs.....	31
3.1 HPLC experimental conditions used to quantify drugs concentrations.	41
4.1 Elemental analysis data for CS and its amphiphilic derivatives.....	48
4.2 The particle sizes and PDI of NSCS micelles with and without MX. Each value represents the mean \pm SD from three independent measurements.....	59
4.3 The particle sizes and polydispersity index (PDI) of polymeric micelles with and without MX. Each value represents the mean \pm SD of three independent measurements.....	59
4.4 The particle sizes and polydispersity index (PDI) of polymeric micelles with 20% MX to polymer and without MX by the evaporation method. Each value represents the mean \pm SD from three independent measurements.....	60
4.5 The particle sizes and PDI of NSCS micelles with and without CUR. Each value represents the mean \pm SD from three independent measurements.....	69
4.6 The particle sizes and PDI of polymeric micelles with and without MX. Each value represents the mean \pm SD of three independent measurements.....	69
A.1 Entrapment efficiency of MX into NSCS with initial drug to polymer (5-40%) by dialysis method.....	96
A.2 Loading capacity of MX into NSCS with initial drug to polymer (5-40%) by dialysis method.....	96

Table	Page
A.3 Entrapment efficiency of MX into NSCS with initial drug to polymer (5-40%) by dropping method.....	96
A.4 Loading capacity of MX into NSCS with initial drug to polymer (5-40%) by dropping method.....	97
A.5 Entrapment efficiency of MX into NSCS with initial drug to polymer (5-40%) by evaporation method.....	97
A.6 Loading capacity of MX into NSCS with initial drug to polymer (5-40%) by evaporation method.....	97
A.7 Entrapment efficiency of MX into NSCS with initial drug to polymer (5-40%) by O/W emulsion method.....	98
A.8 Loading capacity of MX into NSCS with initial drug to polymer (5-40%) by O/W emulsion method.....	98
A.9 Entrapment efficiency of MX into OSCS with initial drug to polymer (5-40%) by evaporation method.....	98
A.10 Loading capacity of MX into OSCS with initial drug to polymer (5-40%) by evaporation method.....	99
A.11 Entrapment efficiency of MX into BSCS with initial drug to polymer (5-40%) by evaporation method.....	99
A.12 Loading capacity of MX into BSCS with initial drug to polymer (5-40%) by evaporation method.....	99
A.13 Entrapment efficiency of CUR into NSCS with initial drug to polymer (5-40%) by dialysis method.....	100
A.14 Loading capacity of CUR into NSCS with initial drug to polymer (5-40%) by dialysis method.....	100
A.15 Entrapment efficiency of CUR into NSCS with initial drug to polymer (5-40%) by dropping method.....	100
A.16 Loading capacity of CUR into NSCS with initial drug to polymer (5-40%) by dropping method.....	101
A.17 Entrapment efficiency of CUR into NSCS with initial drug to polymer (5-40%) by evaporation method.....	101

Table	Page
A.18 Loading capacity of CUR into NSCS with initial drug to polymer (5-40%) by evaporation method.....	101
A.19 Entrapment efficiency of CUR into NSCS with initial drug to polymer (5-40%) by O/W emulsion method.....	102
A.20 Loading capacity of CUR into NSCS with initial drug to polymer (5-40%) by O/W emulsion method.....	102
A.21 Entrapment efficiency of CUR into OSCS with initial drug to polymer (5-40%) by dialysis method.....	102
A.22 Loading capacity of CUR into OSCS with initial drug to polymer (5-40%) by dialysis method.....	103
A.23 Entrapment efficiency of CUR into BSCS with initial drug to polymer (5-40%) by dialysis method.....	103
A.24 Loading capacity of CUR into BSCS with initial drug to polymer (5-40%) by dialysis method.....	103
B.1 The percentage cell viability in Caco-2 cells of NSCS.....	105
B.2 The percentage cell viability in Caco-2 cells of OSCS.....	105
B.3 The percentage cell viability in Caco-2 cells of BSCS.....	106
B.4 The percentage cell viability in HT-29 cells of NSCS.....	106
B.5 The percentage cell viability in HT-29 cells of OSCS.....	107
B.6 The percentage cell viability in HT-29 cells of BSCS.....	107
B.7 The percentage cell viability in HT-29 cells of CUR-loaded NSCS.....	108
B.8 The percentage cell viability in HT-29 cells of CUR-loaded OSCS.....	108
B.9 The percentage cell viability in HT-29 cells of CUR-loaded BSCS.....	109
B.10 The percentage cell viability in HT-29 cells of free CUR.....	109
C.1 % MX release in SGF (pH 1.2) 2 h then changed to SIF (pH 6.8) to 8 h.	111
C.2 % CUR release in SGF (pH 1.2) 2 h then changed to SIF (pH 6.8) to 5 h and then changed to SCF (pH 7.4) to 8 h.....	112

LIST OF FIGURES

Figure	Page
2.1 Anatomy of GI tract in humans.....	11
2.2 Schematic representation of intestinal epithelial cells show potential transepithelial pathways: (A) paracellular route; (B) transcellular passive diffusion; and (C) transcellular receptor-mediated transcytosis.....	12
2.3 Formation and drug loading of polymeric micelles by self-assembly of amphiphilic block copolymers in aqueous solution.....	13
2.4 Various micelle structure by self-assembly that can be formed spontaneously in aqueous solution from different copolymer architectures.....	15
2.5 Physical loading of hydrophobic drugs into polymeric micelles: a) dialysis method, b) o/w emulsion method and c) evaporation method.....	17
2.6 Schematic representation of drug release mechanisms from polymeric micelles: protonation-induced (left) and ionization-induced (right) destabilization.....	26
2.7 <i>In vitro</i> release profile of CDN from PEG ₁₁₅ -b-P(isoBA ₃₅ -co-MAA ₃₈) (open square) and PEG ₁₁₅ -b-P(isoBA ₃₅ -co-tBMA ₃₈) (closed square) polymeric micelles prepared by the solvent evaporation method at pH 1.2 for 2 h followed by 7 h at pH 7.2. Mean ± SD (n=3).....	29
2.8 Chemical structure of chitin and chitosan.....	30
4.1 Synthesis scheme showing the formation of amphiphilic chitosan derivatives.....	48
4.2 ¹ H NMR spectra of NCS, BCS, OCS and CS.....	50
4.3 ¹ H NMR spectra of NSCS, BSCS and OSCS.....	51
4.4 (a) ATR-FTIR spectra of CS, BCS, OCS and NCS; (b) BSCS, OSCS and NSCS.....	52

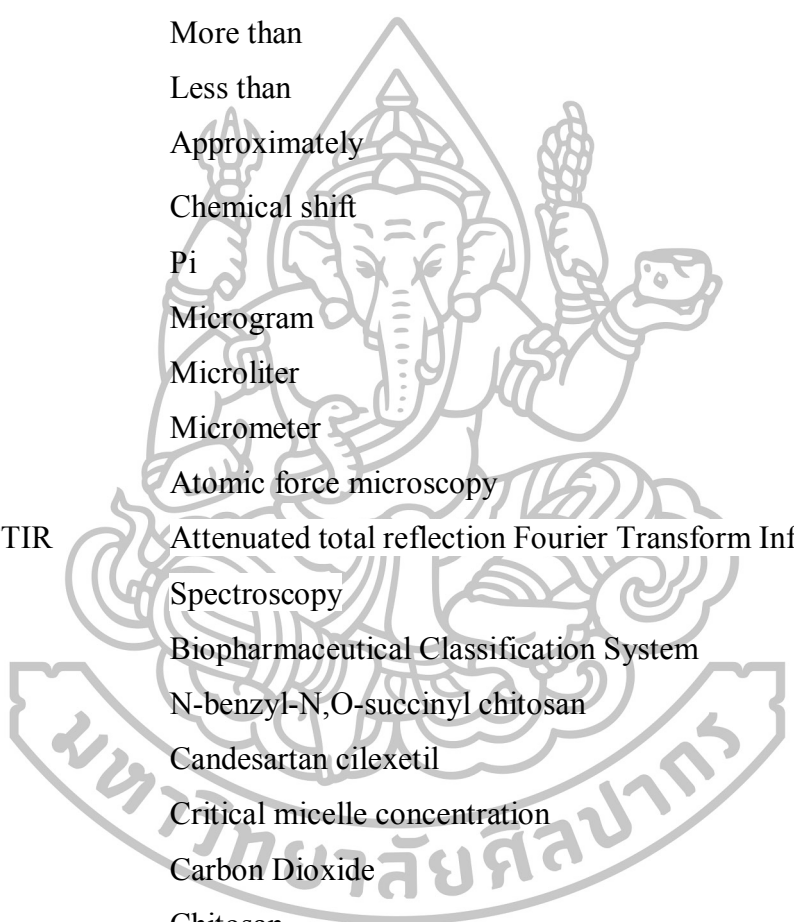
Figure	Page
4.5	53
<p>Fluorescence emission spectra of pyrene in water in the presence of NSCS (a), BSCS (c), and OSCS (e) polymeric micelles; a plot of the change in the intensity ratio (I1/I3) from excitation spectra of pyrene in water at various concentrations of NSCS (b), BSCS (d), and OSCS (f).....</p>	
4.6	55
<p>The percent cell viability in Caco-2 cells at varying concentrations of polymeric micelles; (◻) NSCS, (◼) OSCS, (◽) BSCS. Each value represents the mean ± SD of five wells. * Statistically significant (p < 0.05).....</p>	
4.7	55
<p>The present cell viability in HT-29 cells at varying concentrations of polymeric micelles; (◻) NSCS, (◼) OSCS, (◽) BSCS. Each value represents the mean ± SD of five wells.....</p>	
4.8	57
<p>Effect of entrapment method and initial drug concentration (5–40% to polymer) on (a) the entrapment efficiency, (b) loading capacity of MX-loaded NSCS micelles (◊) dialysis method; (●) dropping method; (■) evaporation method; (▲) emulsion method. Data are plotted as the mean ± S.D. of three measurements.....</p>	
4.9	58
<p>Effect of hydrophobic moieties and initial drug loading (5-40% to polymer) on (a) the entrapment efficiency, (b) loading capacity of MX-loaded polymeric micelles; (◻) MX-loaded NSCS, (◼) MX-loaded OSCS, (◽) MX-loaded BSCS. Data are plotted as the mean ± SD of three measurements. * Statistically significant (p < 0.05).....</p>	
4.10	61
<p>AFM images of NSCS, BSCS and OSCS micelles, and MX-loaded NSCS, BSCS and OSCS micelles at different pH.....</p>	
4.11	62
<p>Polymeric micelles stability by ratio of peak area/[MX]; (◻) MX-loaded NSCS, (◼) MX-loaded OSCS, (◽) MX-loaded BSCS. Data are plotted as the mean ± SD of three measurements.....</p>	

Figure	Page
4.12 MX release profiles from the (◆) MX-loaded NSCS; (■) MX-loaded OSCS; (▲) MX-loaded BSCS; and (●) MX suspension in 0.1 N HCl, pH 1.2 (0-2 h), then in PBS pH 6.8 (2-8 h). Data are plotted as the mean ± SD of three measurements. * Statistically significant ($p < 0.05$).....	65
4.13 (a) The permeation profiles of (◆) MX-loaded NSCS; (■) MX-loaded OSCS; (▲) MX-loaded BSCS; and (●) MX suspension. (b) The fluxes of MX through porcine small intestinal for NSCS, OSCS and BSCS micelles (white bar graph); MX suspension (shaded bar graph). Data are plotted as the mean ± SD of three measurements.....	66
4.14 Effect of entrapment method and initial drug concentration (5–40% to polymer) on (a) the entrapment efficiency, (b) loading capacity of MX-loaded NSCS micelles (◆) dialysis method; (●) dropping method; (■) evaporation method; (▲) emulsion method. Data are plotted as the mean ± S.D. of three measurements.....	67
4.15 Effect of hydrophobic moieties and initial drug loading (5-40% to polymer) on (a) the entrapment efficiency, (b) loading capacity of MX-loaded polymeric micelles; (■) MX-loaded NSCS, (⚡) MX-loaded OSCS, (□) MX-loaded BSCS. Data are plotted as the mean ± SD of three measurements. * Statistically significant ($p < 0.05$).....	68
4.16 AFM images of CUR-loaded OSCS micelles at different pH.....	70
4.17 Polymeric micelles stability by ratio of peak area/[CUR]; (■) CUR-loaded NSCS; (⚡) CUR-loaded OSCS; (□) CUR-loaded BSCS. Data are plotted as the mean ± SD of three measurements.	71

Figure	Page
4.18 CUR release profiles from the (◆) CUR-loaded NSCS; (■) CUR-loaded OSCS; (▲) CUR-loaded BSCS; and (●) CUR suspension in 0.1 N HCl, pH 1.2 (0–2 h), then in PBS pH 6.8(2–5 h) and then, in PBS pH 7.4 (5-8 h). Data are plotted as the mean± SD of three measurements. * Statistically significant (p<0.05).....	72
4.19 Anticancer activity of (■) CUR-loaded NSCS, (▨) CUR-loaded OSCS, (□) CUR-loaded BSCS and (■) CUR free drug against HT-29 cells by MTT assay. Each value represents the mean ± SD of five wells.....	73
4.20 The stability of (◆) CUR-loaded NSCS; (■) CUR-loaded OSCS; (▲) CUR-loaded BSCS; and (●) free CUR drug under the accelerated conditions (at 25°C) compared with the long term conditions (at 4°C) for 90 days. Data are plotted as the mean ± SD of three measurements.....	74
A.1 Meloxicam standard curve.....	94
A.2 Curcumin standard curve.....	95



LIST OF ABBREVIATIONS



®	Registered trademark
% w/v	Percent weight by weight
% v/v	Percent volume by volume
°C	Degree Celsius
>	More than
<	Less than
~	Approximately
δ	Chemical shift
π	Pi
μg	Microgram
μL	Microliter
μm	Micrometer
AFM	Atomic force microscopy
ATR-FTIR	Attenuated total reflection Fourier Transform Infrared Spectroscopy
BCS	Biopharmaceutical Classification System
BSCS	N-benzyl-N,O-succinyl chitosan
CDN	Candesartan cilexetil
CMC	Critical micelle concentration
CO ₂	Carbon Dioxide
CS	Chitosan
CUR	Curcumin
DCM	Dichloromethane
DDA	Degree of deacetylation
DDS	Drug delivery system
DLS	Dynamic light scattering
DMEM	Dulbecco's modified Eagle's medium
DMF	N,N-dimethylformamide
DMSO	Dimethyl Sulfoxide

DS	Degree of substitution
DSS	Degree of N,O-succinylation
EE	Entrapment efficiency
e.g.	exempli gratia (Latin); for example
Eqs	Equation
et al.	And others
etc.	et cetera (Latin); and other things/ and so forth
FBS	Fetal bovine serum
FNB	Fenofibrate
G	Gram
GI	Gastrointestinal
GlcN	Glucosamine
GPC	Gel permeation chromatography
h	Hour
HCl	Hydrochloride
HPLC	High performance liquid chromatography
Hz	Hertz
IC ₅₀	Half maximal inhibitory concentration
ICH	International conference on harmonisation
i.e.	id est (Latin); that is
IND	Indomethacin
KH ₂ PO ₄	Potassium dihydrogen phosphate
kHz	Kilohertz
LC	Loading capacity
M	Molarity
Meq	Milliequivalents
Mg	Milligram
min	Minute
mL	Milliter
mm	Millimeter
mmol	Millimole

Mn	Number average molecular weights
MTT	3-(4,5-dimethylthiazol-2-yl)-2,5 diphenyltetrazolium Bromide
MX	Meloxicam
MW	Molecular weight
N	Mole per liter
NaBH ₄	Sodium borohydride
NaOH	Sodium hydroxide
ng	Nanogram
nm	Nanometer
NSCS	N-naphthyl-N,O-succinyl chitosan
OSCS	N-octyl-N,O-succinyl chitosan
O/W	Oil in water
PAA	Poly(acrylic acid)
PBS	Phosphate buffer solution
pH	Potentia hydrogenii (latin); power of hydrogen
pK _a	-log ₁₀ K _a
PMAA	Poly(methacrylic acid)
PMs	Polymeric micelles
ppm	Part per million
RH	Relative Humidity
RI	Refractive index
rpm	Round per minute
SCF	Simulated colonic fluid
SD	Standard deviation
SGF	Simulated gastric fluid
SIF	Simulated intestinal fluid
UV	Ultraviolet
vs	Versus

CHAPTER 1

INTRODUCTION

1.1 Statement and significance of the research problem

Drug delivery systems (DDS) are processes or methods of pharmaceutical compounds' administration for an improved therapeutic effect in humans or animals body. DDS improve therapeutic efficacy through control of rate, time and place of drug release (Jain, 2008). There are commonly used routes of drug delivery including parenteral delivery, oral delivery, transdermal delivery, mucosal delivery (e.g. pulmonary, ocular, sublingual). Oral administration is the most widely used route of drug delivery due to its convenience in terms of self-administration, pain free and high patient compliance, especially in the case of chronic therapies. However, some properties of drugs are not suitable for oral route due to side effects, rapid metabolism, and poor solubility (Savjani, K. T., Gajjar, and Savjani, 2012). The low solubility of drug, that is classified in Biopharmaceutical Classification System (BCS) class II and class IV, is a crucial obstacle due to low absorption in the gastrointestinal (GI) tract. Accordingly, the low solubility leads to low bioavailability (Li et al., 2009; Lu and Park, 2013). More than 40% of new chemical entities (NCEs) developed in pharmaceutical industry are practically insoluble in water (Kalepu, Manthina, and Padavala, 2013). The techniques used for solubility enhancement of drug include particle size reduction, cosolvents, solid dispersions, complexation (Kumar, A. et al., 2011; Kumar, P. and Singh, 2013; Patel et al., 2012). Recently, scientists have challenged to generate novel carriers of oral drug delivery for obtaining higher levels in bioavailability such as polymeric micelles, microemulsions, nanoparticles (Sharma et al., 2009).

Polymeric micelles as a nano-sized carrier which is prepared through self-assembly of amphiphilic copolymers in an aqueous solution when a concentration of polymer is above the critical micelle concentration (CMC). The inner core is hydrophobic segment which entraps hydrophobic drugs while the outer hydrophilic shell

stabilizes interface between the hydrophobic core and aqueous solution, protects the hydrophobic drugs from the environmental stimuli (e.g. gastric pH, enzyme, temperature) and decreases adverse effect of drugs on healthy cells and tissues (Ghaemy, Ziaei, and Alizadeh, 2014). Polymeric micelles bring some advantages for oral drug delivery such as encapsulating drug to avoid destruction in the GI tract, increasing efficient solubilization, releasing them in spatially controlled manner, which could enhance drug absorption (Kedar et al., 2010; Xu, Ling, and Zhang, 2013; Zhang Y. et al., 2012). Some widely used techniques for drug-incorporated polymeric micelles preparation and the efficacy of drug loading depends on the applied tools. They include techniques of chemical conjugation, physical entrapment, electrostatic and other methods. Physical entrapment is the simplest and the most convenient method and can be implemented via dialysis, O/W emulsion, dropping and evaporation. The hydrophobic drugs can be incorporated into the micelles inner core by hydrophobic interaction between entrapped drug molecules and the hydrophobic inner-core-forming polymer (Murthy, 2015). The hydrophobic interactions also work as a driving force for micelle formation such as hydrophobic force, electrostatic force, π - π interaction and hydrogen bonding. Physical entrapment was selected to use in some studied such as dexamethasone-entrapped into PEGylated poly-4-(vinylpyridine) micelles by dialysis, O/W emulsion or evaporation (Miller et al., 2013), doxorubicin-loaded polyphosphazenes with poly(N-isopropylacrylamide-co-N,N-dimethylacrylamide) polymeric micelles by dialysis or O/W emulsion method (Qui, Wu, and Jin, 2009), and preparation the polymeric micelles of methoxy poly(ethyleneoxide)-block-poly(ϵ -caprolactone) (MePEO-b-PCL) containing cyclosporine A by co-solvent evaporation (Aliabadi et al., 2007). However, the polymeric micelles preparation with high drug loads remains challenging because different techniques may affect the efficacy of drug loading (Kim, S. et al., 2010).

As it is known, pH levels in the GI tract vary from 1-3 in the stomach to 6-7.5 in the small intestine and the variation of pH has been utilized to control drug release from carriers (Bromberg, 2008, Felber, Dufresne, and Leroux, 2012; Xu, Ling, and Zhang, 2013). In oral administration, pH-sensitive polymeric micelle-based carrier can be made to improve the stability of micelles in the stomach and attain a controlled release in the intestine which improves oral bioavailability. The poly(acrylic acid) (PAA)

and poly(methacrylic acid) (PMAA) are generally used as pH-responsive polymers in pH-sensitive polymeric micelles in some studies. These polymers have pendant carboxyl groups with pK_a values of about 4-6 in the chain. For example, pH-responsive amphiphilic poly(acrylic acid-*b*-DL-lactide) (PAAc-*b*-PDLLA) was developed to incorporate prednisone acetate (Xue et al., 2009). This formulation of polymeric micelles showed minimizing drug release at pH 1.4 and burst release at pH 7.4. The pendant carboxyl groups in PAA moieties preserve collapsed states and are protonated in the low pH environment of the stomach; however, PAA swells in the intestines, ionizes, and releases protons (Sant, Smith, and Leroux, 2004). Yang et al. (2011, 2012) developed self-assembled, pH-sensitive micelles from amphiphilic copolymer brushes (e.g., poly(methyl methacrylate-co-methacrylic acid)-*b*-poly(poly(ethylene glycol) methyl ether monomethacrylate) [P(MMA-co-MAA)-*b*-PPEGMA] and poly(lactide)-*b*-poly(methacrylic acid)-*b*-poly(poly(ethylene glycol) methyl ether monomethacrylate) (PLA-*b*-MAA-*b*-PPEGMA) containing ibuprofen and nifedipine, respectively). They found that the drug release rates increased by modifying the MAA blocks. (Yang et al., 2011; Yang et al., 2012).

Chitosan, is produced by Mucorales and other fungi, but on the whole it is manufactured by the deacetylation of chitin isolated from by-products of the marine fisheries. It is soluble in aqueous acidic solutions ($pH < 6.0$) (Muzzarelli et al., 2003; Muzzarelli et al., 2012), however, it cannot form polymeric micelles in water. Chitosan derivatives have been widely utilized in pharmaceutical applications since, they are biodegradable and less expensive (Bonferoni et al., 2014). Presently, chitosan derivatives in the form of polymeric micelles have been investigated for drug delivery. Several modified chitosans, for example *N*-lauryl-carboxymethyl-chitosan, *N*-phthaloylchitosan-*g*-mPEG, *N*-octyl-*O*-sulfate chitosan and *N,N*-dimethylhexadecyl carboxymethyl chitosan (DCMCs) have been utilized for the polymeric micelles preparation (Lia et al., 2014; Miwa et al., 1998; Zhang, C., Qineng, and Zhang, H., 2004). Therefore, in this study pH sensitive amphiphilic chitosan derivatives were developed and prepared as polymeric micelles to improve solubility of poorly water soluble drug and to control the drug release. Two different types of drugs, namely meloxicam and curcumin, were selected as hydrophobic drugs for systemic intestinal absorption and colorectal cancer treatment, respectively.

Meloxicam (MX), is a class of non-steroidal anti-inflammatory drugs with poor aqueous solubility (0.009 mg/mL at 25°C) and high permeability, therefore, it is classified in BCS class II (Kim and Lee, 2007). It acts as an inhibitor of prostaglandin synthetase which has been used to reduce of pain and inflammation. However, the side effects on the GI tract caused by MX after oral administration include indigestion and stomachache (Duangjit et al., 2013), and these effects may reduce the life expectancy of patients with chronic diseases such as rheumatoid arthritis. Thus, MX-loaded into pH sensitive polymeric micelles were prepared by various physical entrapment methods. The influence of the physical entrapment methods, type of amphiphilic chitosan derivatives, amount of drugs on entrapment efficiency, loading capacity, particle size and stability of drugs-loaded polymeric micelles were determined. Moreover, *in vitro* cytotoxicity of human colon adenocarcinoma cells (Caco-2 cells) of micelles, their release behavior and small intestine permeation study were also investigated in this study.

Curcumin (CUR) is a hydrophobic polyphenolic compound from the rhizome of turmeric *Curcuma longa* Linn (Zingiberaceae), one of the most widely used natural active constituents due to low cost and pharmacological safety. Its multiple biological activities have been found such as antibacterial, antifungal, anti-inflammatory, antioxidant (Duan et al., 2016; Wang, Ma, and Tu, 2015). In addition, recently anti-cancer activity of curcumin has been extensively investigated for its potential to use in chemoprevention and treatment of a wide variety of tumors (Mehanny et al., 2016). The extensive studies have shown that curcumin inhibited tumor formation in the initiation and progression stage of carcinogenesis in *in vivo* of colorectal cancer (Kawamori et al., 1999; Rao et al., 1995; Shemesh and Arber, 2014). Curcumin can interfere with multiple cell signaling pathway involved in carcinogenesis, including inhibition of cell cycle progression, slowing proliferation, reducing angiogenesis and induction of apoptosis in colorectal carcinoma cell (Aggrawal et al., 2007; Cen et al., 2009; Guo et al., 2013). For example, curcumin exhibits potent inhibitory activity in human colorectal cancer cell lines, SW480, HT-29, and HTC116 (Cen et al., 2009). It inhibits proliferation and induces apoptosis of human colorectal cells by activating the mitochondria apoptotic pathway (Guo et al., 2013). However, potential of curcumin is hindered by its low aqueous solubility (11 ng/mL in aqueous buffer at pH 5, 400

ng/mL at the physiological pH 7.4), low bioavailability, rapid metabolism, leading to limitation for treatment (Akl et al., 2016; Mehanny et al., 2016). Therefore, nanocarriers or nanoformulations are considered to encapsulate and deliver curcumin to targeted cancer cell such as liposomes, niosomes, solid lipid nanoparticles (SLNs), polymeric nanoparticles, polymeric micelles, nanoemulsions etc (Mehanny et al., 2016). Previous study revealed that curcumin can be loaded into amphiphilic N-benzyl-N,O-succinyl chitosan (BSCS) via dialysis method to increase solubility of curcumin. The BSCS consists of hydrophobic benzyl group and hydrophilic succinyl group that can form self-aggregation micelles in water during dialysis. Curcumin-loaded BSCS micelles show small particle size, highly negative charge, high water solubility, strong cytotoxicity to cervical cancer cells and high amount of drug release in physiological pH 5.5-7.4 (Sajomsang et al., 2014). Therefore, the aim of this study was to entrap curcumin into pH sensitive polymeric micelles and control drug release at colon targeted site by oral route. The influence of the physical entrapment methods, type of amphiphilic chitosan derivatives, amount of drugs on entrapment efficiency, loading capacity, particle size and stability of drugs-loaded polymeric micelles were evaluated. In addition, the *in vitro* cytotoxicity on human colorectal adenocarcinoma cells (HT-29 cells) and their release behavior were investigated.

1.2 Objectives of this research

1. To synthesize pH responsive amphiphilic chitosan derivatives and formulate polymeric micelles for the oral drug delivery
2. To investigate the influence of the physical entrapment methods, type of amphiphilic chitosan derivatives, type and amount of drugs on entrapment efficiency, loading capacity, particle size and stability of drugs-loaded polymeric micelles
3. To evaluate the drug release, intestinal permeation and cytotoxicity of the drug-loaded polymeric micelles

1.3 The research of hypothesis

1. The amphiphilic chitosan derivatives can be synthesized and used to formulate drug-loaded polymeric micelles.

2. The physical entrapment methods, type of amphiphilic chitosan derivatives, type and amount of drugs influence on the characteristics of polymeric micelles (i.e. particle size, size distribution, entrapment efficiency, loading capacity and stability).

3. Drugs-loaded polymeric micelles can be used for oral drug delivery.

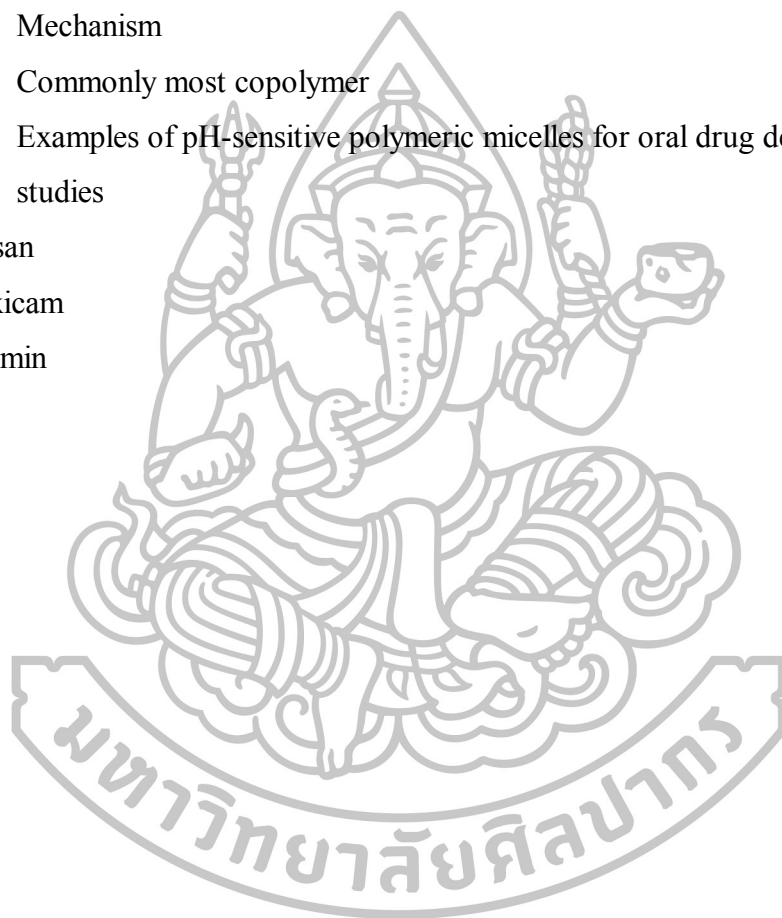


CHAPTER 2

LITERATURE REVIEWS

- 2.1 Drug delivery system (DDS)
 - 2.1.1 Definition
 - 2.1.2 Commonly routes of drug delivery
 - 2.1.2.1 Oral delivery
 - 2.1.2.2 Parenteral delivery
 - 2.1.2.3 Transdermal delivery
 - 2.1.2.4 Mucosal delivery
- 2.2 Oral drug delivery system
- 2.3 Polymeric micelles
 - 2.3.1 Structure of polymeric micelles
 - 2.3.2 Drug loading into polymeric micelles
 - 2.3.2.1 Chemical conjugation
 - 2.3.2.2 Physical entrapment
 - 2.3.2.2.1 Dialysis
 - 2.3.2.2.2 O/W emulsion
 - 2.3.2.2.3 Solvent evaporation
 - 2.3.2.2.4 Other methods
 - 2.3.3 Characterization of polymeric micelles
 - 2.3.3.1 Determination of CMC of polymeric micelles
 - 2.3.3.2 Size determination
 - 2.3.3.3 Drug loading
 - 2.3.3.4 Morphology
 - 2.3.3.5 Stability
 - 2.3.3.6 *In vitro* cytotoxicity
 - 2.3.3.6.1 Lactate dehydrogenase (LDH) release assay
 - 2.3.3.6.2 Neutral red uptake assay
 - 2.3.3.6.3 Methyl tetrazolium (MTT) assay

- 2.3.3.7 *In vitro* drug release study
- 2.3.4 Application of polymeric micelles in drug delivery
 - 2.3.4.1 Solubilization
 - 2.3.4.2 Controlled or sustained release of a drug
 - 2.3.4.3 Targeting
- 2.4 pH sensitive polymeric micelles for oral drug delivery
 - 2.4.1 Mechanism
 - 2.4.2 Commonly most copolymer
 - 2.4.3 Examples of pH-sensitive polymeric micelles for oral drug delivery studies
- 2.5 Chitosan
- 2.6 Meloxicam
- 2.7 Curcumin



2.1 Drug delivery system (DDS)

2.1.1 Definition

Drug delivery system (DDS) is defined as a formulation or a device that enables the introduction of a therapeutic substance in the body and improves its efficacy and safety by controlling the rate, time, and place of release of drugs in the body (Jane, 2008).

2.1.2 Commonly routes of drug delivery

The route of administration or delivery is a important factor in designing DDS. The selection of the route of administration depends on the disease, the desired onset and duration of drug effect, patient's discomfort, compliance and the product available. Drugs or therapeutic substances may be administered directly to the organ affected by disease or given systemically and targeted to the diseased organ (Jane, 2008). The commonly used routes of drug delivery include the following:

2.1.2.1 Oral delivery

This route is the oldest way developed both in conventional and novel drug delivery because of ease of administration and the highly accepted history by patients. The most common dosage forms include liquids, solids and dispersed system.

2.1.2.2 Parenteral delivery

In term of parenteral means the introduction of substances or drugs into the body through different routes other than the oral route (mainly by injection). Parenteral routes are often used when the administration of drugs through oral route is ineffective and also used for drugs that are too irritating to be given by mouth. These routes include intravenous (IV), intramuscular (IM), subcutaneous (SC) and intradermal (ID).

2.1.2.3 Transdermal delivery

The transdermal drug delivery is used to deliver drugs through the skin. It has been used to apply for medical treatment systemic effect. This route can transfer drugs or substances directly to the systemic circulation without GI

metabolism. Thus, transdermal delivery is used as one alternative route such as transdermal patch.

2.1.2.4 Mucosal delivery

Delivery of drugs via the absorptive mucosa in various easily accessible body cavities like the buccal, nasal, ocular, sublingual, rectal, and vaginal mucosa offers distinct advantages over peroral administration for systemic drug delivery. An advantage of these routes' use is avoidance of the first-pass effect of drug clearance (Sinko, 2011).

2.2 Oral drug delivery system

The oral administration is widely used for treatments both conventional as well as novel drug delivery. The reasons of this route is favored because it is simplest, easiest, most convenient and painless self-medication, especially for chronic therapies (Gaucher et al., 2010; Satturwar et al., 2007). However, there are many limitations of oral route that may affect drug bioavailability such as poor adsorption, the first-pass metabolism, degradation some drug in high acid content or digestive enzyme in GI tract and poorly solubility etc (Jane, 2008). Based on that, the Biopharmaceutic Classification System (BCS) defines four categories of drugs (Table 2.1). Two important parameters, solubility and permeability, influence on the bioavailability of oral drugs. Many new drugs or therapeutic substances candidates are practically insoluble in water which are classified in BCS class II and class IV. The low solubility parameter limits the drugs dissolution rate and its absorption in GI tract that resulting in low bioavailability of the orally administered drugs (Xu, Ling, and Zhang, 2013).

Table 2.1 BCS drug classification

	High permeability	Low permeability
High solubility	Class I	Class III
Low solubility	Class II	Class IV

The anatomy of the GI tract was shown in Figure 2.1. The organs and glands in GI tract work together to extract nutrients from ingested food. The pH varies

according to the locations, pH 1-3 in the stomach, pH 5-7 in the small intestine and pH 6-7.5 in the colon (Daugherty and Mrsny, 1999; Gaucher et al., 2010). In oral DDS, the drug must be absorbed through 3 main pathway of small intestine site as following (Figure 2.2).

(1) Paracellular pathway

This way allows small molecule and hydrophilic property (e.g., mannitol) through between adjacent epithelial cells.

(2) Transcellular pathway

The small hydrophobic molecules are able to diffuse through lipid bilayer and the membrane-bound protein regions of the cell membrane.

(3) Receptor-mediated transcytosis via endocytosis

The molecules must be used receptor and energy. This pathway, polymeric micelles are thought to absorb in the intestine and accumulate in the bloodstream.

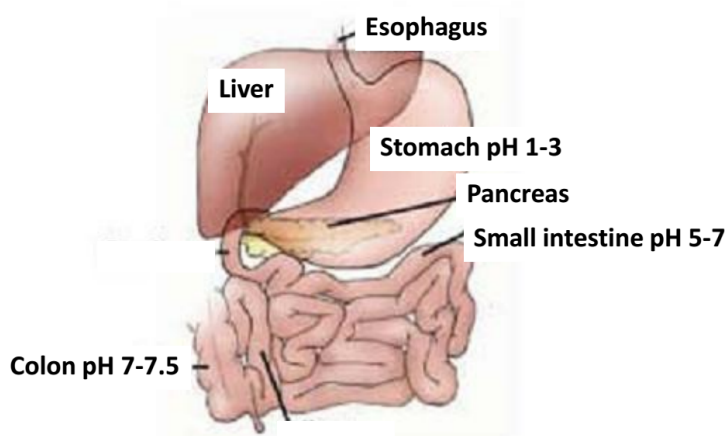


Figure 2.1 Anatomy of GI tract in humans. Adapted in part from Godfroy, 2007

Source: Godfroy, I. "Polymeric micelles-The future of oral drug delivery."

Journal of Biomaterials Applications Reviews 3: 216-232.

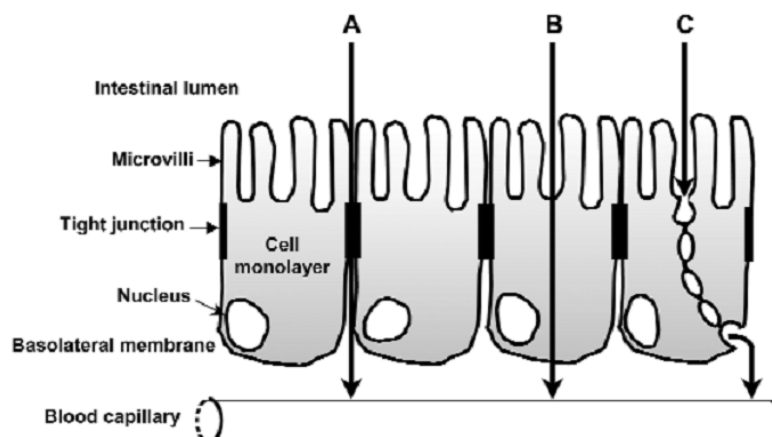


Figure 2.2 Schematic representation of intestinal epithelial cells show potential transepithelial pathways: (A) paracellular route; (B) transcellular passive diffusion; and (C) transcellular receptor-mediated transcytosis.

Source: Francis, M.F., Cristea, M., and Winnik, F.M. "Polymeric micelles for oral drug delivery: Why and how." **Pure and Applied Chemistry** 76, 7-8: 1321-1335.

In order to improve the solubility of drugs, several strategies were used include salt formation, reduction of drug particle size, cosolvents, solid dispersions etc. Recently, novel carriers have been developed for oral drug delivery such as microemulsions, self-nanoemulsifying drug delivery systems (SNEDDS), nanoparticles and polymeric micelles (Bernkop-Schnürch, 2013; Gaucher et al., 2010).

2.3 Polymeric micelles

Polymeric micelles are macromolecules that are generally formed by self-assembly in an aqueous solution from synthetic amphiphilic block copolymers or graft copolymers (see Figure 2.3). Usually, it has a spherical inner core and an outer shell (Yokoyama, 2011). The self-assembly micelles have distinct hydrophobic (non-polar) and hydrophilic (polar, water-loving) domains. Generally, formation of micelles from both surfactant and polymeric micelles in aqueous solution occurs when the concentration of the copolymer increases above a certain concentration named the critical micelle concentration (CMC). The CMC depends on the relative

sizes of both the hydrophobic and hydrophilic domain. A larger hydrophobic domain will result in a lower CMC, and a higher hydrophilic domain area will result in a higher CMC (Ding et al., 2012). Polymeric micelles show very low CMC values in range from 1 mg/L to 10 mg/L (Murthy, 2015). These values are lower than typical CMC of low-molecular weight surfactants. It is described polymeric micelles are more stable than surfactant micelles.

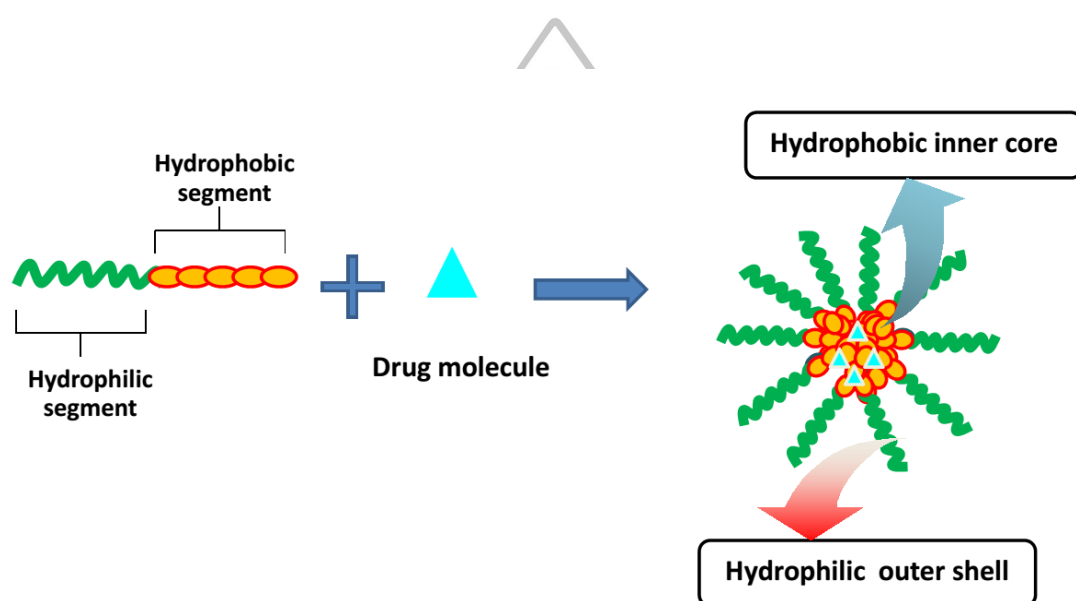


Figure 2.3 Formation and drug loading of polymeric micelles by self-assembly of amphiphilic block copolymers in aqueous solution

2.3.1 Structure of polymeric micelles

As shown in Figure 2.3, the polymeric micelles present a great potential as a DDS for hydrophobic drugs which exhibit poor bioavailability. The inner hydrophobic cores are able to incorporate poorly water-soluble drugs to improve their solubility, stability and bioavailability. Moreover, undesirable side effects are lessened, as contact of the drug with inactivating species, such as enzymes present in biological fluids, are minimized, in comparison with free drug. The core-shell structure of polymeric micelles can be formed as a result of two forces. One is an attractive force which produced micelle formation and a repulsive force which can prevent micelles unlimited growth. The drugs are encapsulated in the hydrophobic inner core through their attractive interactions such as hydrophobic, electrostatic, π - π

interactions, and hydrogen bonding. Typically, the polymeric micelles are formed by hydrophobic interactions which work as driving force because most of drugs molecules are hydrophobic structure.

The choice of amphiphilic copolymer architecture can create several different possible micellar morphologies (Figure 2.4) (Mondon et al., 2008). Generally, amphiphilic copolymers are commonly designed diblock copolymer of linear A-B type, where A represents a hydrophilic block and B represents a hydrophobic block because of the close relationship between the properties of micelles the structure of polymers (Xu, Ling, and Zhang, 2013), for example, self-assembled pH-responsive MPEG-*b*-(PLA-co-PAE) block copolymer micelles for anticancer drug delivery (Zhang, C.Y. et al., 2012); Poly(ethylene oxide)-block-poly(L-amino acid) micelles for drug delivery (Lavasanifar et al., 2002); pH-Responsive composite based on prednisone-block copolymer micelle intercalated inorganic layered matrix: Structure and *in vitro* drug release (Li et al., 2009). Moreover, nonlinear composition having more complex architectures like star or branch type also has been studied for drug delivery such as pH-sensitive micelles self-assembled from multi-arm star triblock co-polymers poly(ϵ -caprolactone)-*b*-poly(2-(diethylamino)ethylmethacrylate)-*b*-poly(poly(ethylene glycol) methyl ether methacrylate) for controlled anticancer drug delivery (Yang et al., 2013); synthesis of star-branched PLA-*b*-PMPC copolymer micelles as long blood circulation vectors to enhance tumor-targeted delivery of hydrophobic drugs *in vivo* (Long et al., 2016); Preparation of pH-sensitive micelles from miktoarm star block copolymers by ATRP and their application as drug nanocarriers (Huang et al., 2016).

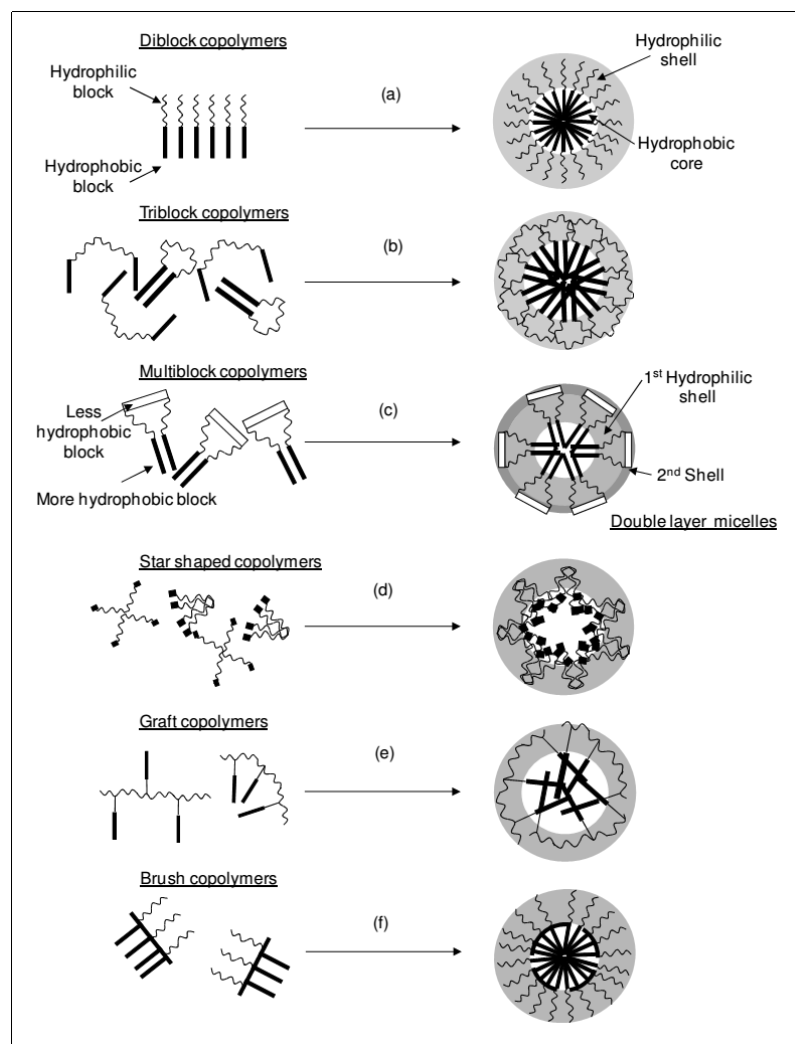


Figure 2.4 Various micelle structure by self-assembly that can be formed spontaneously in aqueous solution from different copolymer architectures (Mondon et al., 2008).

Source: Mondon, K., Gurny, R., and Moller, M. "Colloidal drug delivery system-recent advances with polymeric micelles." *CHIMIA* 62, 10: 832-840.

2.3.2 Preparation of drug loading into polymeric micelles

Polymeric micelles have been loaded with an extensive variety of drugs such as paclitaxel (Kim et al., 2008), cisplatin (Oberoi et al., 2011), doxorubicin (Soppimath, Tan, and Yang, 2005), ibuprofen (Yang et al., 2011), prednisone acetate (Wang et al., 2009), candesartan cilexetil (Satturwar et al., 2007) etc. In general,

drug-loaded polymeric micelles can be prepared by two major approaches: chemical conjugation and physical entrapment method (Pu et al., 2012; Murthy, 2015).

2.3.2.1 Chemical conjugation

According to this method, a drug is chemically conjugated to the core forming block of the copolymer via carefully designed enzyme- or pH-sensitive linker. It can be cleaved to release a drug in its active form within a cell such as a hydrazone bond, which can be cleaved under acidic conditions (Yoo et al., 2002). The appropriate choice of conjugating bond depends on specific applications (Batrakova et al., 2006).

2.3.2.2 Physical entrapment

The physical entrapment method is generally preferred over micelle-forming polymer-drug conjugates, especially for hydrophobic drug molecules. It is the simplest and the most convenient technique, and can be implemented via dialysis, oil-in water (O/W) emulsion, solvent evaporation and other methods.

2.3.2.2.1 Dialysis

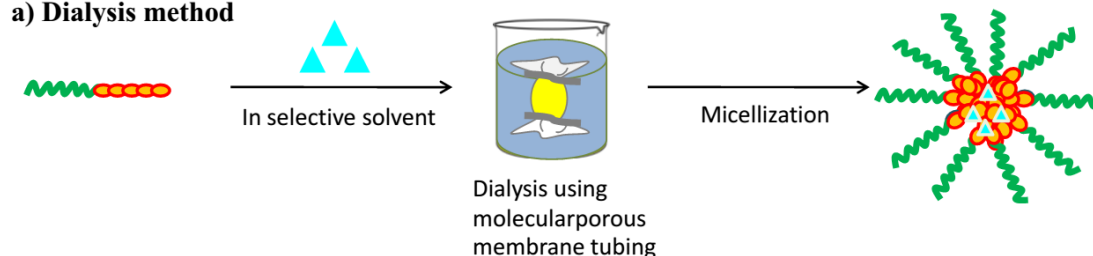
In the dialysis method, the copolymers and hydrophobic drugs are dissolved in a water-miscible organic solvent like dimethyl sulfoxide (DMSO), dimethylformamide (DMF), acetone, ethanol and placed in the dialysis bag. Then, the solution is exchanged with water or aqueous media for several hours to remove the organic solvent (Figure 2.5 (a)).

2.3.2.2.2 O/W emulsion

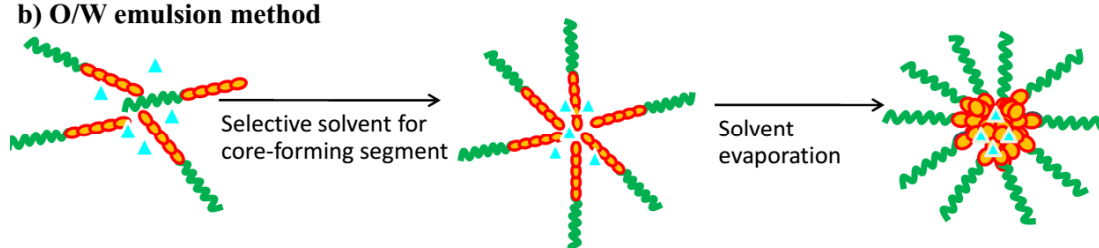
In O/W emulsion method, the procedure involves the addition of a solution consisting of the copolymers, drugs and volatile, non-water-miscible organic solvent like chloroform, dichloromethane (DCM) or a mixture of solvents like chloroform and ethanol, into vigorous stirring aqueous media or water to form an emulsion with an internal organic phase and continuous aqueous phase, which rearranges the polymer to form micelles. Then, the solvent was evaporated (Figure 2.5 (b)) (Kwon and Okano, 1996). Some case study, this method was prepared two steps because the incompatibility of copolymers and drugs occurred when these are dissolved in some organic solvent. First, blank polymeric micelles

was prepared by dialysis method. Second, the drugs in volatile, non-water-miscible organic solvent was injected under vigorous stirring into blank polymeric micelles, and the evaporation of the solvent (Miller et al., 2013).

a) Dialysis method



b) O/W emulsion method



c) Evaporation method

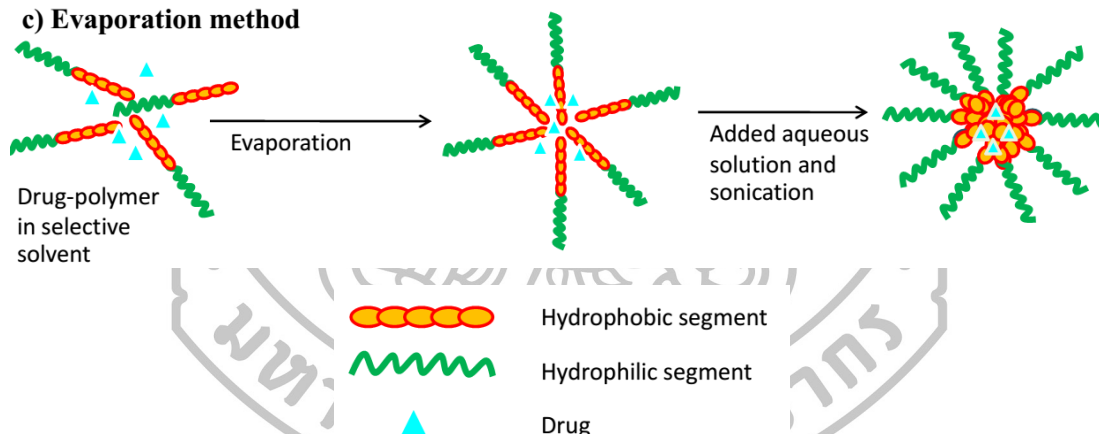


Figure 2.5 Physical loading of hydrophobic drugs into polymeric micelles: a) dialysis method, b) o/w emulsion method and c) evaporation method.

2.3.2.2.3 Solvent evaporation

In solvent evaporation or solution-casting method, the copolymers and drugs are dissolved in a volatile organic solvent like acetone, acetonitrile, a mixture of solvents like acetone and DMF. Then, the thin film is formed by evaporating the solvent. Drug-loaded polymeric micelles are obtained by reconstitution of film with water or aqueous media (Murthy, 2015, Miller et al., 2013) (Figure 2.5 (c)).

2.3.2.2.4 Other methods

The other methods were also used such as lyophilization, dropping, separation method, and various solvent evaporation procedures (Pu et al., 2012).

2.3.3 Characterization of polymeric micelles

2.3.3.1 Determination of CMC of polymeric micelles

The concentration of the amphiphilic molecule at which spontaneous self-assembly or micellization starts is termed the CMC. There are several methods available to determine the CMC value in aqueous solutions of micelles, including surface tension measurements, chromatography, light scattering, differential scanning calorimetry and fluorescent probes. Among various methods, the determination of CMC using the fluorescent probe pyrene is the most effective, convenient and reliable (Biswas et al., 2013, Jones and Leroux, 1999). Pyrene, a hydrophobic fluorescence probe, preferentially partitions into the hydrophobic core of micelles, with a synchronous change in its fluorescent properties such as vibrational changes in the emission spectrum and red shift in the excitation spectrum (Kedar et al., 2010). The CMC value can be determined as the point of cross-section of the extrapolation of the change in absorbance over a wide range of the concentration of polymer.

2.3.3.2 Size determination

Micelles was classified in the category of colloidal dispersions, where colloids or a dispersed phase are distributed uniformly in the aqueous dispersion media. The dispersed phase or colloids have a diameter of approximately 5–500 nm (Biswas et al., 2013). However, small size (10-200 nm) is one of the most interesting features of polymeric micelles. Generally, size and size distribution of polymeric micelles can be determined by static and dynamic light scattering (DLS) as well as microscopic techniques.

As reported the uptake of particles within the intestine and the extent of drug absorption increase with decreasing particle size and increasing specific surface area (Francis, Cristea, and Winnik, 2004). Jani et al. (1989, 1990)

evaluated the size-dependence of the uptake of nanoparticles by the rat intestine by monitoring their appearance in the systemic circulation and their distribution in different tissues. They found that, after administration of the equivalent doses, 33 % of the 50 nm nanoparticles and 26% of the 100 nm nanoparticles were detected in the intestinal mucosa and gut-associated lymphoid tissues, whereas, in the case of 500 nm particles, only 10 % were found in the intestinal tissues. Thus size characterization of polymeric micelles is smaller than 500 nm that is appropriate in designing of nanoparticles for oral DDS.

The size of micelles is controlled by the length of the core-forming segment and the length of the corona-forming chain or molecular weight of block copolymer. For example, Aliabadi et al. (2007) reported that increasing average molecular weight of hydrophobic chain of methoxy poly(ethylene oxide)-block-poly(ϵ -caprolactone) (MePEO-b-PCL) micelles from 5000-5000 to 5000-24000 g/mol MePEO-b-PCL resulted in increase in the mean particle size of micelles from 68.5 nm to 93.6 nm. Moreover, it depends also on the method of micellization selected for the preparation of micelles. For instance, the dexamethasone-loaded PEGylated poly-(4-vinylpyridine) (PEG-PVPy) micelles produced using the cosolvent evaporation methods showed mean particle size of 45 nm, while dialysis method showed micelles size of 67 nm (Miller et al., 2013).

2.3.3.3 Drug loading

The hydrophobic core of self-assembled micelles is expected to serve as the loading space for various hydrophobic drugs. The polymeric micelles were designed in nanometric size to deliver drug which this space was limited. As literature, drug loaded into polymeric micelles core by hydrophobic interactions and other interactions between hydrophobic polymer blocks and drugs (Biswas et al., 2013). Thus, in order to enhance of solubility of drug in water, the many factors that control loading efficiency and loading capacity was studied. Several of the major factors which influence the loading capacity and loading efficiency of block copolymer micelles are nature of the core forming block, length of hydrophobic core, nature and length of outer micelle shell (corona), total copolymer molecular weight, nature of the solute and preparation of micelles (Sezgin, Yuksel, and Baykara, 2006; Miller et al., 2013).

Jette et al. (2004) examined the effect of the length of the core-forming block on loading efficiency of fenofibrate into poly(ethylene glycol)-block-poly(ϵ -Caprolactone) (PEG-b-PCL) micelle. The length of the PEG block was constant at 5000 g/mol, whereas the PCL block length varied (1000, 2500, and 4000 g/mol). They found nearly a 90% loading efficiency was obtained with PEG-b-PCL (5000:4000) and (5000:2500) micelles, whereas PEG-b-PCL (5000:1000) micelles only obtained a loading efficiency of 29%. It was explained that likely due to the smaller core of PEG-b-PCL (5000:1000) micelles compared to PEG-b-PCL (5000:4000) and (5000:2500) micelles. This result was related to study of chain length effect of MePEO-b-PCL micelles on the encapsulation of cyclosporine A (Cy A) (Aliabadi et al., 2007). The average molecular weight of 5000, 13000 and 24000 PCL hydrophobic chain and 5000 of MePEO parts were used. As the reported an increase in the PCL molecular weight from 5000 to 13,000 and 24,000 led to an increase the molar loading of CyA in polymeric micelles.

Miller et al. (2013) studied effect of different physical entrapment method (direct dialysis, O/W emulsion and cosolvent evaporation) on entrapment efficiency and capacity of PEG-PVPy micelles containing dexamethasone. They observed drug loading via direct dialysis from acetone was a less effective loading method which led to dexamethasone loads < 2% w/w. O/W emulsion technique from DCM increased drug load up to ~13% w/w and optimized cosolvent evaporation increased load up to ~19% w/w.

In addition, drug loading capacity and efficiency depend on the compatibility between polymers and drugs which directly related to drug solubilization as determined by Flory–Huggins interaction parameter (Letchford et al., 2008).

2.3.3.4 Morphology

Microscopic technique has been used to observe the morphology of the nanoparticles. It includes scanning electron microscopy (SEM), transmission electron microscopy (TEM), atomic force microscopy (AFM), confocal microscopy, and others.

Electron microscopy (SEM and TEM), have been widely used for the direct visualization, size and shape determination of particularly block copolymer micelles.

AFM technique makes use of a mechanical imaging instrument employed to observe morphology and particle size of polymeric micelles. In this technique, a probe tip with atomic-scale sharpness is rastered over the sample to produce a topological map based on the forces at play between the tip and the surface. The probe can be placed in contact or noncontact mode with the sample (Kedar et al., 2010).

Confocal microscopy is used to track colloidal particles in three dimensions with great precision over large time scales by excluding aberrant rays of scattered light from regions outside the image plane of interest. A better resolution in image was found when compared with conventional microscopy (Kedar et al., 2010).

2.3.3.5 Stability

In DDS, polymeric micelles must remain intact during formulation and administration to prevent drug cargo release before reaching the target cells. The stability of polymeric micelles can be thought of generally in terms of thermodynamic and kinetic stability. Thermodynamic stability describes how the system acts as micelles are formed and reach equilibrium, which used CMC as a fundamental parameter for characterization. Kinetic stability describes the behavior of the system over time and details the rate of polymer exchange and micelle disassembly. HPLC-based gel permeation chromatography can be applied to observe kinetic stability (Owen et al., 2012). Jette et al. (2004) used this technique to examine the stability and dissociation of the polymeric micelles upon dilution, and confirm drug loading of PEG-b-PCL micelles, with and without fenofibrate. In the chromatogram, it was observed micelles formation that the peaks of micelle detected by refractive index (RI) detector (for polymer). They found that an increased length of the PCL block led to greater the stability of the PEG-b-PCL micelle upon dilution. Fenofibrate, detected by monitoring the absorbance at 288 nm, eluted with PEG-b-PCL micelles, which showed the same retention time indicating drug encapsulation.

2.3.3.6 *In vitro* cytotoxicity

The predictive value of *in vitro* cytotoxicity tests is based on the idea that toxic chemicals affect basic functions of cells that are common to all cells. The toxicity can be measured by assessing cellular damage (Kedar et al., 2010). For the *in vitro* cytotoxicity test of drug loading into polymeric micelles, various types of cell lines are used, as shown in Table 2.2.

Table 2.2 *In vitro* cytotoxicity

Drug	Copolymer	Cells	References
Adriamycin	Poly(L-histidine)-b-PEG	Human breast adenocarcinoma cells	Zhiang et al., 2009
Camptothecin	N-phthaloylchitosan-g-mPEG	HeLa cells	Opanasopit et al., 2007
Camptothecin	Poly(ketal adipate)-co-PEG	NIH 3T3 and SW620 human colon cancer cells	Lee et al., 2013
Cyclosporin A	mPEG-b-poly(D,L-lactic acid)	Caco-2 cells	Zhang, Y. et al., 2010
Docetaxel	PLGA-lecithin-PEG	HeLa and HepG2 cells	Nishiyama and Kataoka, 2001
Paclitaxel and Etoposide	PEG-b-PLA	CT-26 murine colorectal cells	Cho et al., 2004
Prednisone acetate	Poly(acrylic acid-b-DL-lactide)	HeLa cells	Xue et al., 2009

The common methods for the detection of the cytotoxicity or cell viability following exposure to toxic substances include a lactate dehydrogenase (LDH) release assay, the neutral red uptake assay and methyl tetrazolium (MTT) assay (Fotakis and Timbrell, 2006).

2.3.3.6.1 Lactate dehydrogenase (LDH) release assay

The LDH leakage assay, the level of extracellular LDH released from damaged cells is measured as an indicator of cytotoxicity. This assay was used to measure neuronal cell death occurring via necrosis (Koh and Choi, 1987) and neuronal apoptosis in cortical cultures (Koh and Cotman, 1992). The assay is a two-step process, firstly step, LDH produces reduced nicotinamide adenine dinucleotide (NADH) when it catalyzes the oxidation of lactate to pyruvate. In the second step, a tetrazolium salt is converted to a colored formazan product using newly synthesized NADH in the presence of an electron acceptor (Wang et al., 2012; Chan, Moriwaki, and Rosa, 2013).

2.3.3.6.2 Neutral red uptake assay

The neutral red uptake assay is used to measure cell viability. It has been used as an indicator of cytotoxicity in cultures of primary cells and other cell lines from diverse origin. Living cells take up the neutral red, which is concentrated within the lysosomes of cells (Fotakis and Timbrell, 2006).

2.3.3.6.3 Methyl tetrazolium (MTT) assay

The MTT assay is used to determine disruption of a critical biochemical function. This assay quantifies mitochondrial activity by measuring the formation of a purple formazan product formed by cleavage of the tetrazolium ring by succinate dehydrogenase within the mitochondria (Fotakis and Timbrell, 2006; Lobner, 2000). The MTT assay was determined for its validity in various cell lines (Mossmann, 1983).

2.3.3.7 *In vitro* drug release study

Polymeric micelles improve solubility of many poorly water-soluble drugs by encapsulation in the hydrophobic core. However, the drug has to be released from the micelles to exhibit its function. After reaching the target site, efficient drug release from micelles becomes important for the bioavailability of the drug (Biswas et al., 2013).

In vitro drug release behavior from polymeric micelles is studied by placing the fixed amount of drug-loaded polymeric micelles in a dialysis bag into a flask containing release medium, kept at a constant stirring rate and

temperature with sink condition maintained. At predetermined time intervals, aliquots of the release medium are taken, and fresh medium are replaced. The content of drug released in the medium is determined by spectroscopic or other suitable method such as UV-Vis spectrophotometry, High performance liquid chromatography (HPLC) (Murthy 2015).

2.3.4 Application of polymeric micelles in drug delivery

The studies on the application of polymeric micelles in drug delivery have focused to improve three fundamental parameters in drug performance: (1) the solubilization of hydrophobic or water-insoluble drugs, (2) the controlled or sustained release of a drug and (3) targeting a certain cell type or organ, which will be explained below.

2.3.4.1 Solubilization

Nowadays, it is estimated that around 40% or more of the new chemical entities generated through drug discovery have poor aqueous solubility and belong to class II or IV in the BCS (Movassaghian et al., 2015). Here, the hydrophobic drugs can be incorporated into the hydrophobic core of the polymeric micelles. As reported the results showed that micelles promisingly increase the water solubility of many drugs 10- to 8400-fold (Savic, Eisenberg, and Maysinger, 2006; Chiappetta et al., 2011). The solubilization process leads to enhancement of their water solubility and thereby bioavailability. However, the extent of solubilization depends upon the micellization process, the compatibility between the drug and the core forming block, chain length of the hydrophobic block, concentration of polymer and nature of the drug.

2.3.4.2 Controlled or sustained release of a drug

In order to show controlled or sustained release from the polymeric micelles that they requires specific properties. The micelles must be stable to dilution due to their high thermodynamic stability (low CMC) or to a high kinetic stability based on highly viscous, low chain mobility core properties for prolonging the circulation time. However, drugs which are physically entrapped in polymeric micelles should have low diffusion coefficients to qualify for a sustained release profile. In addition, the chemical manipulation of the hydrophobic block

may be used to increase the hydrophobicity and rigidity of the micellar core, restricting the loss of the drug (Movassaghian et al., 2015).

2.3.4.3 Targeting

Most of the studies targeting via polymeric micelles have received considerable scientific attention to deliver drug, especially anticancer drug due to several reasons. At first, anticancer drugs are water-insoluble and are limited by undesirable properties such as low therapeutic efficacy, cytotoxicity to normal tissue, low tumor targeting, insufficient cellular drug uptake. Second, polymeric micelles can preferentially accumulate in the tumor via the enhanced permeability and retention (EPR) effect for passive targeting. Finally, polymeric micelles can also be modified with ligands or antibodies for active targeting, which specifically recognize the receptors overexpressed on the surface of tumor cells and/or tumor endothelium, resulting in highly efficient intracellular delivery of micellar drugs (Liu et al., 2013; Tan, Wang, and Fan, 2013).

Although polymeric micelles have been reported to accumulate preferably in tumor due to passive targeting and/or receptor-mediated active targeting, the inefficient drug release in the tumor cells can be another barrier that may significantly lower drug's efficacy. Thus, the other targeting approach for improved drug efficiency is the use of stimuli-responsive polymeric micelles that can be controlled micellar dissociation and triggered drug release (Movassaghian et al., 2015; Liu et al., 2013). At present, several examples the studies stimuli-responsive polymeric micelles, which respond to internal or external stimuli, such as pH, temperature, enzyme, ultrasound by including thermo- or pH-sensitive components or by attaching specific targeting moieties to the outer hydrophilic surface of polymeric micelles have been developed (Nakayama, Akimoto, and Okano, 2014).

For oral drug administration, besides protecting the payload of polymeric micelles from the harsh environment in the GI tract and facilitating the safe transport through the GI tract. In stimuli-responsive system, pH-sensitive micelles can be used to control drug release at the target region, which it is explained in next section.

2.4 pH-sensitive polymeric micelles for oral drug delivery

As it is known, the pH in GI tract varies according to the sites from high acidity in the stomach (pH 1-3) to a neutral or slightly alkaline in the small intestine (pH 5-7) and the colon (pH 6-7.5) (Daugherty and Mrsny, 1999; Gaucher et al., 2010). The normal transit time in stomach (pH 1-2) is 2 h (although this may vary) and the transit time in the small intestine is 2-3 h (Li et al., 2009; Sinha and Kumria, 2002). Here, this point can be applied to develop various pH sensitive drug carrier in a controlled drug release to target sites for oral DDS.

2.4.1 Mechanism

pH sensitive polymeric micelles are developed by designing compositions of building block or graft of copolymers with various polyacids. An acidic units in polyacids such as carboxylic acids (COOH) are uncharged when protonated at low pH. The copolymer can be formed micelle and contained drug in the inner core. When become high pH (above the pK_a of polymer), the polymeric micelles were dissociated by caused electrostatic repulsions that showed negative charge and drug were released (Figure 2.6).

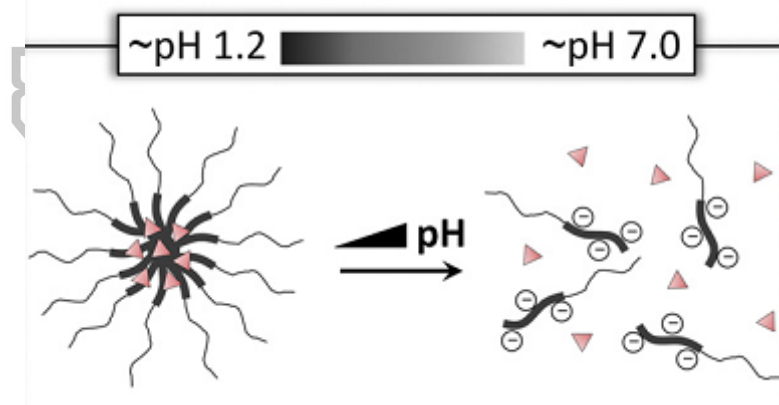


Figure 2.6 Schematic representation of drug release mechanisms from polymeric micelles: protonation-induced (left) and ionization-induced (right) destabilization.

Source: Felber, A.E., Dufresne, M., and Leroux, J. “pH-sensitive vesicles, polymeric micelles, and nanospheres prepared with polycarboxylates.” *Advanced Drug Delivery Reviews*, 64: 979-992.

2.4.2 Commonly most copolymer

A promising strategy to pH-dependent micellization behavior in aqueous media was presented in Table 2.3. Acrylic-based polymers are widely used for forming pH sensitive polymeric micelles to deliver oral drug, such as poly(methacrylic acid) (PMAA), poly(acrylic acid) (PAA). PMAA and PAA, bearing the carboxylic group with pK_a around 4–6, retain a collapsed state in the low pH of the stomach and swells as it transits through the intestines.

Table 2.3 pH sensitive polymer typically used to prepare polymeric micelles for oral drug delivery.

Amphiphilic copolymer	Drug (low solubility)	Years
PEG-b-P(AIA-co-MAA)	Fenofibrate	2005
PEG-b-P(VBODENA-co-AA)	Paclitaxel	2008
PEO-b-PMAA	Naproxen	2009
PAAc-b-PDLLA	Prednisone acetate	2009
P(MMA-co-MAA)-b-PPEGMA	Ibuprofen	2011
PLA-b-PMAA-b-PPEGMA	Nifedipine	2012
PEG-[b-PCL-b-PAA] ₂	Naproxen	2014
BSCS	Curcumin	2014

Poly(ethylene glycol) (PEG); Poly(methacrylic acid) (PMAA); Acrylic acid (AA); Poly(DL-lactide) (PDLLA); Poly(polyethylene glycol) methyl ether monomethacrylate) (PPEGMA); poly(ethylene oxide) (PEO); poly(ϵ -caprolactone); N-benzyl-N,O-succinyl chitosan (BSCS).

2.4.3 Examples of pH-sensitive polymeric micelles for oral drug delivery studies

Over the past decade, the self-assembly polymeric micelles have been extensively studied for oral DDS. For instance, PEG-b-P(alkyl(-meth-)acrylate-co-methacrylic acid)s (PEG-b-P(AI(M)A-co-MAA)s)-based polymeric micelles have been investigated for containing indomethacin (IND) or fenofibrate (FNB) or candesartan cilexetil (CDN) by various methods (i.e. o/w emulsion, dialysis, solvent evaporation) (Sant, Smith, and Leroux, 2004; Satturwar et al., 2007). These

polymeric micelles display a pH-dependent micellization behavior in aqueous media. As shown in Figure 2.7 shows the in vitro cumulative release profiles of CDN, a poorly ionizable drug, from pH-sensitive PEG-b-P(isoBA-co-MAA) and pH-insensitive PEG-b-P(isoBA-co-tert-butyl methacrylate) (PEG-b-P(isoBA-co-tBMA)) micelles. The polymeric micelles were immersed in SGF (pH 1.2) for 2 h and then exposed to pH 7.2 for an additional 7 h. It can be seen both formulations showed relatively low drug leakage in SGF, with about 10% of CDN released after 2 h. When pH was shifted from 1.2 to 7.2 resulted in a sudden increase in the release rate from PEG-b-P(isoBA-co-MAA) micelles, whereas the release behavior from the pH-insensitive formulation was not affected. Due to the presence of pendant carboxylic groups in the hydrophobic part (MAA moieties), PEG-b-P(isoBA-co-MAA) exhibits pH-dependent aggregation behavior and form micelles at acidic pH, while dissociate partially or completely with increase in pH owing to the ionization of carboxylic groups (Satturwar et al., 2007). Alternatively, N-benzyl-N,O-succinyl chitosan is graft copolymer which were rendered pH-sensitive from succinic segment. It exhibited release behavior through pH-dependent. At pH 1.2 release rate of curcumin is slow (< 30% within 24 h) while at pH 5.5, 6.8, 7.4 the accumulative release showed about 70% within 24 h (Sajomsang et al., 2014).



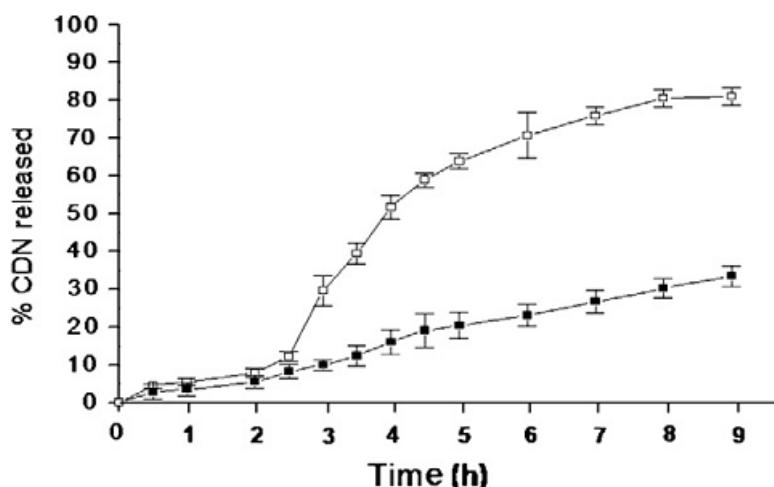


Figure 2.7 *In vitro* release profile of CDN from PEG₁₁₅-b-P(isoBA₃₅-co-MAA₃₈) (open square) and PEG₁₁₅-b-P(isoBA₃₅-co-tBMA₃₈) (closed square) polymeric micelles prepared by the solvent evaporation method at pH 1.2 for 2 h followed by 7 h at pH 7.2. Mean \pm SD (n=3). Adapted in part from Satturwar et al., 2007

Source: Gaucher, G. et al. "Polymeric micelles for oral drug delivery." **European Journal of Pharmaceutics and Biopharmaceutics** 76, 2 (October): 147-158.

2.5 Chitosan

Chitosan is a randomly deacetylated derivative of chitin which is the second most abundant natural polysaccharide after cellulose and is abundantly available in marine crustaceans (Fu et al., 2013). The chemical structure of chitosan consists of D-glucosamine and N-acetyl-D-glucosamine as shown in Figure 2.8 (Tran et al., 2011). It has been proved that chitosan has excellent biocompatibility, biodegradability, low immunogenicity, and toxicity, as well as versatile biological activities. However, the poor solubility of chitosan in water or aqueous media at pH greater than 6.0 due to amino groups (pK_a 6.2-7.0) in structure has so far limited its widespread application. Thus, the chitosan can be modified for utilizing in various application.

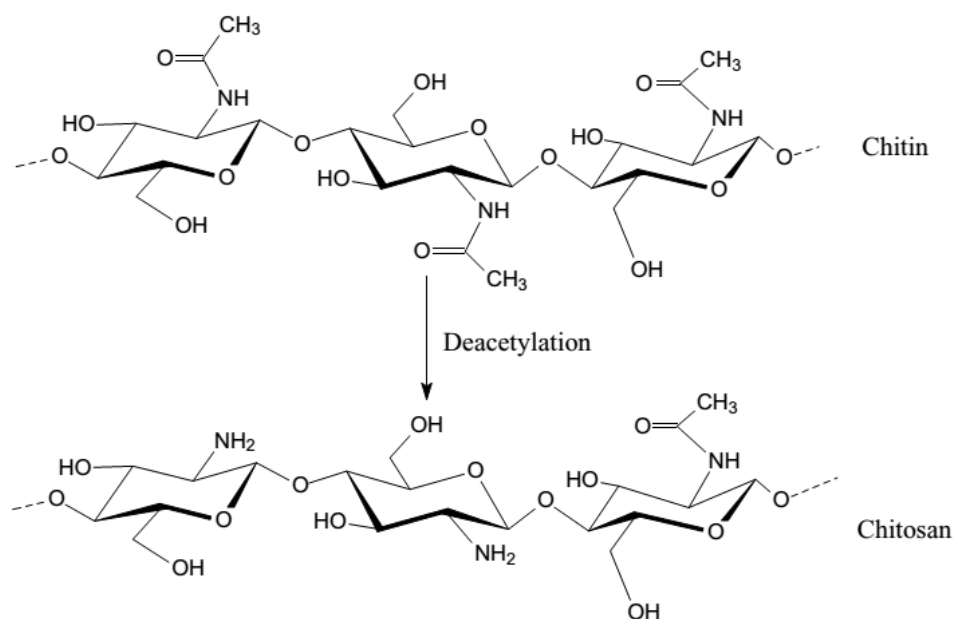


Figure 2.8 Chemical structure of chitin and chitosan

Source: Tran, D.L. et al. "Some biomedical applications of chitosan-based hybrid nanomaterials." **Advances in Natural Sciences: Nanoscience and Nanotechnology** 2, 4 (December): 1-6.

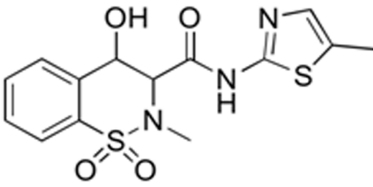
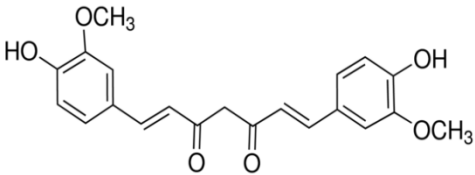
The modification of the chitosan can be done through the derivatization of the amino and hydroxyl functional groups which improves its water solubility at higher pH, its biodegradability and biocompatibility, and decreases toxicity (Bashir et al., 2015). Several modification methods are used such as quaternization, alkylation, acylation, sugar derivatives. The most widely used modification method is N-substitution which chemical reaction may occur via reductive amination procedure in designing molecules react with the amino groups of chitosan. Some polymers terminated by the designed groups can also be grafted on chitosan through this method. Moreover, O-substitution means the reaction between designed small molecules or polymers and the hydroxyl groups of chitosan (Wang et al., 2016).

Chitosan has been successfully modified and employed in various DDS; for example, vitamin D₃ loaded into N,N-dimethylhexadecyl carboxymethyl chitosan (DCMCs) micelles (Lia et al., 2014), 5-fluorouracil loaded CS microspheres (Sun et al., 2010), and ketoprofen loaded chitosan grafted with β-cyclodextrin (CD-g-CS) nanoparticles (Yuan et al., 2013).

2.6 Meloxicam

Meloxicam (MX), 4-hydroxy-2-methyl-N-(5-methyl-1,3-thiazol-2-yl)-2H-1,2-benzothiazine-3-carboxamide 1,1-dioxide, is a non-steroidal anti-inflammatory drug (NSAID) in class of enolic acid compounds. MX is a potent inhibitor of cyclo-oxygenase (COX), which has a greater affinity to inhibit the activity of COX-2 than COX-1 (Villalba et al., 2016). COX-2 inhibition is related to anti-inflammatory effects of MX, since it reduces prostaglandin synthesis in an inflamed site (Lopez-Garcia and Laird, 1998). It is used in the treatment for painful conditions and inflammatory disorders such as rheumatoid arthritis, gout, osteoarthritis and ankylosing spondylitis (Luger et al., 1996). However, COX-1 inhibition is related to the side effects of the drug on the GI tract (Mitchell et al., 1993; Engelhardt et al., 1996). The physicochemical properties of MX were presented in Table 2.4. MX is practically insoluble in water that can be classified in BCS class II (low aqueous solubility and high permeability) (Kim and Lee, 2007).

Table 2.4 Physicochemical properties of the drugs

Drug	Structure	MW (g/mol)	pK _a	Solubility mg/mL
MX		351.41	1.09, 4.18	0.009
CUR		368.38	8.54, 9.30, 10.69	0.000011

Source: Wang J., Ma W., and Tu P. "The mechanism of self-assembled mixed micelles in improving curcumin oral absorption: In vitro and in vivo."

Colloids and Surfaces B: Biointerfaces 133 (September): 198-119.

Mehanny, M. et al. "Exploring the use of nanocarrier systems to deliver the magical molecule; Curcumin and its derivatives." **Journal of Controlled Release** 225 (March): 1-30.

2.7 Curcumin

Curcumin [1,7-bis(4-hydroxy-3-methoxyphenyl)-1,6-heptadiene-3,5-dione] is a yellow-orange pigment hydrophobic polyphenol derived from the rhizome of the turmeric *Curcuma longa* Linn (Zingiberaceae) (Table 2.4). It is widely used to treat disorders due to low cost and pharmacological safety. It has been found to be non-toxic to humans up to the dose of 10 g/day (Shen and Ji, 2007). Curcumin has many pharmacologic effects including antioxidant, antibacterial, antifungal, anti-inflammatory, chemopreventive and chemotherapeutic (Duan et al., 2016; Wang, Ma, and Tu, 2015). In recent years, several researches preclinical and clinical support the idea that curcumin has potential anticancer activity to use in chemoprevention and treatment of many tumor cells such as head and neck, melanoma, brain, breast, ovarian, pancreatic, prostate and colon cancers (Mehanny et al., 2016; Ramasamy et al., 2015). It has been reported that curcumin can interfere with multiple cell signaling pathway involved in carcinogenesis, including inhibition of cell cycle progression, slowing proliferation, reducing angiogenesis and induction of apoptosis in colorectal carcinoma cell (Aggrawal et al., 2007; Cen et al., 2009; Guo et al., 2013). Curcumin was reported to inhibit the proliferation of human colorectal cancer cell lines such as SW480, HT-29, HCT116 cells (Cen et al., 2009; Sandur et al., 2009), LoVo cells (Guo et al., 2013) and Colo205 cells (Su et al., 2006). Although curcumin has a great potential anticancer activity in various tumors, its low aqueous solubility (11 ng/mL in aqueous buffer at pH 5, 400 ng/mL at the physiological pH 7.4) may be due to low bioavailability and rapid metabolism. In order to improve the bioavailability and stability of curcumin that various nanotechnology-based formulations have been considered to encapsulate and deliver curcumin to targeted cancer cell such as liposomes, niosomes, solid lipid nanoparticles (SLNs), polymeric nanoparticles, polymeric micelles, nanoemulsions etc. (Mehanny et al., 2016). Previous studies reported support that curcumin loaded into nanocarriers revealed an increase in efficacy of anticolorectal cancer activity compared with free curcumin; for example, curcumin-loaded lipopolysaccharide nanocarriers (C-LPNCs) (Chaurasia et al., 2015), curcumin-loaded stearic acid-g-chitosan oligosaccharide (CSO-SA) micelles (Wang et al., 2012), curcumin-containing chitosan nanoparticles (CUR-CS-NP) (Chuah et al., 2014).

CHAPTER 3

MATERIALS AND METHODS

- 3.1 Materials
- 3.2 Equipments
- 3.3 Methods
 - 3.3.1 Synthesis of pH sensitive amphiphilic chitosan derivatives
 - 3.3.2 Characterization of pH sensitive amphiphilic chitosan derivatives
 - 3.3.2.2 Proton nuclear magnetic resonance (^1H NMR)
 - 3.3.2.3 Attenuated total reflection Fourier Transform Infrared Spectroscopy (ATR-FTIR)
 - 3.3.3 Characterization of polymeric micelles
 - 3.3.3.1 Critical micelle concentration (CMC)
 - 3.3.3.2 *In vitro* cytotoxicity
 - 3.3.4 Drugs-loaded polymeric micelles
 - 3.3.4.1 Physical entrapment methods
 - 3.3.4.1.1 Dialysis method
 - 3.3.4.1.2 O/W emulsion method
 - 3.3.4.1.3 Dropping method
 - 3.3.4.1.4 Evaporation method
 - 3.3.4.2 Entrapment efficiency
 - 3.3.4.3 Characterizations of drugs-loaded polymeric micelles
 - 3.3.4.3.1 Particle size
 - 3.3.4.3.2 Morphology
 - 3.3.4.3.3 The stability of drug-loaded micelles
 - 3.3.4.4 *In vitro* releases study
 - 3.3.4.4.1 MX-loaded polymeric micelles
 - 3.3.4.4.2 CUR-loaded polymeric micelles
 - 3.3.4.5 *In vitro* intestinal permeation

3.3.4.6 Cytotoxic activity

3.3.5 Stability

3.3.6 Statistical analysis



3.1 Materials

- Acetone (RCI Labscan Limited, Bangkok, Thailand)
- Acetonitrile HPLC grade (RCI Labscan Limited, Bangkok, Thailand)
- Benzaldehyde (Sigma Aldrich[®], St. Louis, MO, USA)
- Chitosan (Degree of deacetylation; DDA 96%, MW 10-13 kDa) (OilZac Technologies Co., Ltd., Bangkok, Thailand)
- Curcumin (Sigma Aldrich[®], St. Louis, MO, USA)
- Deionized water
- Dichloromethane
- Dimethyl sulfoxide (Fisher Scientific, UK Limited, UK)
- Dulbecco's modified Eagle's medium (DMEM) (GIBCO[®], Grand Island, NY, USA)
- Ethanol (Merck, Germany; purity $\geq 99.9\%$)
- Fetal bovine serum (FBS) (GIBCO[®], Grand Island, NY, USA)
- Glacial acetic acid (Merck, Germany; purity $\geq 99.8\%$)
- Human colon adenocarcinoma (Caco-2) cell line (Rockville, MD, USA)
- Human colorectal adenocarcinoma cells (HT-29) cell line (Rockville, MD, USA)
- Hydrochloric acid (Scharlau Chemie S.A., Spain; purity $\geq 99.8\%$)
- Methanol (Merck, Germany; purity $\geq 99.9\%$)
- Meloxicam (Siam Pharmaceutical Co., Ltd., Bangkok, Thailand)
- N,N-dimethylformamide (DMF, 99.8%) (Brightchem Sdn Bhd, Malaysia)
- 2-Naphthaldehyde (Sigma Aldrich[®], St. Louis, MO, USA)
- Octaldehyde (Sigma Aldrich[®], St. Louis, MO, USA)
- Penicillin-streptomycin (GIBCO[®], Grand Island, NY, USA)
- Potassium chloride (Ajax Finechem Australia, New Zealand)
- Potassium dihydrogen phosphate (Ajax Finechem Australia, New Zealand)
- Succinic anhydride (Sigma Aldrich[®], St. Louis, MO, USA)
- Sodium borohydride (Sigma Aldrich[®], St. Louis, MO, USA)
- Sodium dihydrogen phosphate (Ajax Finechem Australia, New Zealand)
- Trisodium phosphate (Ajax Finechem Australia, New Zealand)
- Trypsin-EDTA (0.25 %) solution (GIBCO[®], Grand Island, NY, USA)

3-(4,5-Dimethylthiazol-2-yl)-2,5-diphenyl-tetrazolium bromide (MTT) (Sigma Aldrich[®], St. Louis, MO, USA)

3.2 Equipments

1.5 mL microcentrifuge tube (Eppendorf[®], Corning Incorporated, NY, USA)

15, 50 mL centrifuge tubes-sterile (Biologix Research Company, KS, USA)

Analytical balance (Sartorius CP224S; Scientific Promotion Co., Ltd., Bangkok, Thailand)

Aluminium foil

Atomic-force microscope (AFM) (SPA400, Seiko, Japan)

Beaker (Pyrex, USA)

Bruker AVANCE 500 spectrometer (Bruker, Switzerland)

Centrifuge tube (Biologix Research Company, KS, USA)

CO₂ incubator (Heraeus HERA Cell 240, Heraeus Holding GmbH., Germany)

Dialysis bag (CelluSep[®] (6000–8000 MWCO) Membrane Filtration Products, USA)

Duran bottle 500, 1,000 mL

Franz diffusion cells

Freeze-dryer (Model: Freezone 2.5, LABCONCO, USA)

Freezer/Refrigerator -20 °C, -80 °C, 5°C

Hot air oven (WTB Binder, Germany)

High performance liquid chromatography (HPLC) instrument (Agilent 1100 series, Agilent Technologies, USA)

HPLC column (Eclipse XDB-C18, 5 μm, 15 cm x 4.6 mm) (Santa Clara, CA, USA)

High voltage power supply (Model: Gamma High Voltage Research, USA)

Incubated shaker (Model: KBLee 1001, Daiki sciences, Bio-Active, Bangkok, Thailand)

Laminar air flow (BIO-II-A, Telstar Life Science Solutions, Spain)

Magnetic stirrer (Framo, Germany) and magnetic bar

Micropipette 0.1-2.5 μL, 2–20 μL, 20–200 μL, 100–1000 μL, 1–5 mL, and micropipettetip

Microcentrifuge (Microfuge 16[®], Model: A46473, Beckman Coulter Inc.,

Germany)

Microcentrifuge tube (Eppendorf[®], Corning Incorporated, NY, USA)

Microplate reader (Universal Microplate Analyzer, Model AOPUS01 and AI53601, Packard BioScience, CT, USA)

Nicolet 6700 spectrometer (Thermo Company, USA)

Nylon membrane filter (diameter 47 mm, pore size 0.45 μm)

pH meter (Horiba compact pH meter B-212, Japan)

Probe-type sonicator (model CV 244, Sonics VibraCellTM, USA)

Round bottom flask (Pyrex, USA)

Sonicate Bath

SPSS version 16.0 for Windows (SPSS Inc., Chicago, IL)

Volumetric flask (Pyrex, USA)

Vortex mixer (VX100, Model: Labnet, NJ, USA)

Water bath (HETOFRIG CB60; Heto High Technology of Scandinavia, Birkerød, Denmark)

Well-plate (96 Well plate) (Corning Incorporated, NY, USA)

ZetasizerNano ZS (Malvern Instruments, Malvern, UK)

3.3 Methods

3.3.1 Synthesis of pH sensitive amphiphilic chitosan derivatives

The amphiphilic chitosan derivatives, i.e. *N*-naphthyl-*N,O*-succinyl chitosan (NSCS), *N*-octyl-*N,O*-succinyl chitosan (OSCS) and *N*-benzyl-*N,O*-succinyl chitosan (BSCS), were synthesized by reductive *N*-amination and *N,O*-succinylation. Two grams of chitosan was dissolved in 150 mL of 1% (v/v) aqueous acetic acid. Then, 100 mL of ethanol was added to the solution. 2-Naphthaldehyde, octanaldehyde or benzaldehyde (2.0 meq/GlcN) was added, and the reaction mixture was stirred at room temperature for 24 h. At this point, the pH of the solution was adjusted to 5 by adding 1 M NaOH, and 2.0 g of NaBH₄ (52.9 mmol) was added to the reaction mixture and stirred at room temperature for 24 h. The precipitate was collected by filtration, washed several times with ethanol, before being dried under a vacuum at room temperature to obtain the *N*-naphthyl chitosan (NCS), *N*-octyl chitosan (OCS)

or *N*-benzyl chitosan (BCS). The *N,O*-succinylation was conducted using succinic anhydride. Briefly, 1.0 g of NCS, OCS or BCS was dispersed in 40 mL of *N,N*-dimethylformamide (DMF)/dimethyl sulfoxide (DMSO), (1:1 v/v), and 3.0 g of succinic anhydride (5.0 meq/GlcN) was added. The reaction was heated at 100°C under nitrogen atmosphere for 24 h. Next, the reaction mixture was cooled to room temperature and filtered to remove undissolved NCS, OCS or BCS. The clear solution was dialyzed with distilled water for 3 days to remove excess succinic anhydride and DMF/DMSO. The powdered NSCS, OSCS or BCS were then obtained by lyophilization. The number average molecular weights (M_n) of chitosan derivatives were evaluated based on the theoretical molecular weight increase of the derivatives and the degree of substitution.

3.3.2 Characterization of pH sensitive amphiphilic chitosan derivatives

3.3.2.2 Proton nuclear magnetic resonance (^1H NMR)

The ^1H -NMR spectra of chitosan and its derivatives were measured on a Bruker AVANCE 500 spectrometer (Bruker, Switzerland) using $\text{D}_2\text{O}/\text{CD}_3\text{COOD}$ (99:1 v/v) solution and DMSO- d_6 , respectively, at 10 mg/mL polymer concentrations. All measurements were performed at 300 K, using the pulsed accumulation of 64 scans and an LB parameter of 0.30 Hz. Tetramethylsilane was used as an internal standard.

3.3.2.3 Attenuated total reflection Fourier Transform Infrared Spectroscopy (ATR-FTIR)

ATR-FTIR spectra were collected on a Nicolet 6700 spectrometer (Thermo Company, USA) using a single-bounce ATR-FTIR Smart Orbit accessory with a diamond internal reflection element (IRE) at ambient temperature (25°C). All spectra were taken from 400-4000 cm^{-1} . Typically, 32 scans at a resolution of 4 cm^{-1} were accumulated by using rapid-scan software in OMNIC 7.0 to obtain a single spectrum.

3.3.3 Characterization of polymeric micelles

3.3.3.1 Critical micelle concentration (CMC)

The CMC of graft copolymers in aqueous medium was determined using fluorescence spectroscopy with pyrene employed as a fluorescent probe. An aliquot (10 μL) of 1 mM pyrene solution in acetone was added to each vial of a series of aqueous polymer solutions (4 mL, $0.5\text{--}3.9\times 10^{-3}$ mg/mL). The final concentration of pyrene in each sample solution was 2.5×10^{-6} M. The mixtures were sonicated for 15 min, heated at 50°C for 2 h, and then kept in the dark at room temperature overnight to equilibrate. Fluorescence spectra were recorded at an excitation wavelength of 335 nm, and the emission spectra were monitored over a range of 350–500 nm. The change in the intensity ratio of the first and third vibration bands (I_1/I_3) at 373 nm (I_1) and 382 nm (I_3) in the emission spectra was used to investigate the shift in graft copolymer hydrophobic microdomains. The CMC was calculated after fitting the semi-log plot of the intensity ratio I_1/I_3 vs. the concentration.

3.3.3.2 *In vitro* cytotoxicity

The cytotoxicity of blank polymeric micelles was evaluated using an MTT cytotoxicity assay. The Caco-2 cells and HT-29 cells were cultured until 60–70% confluency in Dulbecco's modified Eagle's medium (DMEM) at pH 7.4 supplemented with 10% fetal bovine serum (FBS), 2 mM L-glutamine, 1% non-essential amino acid solution and 0.1% penicillin-streptomycin solution in a humidified atmosphere (5% CO_2 , 95% air, 37°C). The cells were seeded into each well of 96-well plates and preincubated for 24 h at a seeding density of 10,000 cells/well. Then, the cells were treated with blank polymeric micelles at various concentrations. After treatment, the solution was removed, fresh medium was added. Then, the mixture was incubated with MTT solution (final concentration 1 mg/mL) for 4 h at 37°C . The culture medium was removed, and the formazan crystals formed in the living cells were solubilized in 100 μL DMSO. Relative cell viability was calculated based on the absorbance at 550 nm using a microplate reader (Universal Microplate Analyzer, AOPUS01 and AI53601, Packard BioScience, CT, USA). The viability of non-treated control cells was arbitrarily defined as 100%.

3.3.4 Drugs-loaded polymeric micelles

3.3.4.1 Physical entrapment methods

3.3.4.1.1 Dialysis method

Overall, 5 mg of the amphiphilic copolymers (NSCS, OSCS and BSCS) and hydrophobic drugs (MX and curcumin) were dissolved in 2 mL of DMSO in a glass bottom container. Then, the mixture was stirred at room temperature until completely dissolved and transferred to dialysis bag (molecular weight cut-off, MWCO 6000-8000). The deionized water was replaced every 4 h for 24 h. The solution was centrifuged at 1000 rpm for 5 min. Then, the supernatant was filtered through a 0.45- μ m membrane filter and collected.

3.3.4.1.2 O/W emulsion method

The copolymers (NSCS, OSCS and BSCS) were prepared as for dialysis method. Then, drug was dissolved in DCM and was injected under constant stirring into 2 mL of blank polymeric micelles solution. Then, DCM was evaporated by overnight stirring at room temperature. The solution was centrifuged at 1000 rpm for 5 min. Then, the supernatant was filtered through a 0.45- μ m membrane filter and collected.

3.3.4.1.3 Dropping method

Five milligrams of copolymer and drugs were dissolved in 0.5 mL DMSO. The solution was slowly dropped into stirred water, and the mixed solution was stirred overnight. The final ratio of DMSO : water was 1:5. The mixture was then placed in a dialysis bag and dialyzed against deionized water overnight. The solution was centrifuged at 1000 rpm for 5 min. Then, the supernatant was filtered through a 0.45- μ m membrane filter and collected.

3.3.4.1.4 Evaporation method

Five milligrams of copolymer and drug were dissolved in DMF in a glass bottom container. The solution was mixed with acetone (1/3 of DMF) and stirred at room temperature under nitrogen gas flow until the solvent completely evaporated. Then, 3 mL of deionized water was added, and the solution was sonicated using a probe-type sonicator (CV 244, Sonics VibraCell™, Newtown,

CT, USA) in a cycle with a sonication time of 5 min and a standby time of 5 min for 20 min. The solution was centrifuged at 1000 rpm for 5 min. Then, the supernatant was filtered through a 0.45- μ m membrane filter and collected.

3.3.4.2 Entrapment efficiency

The drug-loaded polymeric micelles of each method were dissolved in a mixture solution of DMSO : H₂O (9:1). The amount of drug loaded into the polymeric micelles was determined using the high performance liquid chromatography (HPLC) (Agilent 1100 Series HPLC System, Agilent Technologies, USA) equipped with Eclipse XDB-C18 column (particle size 5 μ m, 15 cm \times 4.6 mm). The injection volume was 20 μ L. The mobile phase used for each drug was described in Table 3.1. The entrapment efficiency and loading capacity were calculated with the following Eqs. (1) and (2), respectively.

$$\text{Entrapment efficiency (\%)} = (C_1/C_2) \times 100 \quad (\text{Eq.1})$$

where C_1 is the amount of drug in polymeric micelles and C_2 is the initial of amount drug used for preparation

$$\text{Loading capacity } (\mu\text{g}/\text{mg}) = L_1/L_2 \quad (\text{Eq.2})$$

where L_1 is the amount of drug in micelles and L_2 is the amount of graft copolymer used for preparation.

Table 3.1 HPLC experimental conditions used to quantify drugs concentrations

Drug	Mobile phase	Flow rate (mL/min)	Wavelength (nm)
MX	Potassium dihydrogen phosphate (pH 4.4):methanol:acetonitrile (45:45:10, v/v/v)	1.0	365
Curcumin	Acetonitrile:1%v/v acetic acid (43:57, v/v)	1.0	428

3.3.4.3 Characterizations of drugs-loaded polymeric micelles

3.3.4.3.1 Particle size

The micelle samples were diluted with different pH medium (pH 1.2, 5.0, and 6.8) prior to use. The mean particle size and size distribution of the polymeric micelles with and without drugs were determined in triplicate at 25°C using the dynamic light scattering (DLS) (Malvern, Worcestershire, UK).

3.3.3.3.2 Morphology

Atomic force microscopy (AFM) was performed in order to investigate the morphology of the polymeric micelles with and without drugs. The samples in different pH medium (pH 1.2, 5.0 and 6.8) were prepared by dropping onto a mica surface, followed by air drying. Subsequently, the nanoparticles were imaged by scanning a 1 μm x 1 μm area in tapping mode using an NSG01 cantilever with 115–190 kHz resonance frequencies and a constant force ranging from 2.5–10 N/m. All images were recorded in air at room temperature at a scan speed of 1 Hz, and the phase and topology images were used to determine the morphology.

3.3.4.3.3 The stability of drug-loaded micelles

The stability of drug-loaded micelles was determined by gel permeation chromatography (GPC) as described previously (Opanasopit et al., 2004). GPC was carried out using an Agilent HPLC system (Agilent 1100 series, USA) equipped with a Shodex[®] GFC SB804 HQ column at 40°C. Drug-loaded polymeric micelles freshly prepared solutions (50 μL), were passed through a 0.45- μm membrane filter and then injected into the column and eluted with deionized water at a flow rate of 1 mL/min. Detection was performed by refractive index (RI) and UV detector.

3.3.4.4 *In vitro* releases study

3.3.4.4.1 MX-loaded polymeric micelles

The release of MX from MX-loaded polymeric micelles was determined by dialysis method. In detail, one milliliter of MX-loaded micelles was placed in a dialysis bag. Twenty milliliters of 0.1 N HCl (pH 1.2) were

used for medium for 2 h, then the pH of the medium was changed to 6.8 with trisodiumphosphate and 0.2 M NaOH for 6 h. The dialysis bag was immersed in the medium under constant stirring with sink conditions at $37 \pm 0.5^\circ\text{C}$. At the time intervals of 0.5, 1, 2, 4, 6 and 8 h, 1 ml aliquot of the medium was withdrawn, and the same volume of fresh medium was added. The sample solution was analyzed by HPLC. All experiments were done in triplicate.

3.3.4.4.2 CUR-loaded polymeric micelles

The release of CUR from CUR-loaded polymeric micelles was performed the same way as mentioned in the MX release, but the medium was supplemented for three different stages with 0.1 N HCl (pH 1.2) for 2 h, then the pH of the medium was changed to 6.8 with potassium dihydrogen phosphate (KH_2PO_4) and 5.0 M NaOH for 3 h and then pH was changed to 7.4 until for 8 h (Sajomsang et al., 2014). Curcumin-loaded micelles was transferred to a dialysis bag and immersed in the medium containing 30% (v/v) methanol and 1% (v/v) Tween 20 under constant stirring with sink conditions at $37 \pm 0.5^\circ\text{C}$. At the time intervals of 1, 2, 3, 4, 5, 6, 8 h, 1 ml aliquot of the medium was withdrawn, and the same volume of fresh medium is added. The sample solution was analyzed by HPLC. All experiments were done in triplicate.

3.3.4.5 *In vitro* intestinal permeation

Porcine duodenum tissues were sectioned and washed with phosphate-buffered saline (PBS, pH 7.4) to remove lumen contents. The *in vitro* permeation studies of MX through porcine small intestine were performed using Franz diffusion cells. Briefly, the intestinal tissues were mounted on Franz cells. MX-loaded polymeric micelles was added to the lumen surface in the donor compartment and sealed with Parafilm[®] immediately to prevent water evaporation, and the receptor compartment of the cell was filled with 6 mL of PBS (pH 7.4) and was kept at $37 \pm 0.5^\circ\text{C}$ by a circulating-water jacket under constant stirring. Samples of 0.8 mL were withdrawn periodically from the receptor chamber at time intervals of 0.5, 1, 2, 4, and 6 h and replaced with the same volume of PBS. The amount of drug was analyzed by HPLC. The cumulative amount of permeated drug was plotted against time, and the pseudo steady state flux was determined by linear regression.

3.3.4.6 Cytotoxic activity

Testing of the anticancer activity, CUR-loaded polymeric micelles and pure CUR were performed with MTT assay. HT-29 cells were cultured until 60–70% confluency with DMEM at pH 7.4, 10% FBS, 2 mM L-glutamine, 1% non-essential amino acid solution and 0.1% penicillin-streptomycin solution in a humidified atmosphere (5% CO₂, 95% air, 37°C). The HT-29 cells were seeded into each well of 96-well plates and preincubated for 24 h at a seeding density of 10,000 cells/well. After 24 h the cells were treated with fresh medium containing different concentrations of samples and incubated at 37°C and 5% CO₂ for 24 h. The cells were investigated using MTT test as mentioned in cytotoxicity evaluation.

3.3.5 Stability

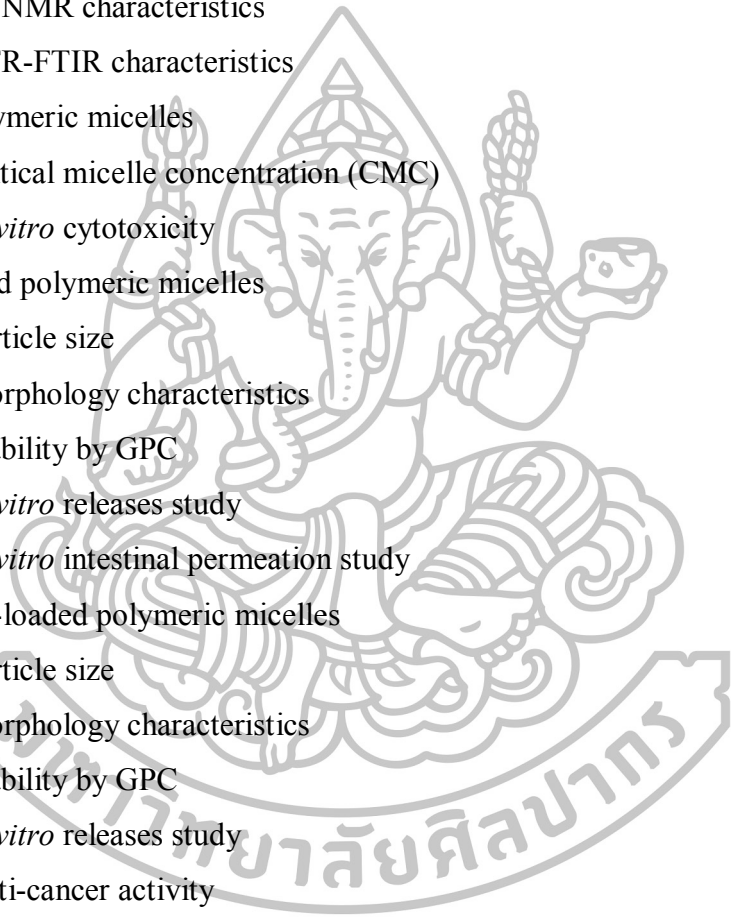
The stability of 20% initial CUR-loaded polymeric micelles after lyophilization process was evaluated according to ICH guideline for storage under accelerated condition (25°C ± 2°C and 60 ± 5%RH) comparing with long term condition in refrigerator (5°C ± 3°C) for 90 days. The amount of curcumin from CUR-loaded polymeric micelles was determined after keeping for 0, 30 and 90 days.

3.3.6 Statistical analysis

All experimental measurements were collected in triplicate. Data are expressed as mean ± standard deviation (SD). Statistical significance of differences was examined using one-way analysis of variance (ANOVA) (SPSS version 16.0 for Windows (SPSS Inc., USA)).

CHAPTER 4

RESULTS AND DISCUSSION

- 4.1 Synthesis and characterizations of pH sensitive amphiphilic chitosan derivatives
 - 4.1.1 ^1H NMR characteristics
 - 4.1.2 ATR-FTIR characteristics
 - 4.2 Blank polymeric micelles
 - 4.2.1 Critical micelle concentration (CMC)
 - 4.2.2 *In vitro* cytotoxicity
 - 4.3 MX-loaded polymeric micelles
 - 4.3.1 Particle size
 - 4.3.2 Morphology characteristics
 - 4.3.3 Stability by GPC
 - 4.3.4 *In vitro* releases study
 - 4.3.5 *In vitro* intestinal permeation study
 - 4.4 Curcumin-loaded polymeric micelles
 - 4.4.1 Particle size
 - 4.4.2 Morphology characteristics
 - 4.4.3 Stability by GPC
 - 4.4.4 *In vitro* releases study
 - 4.4.5 Anti-cancer activity
 - 4.4.6 Stability test
- 

4.1 Synthesis and characterizations of pH sensitive amphiphilic chitosan derivatives

The synthesis of the amphiphilic chitosan derivatives i.e. NSCS, OCS and BSCS, was carried out by reductive N-amination and N,O-succinylation (Sajomsang et al., 2014). as shown in Figure 4.1. Overall, the N-alkyl or N-aryl CSs were formed from the corresponding Schiff base intermediates before the reduction using sodium borohydride. The homogenous N,O-succinylation of NCS, OCS and BCS was carried out by using succinic anhydride in the mixture of solvents consisting of DMF and DMSO at 100°C. The successful synthesis of all amphiphilic CS derivatives was confirmed by ¹H NMR, ATR-FTIR and elemental analysis. The series of amphiphilic CS derivatives with different N-hydrophobic substituents were obtained as shown in Table 4.1. The degree of substitution (DS), defined as the number of N-hydrophobic groups, and the degree of N,O-succinylation (DSS), defined as the number of N,O-succinyl groups per hundred glucosamine units of CS, were determined by elemental analysis. The DS and DSS were calculated by comparing the C/N molar ratios obtained from the elemental analyses using Eqs. (3) and (4), respectively (Huo et al., 2012).

$$\text{DS of hydrophobic group (\%)} = \frac{(C/N)_{\text{ACS}} - (C/N)_{\text{CS}}}{X} \times 100 \quad (\text{Eq.3})$$

$$\text{DSS of succinylgroup (\%)} = \frac{(C/N)_{\text{sCS}} - (C/N)_{\text{ACS}}}{4} \times 100 \quad (\text{Eq.4})$$

where (C/N)_{ACS} represents the C/N ratio of amphiphilic CS derivatives, (C/N)_{CS} represents the C/N ratio of CS, (C/N)_{sCS} represents the C/N ratio of succinylated amphiphilic CS derivatives, and X represents the number of carbon atoms on the hydrophobic moieties of the CS backbone, which are 11, 8, and 7 for naphthyl, octyl, and benzyl substituents, respectively.

Both aliphatic and aromatic aldehydes at 2-fold molar ratios relative to the glucosamine (GlcN) residues of CS were used to study the DS. By varying the hydrophobic substituents on the CS backbone, the impact of the steric and electronic factors on this procedure could be elucidated. As shown in Table 4.1, the N-benzylation of CS by benzaldehyde had a higher DS than the N-naphthylation and

N-oxylation by 2-naphthaldehyde and octanaldehyde, respectively, at similar molar ratios of aldehyde to GlcN. The DS order of N-hydrophobically modified CS was N-benzyl (0.69) > N-naphthyl (0.52) > N-octyl (0.47). This indicated that octanaldehyde was less reactive than benzaldehyde and 2-naphthaldehyde. This could be attributed to the relative stability of the Schiff base intermediate and steric hindrance effect. In the case of benzaldehyde and 2-naphthaldehyde, the Schiff bases were stabilized by resonance with the aromatic ring, while the Schiff base of octanaldehyde with CS could not be stabilized by the resonance effect. Compared with 2-naphthaldehyde, benzaldehyde showed lower steric hindrance, leading to a higher DS. Moreover, the hydrophobic moieties (i.e., the naphthyl, octyl, and benzyl groups) effectively substituted onto the primary amino groups, while the succinyl groups were added to both the primary amino and hydroxyl groups on the CS backbone. The M_n of all CS derivatives could be calculated based on the increase of theoretical molecular weight of the derivatives due to the DS of the hydrophobic groups and the DSS of the succinyl groups. The M_n of CS was determined to be 7,633 g/mol (47 repeating units) by GPC. The DS values of NCS, OCS, and BCS were calculated to be 0.54 (approximately 25 repeating units), 0.47 (approximately 22 repeating units), and 0.69 (approximately 32 repeating units), while the DSS values were 0.52 (approximately 24 repeating units), 1.13 (approximately 53 repeating units), and 1.07 (approximately 50 repeating units), respectively (Table 4.1). According to the DS and DSS, the hydrophobic/hydrophilic ratios on the CS backbone were 1.04, 0.42, and 0.65 for NCS, OCS, and BCS, respectively.

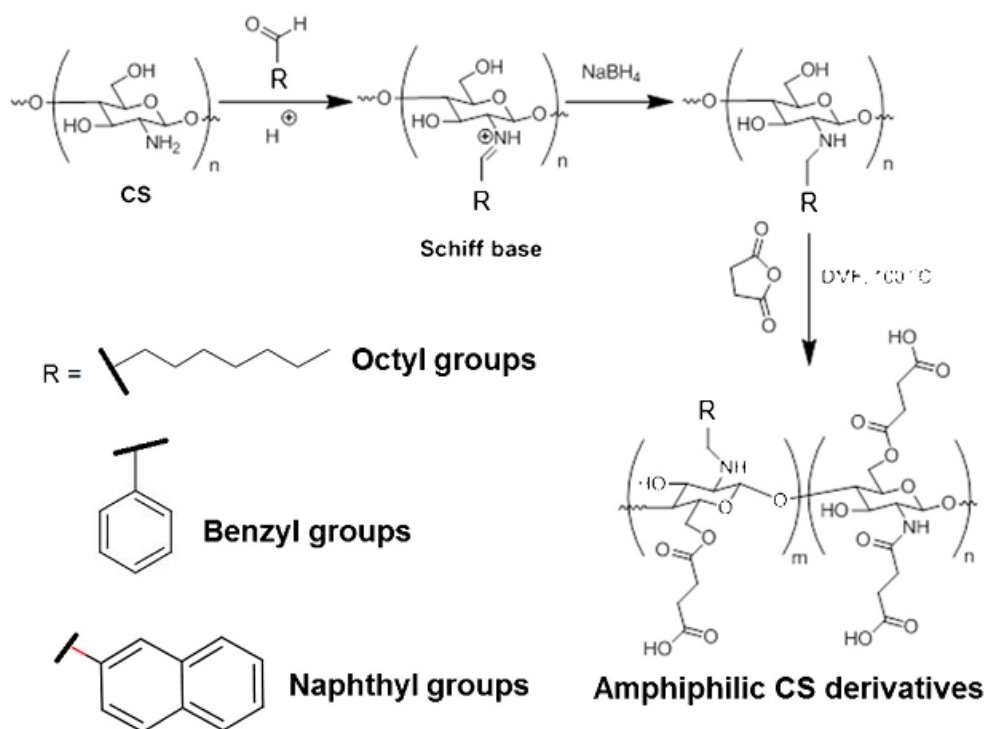


Figure 4.1 Synthesis scheme showing the formation of amphiphilic chitosan derivatives.

Table 4.1 Elemental analysis data for CS and its amphiphilic derivatives

Sample	%C	%H	%N	C/N	DS ^a	DS ^b	DSS ^c	M _n (g/mol)
CS	44.3	7.87	8.38	5.28	-	-	-	7633 ^d
NCS	66.79	11.29	5.97	11.18	0.52	0.54	-	10907 ^e
OCS	49.49	12.68	5.47	9.04	0.37	0.47	-	10046 ^e
BCS	65.48	11.76	6.45	10.15	0.65	0.69	-	10467 ^e
NSCS	54.97	10.41	4.14	13.27	-	0.54	0.52	13351 ^e
OSCS	49.17	11.28	3.61	13.59	-	0.47	1.13	15321 ^e
BSCS	56.89	9.97	3.93	14.44	-	0.69	1.07	15462 ^e

^a The degree of *N*-substitution (DS) determined by ¹H-NMR

^b The degree of *N*-substitution (DS) determined by elemental analysis

^c The degree of *N,O*-succinylation (DSS) determined by elemental analysis

^d Measured by GPC

^e Determined by elemental analysis

4.1.1 ¹H NMR characteristics

The ¹H-NMR spectrum of CS, NCS, OCS, BCS, NSCS, OSCS and BSCS are shown in Figure 4.2 and 4.3, respectively. In comparison with the ¹H NMR spectra of CS that contains no aromatic protons, the ¹H NMR NCS spectra and BCS exhibited broad multiple protons at δ ranging from 7.42 to 7.89 ppm and at δ 7.32 ppm due to the presence of the naphthyl and benzyl groups, respectively. The OCS showed the proton signals at δ 0.82 ppm and 1.21 ppm due to the methyl and methylene protons of long chain hydrocarbon (Figure 4.2). Moreover, the proton signal at δ 2.45 ppm in NSCS, OSCS and BSCS represented the methylene protons of the succinyl moiety on the CS backbone (Figure 4.3) (Lim et al., 2013; Sajomsang et al., 2014). Based on the ¹H-NMR spectra, the DS values of NCS, OCS, and BCS were calculated using Eqs. (5)–(7), respectively. The DS values were 0.52, 0.37, and 0.65 for NCS, OCS, and BCS, respectively.

$$DS = \left(\frac{I_{Nap}/7}{I_{H2-H6}/6} \right) \quad (\text{Eq.5})$$

where I_{Nap} represents the total area (integration) of the N-naphthyl protons, and I_{H2-H6} represents the peak area of protons C2–C6 on the CS backbone.

$$DS = \left(\frac{I_{Me}/3}{I_{H2-H6}/6} \right) \quad (\text{Eq.6})$$

where I_{Me} represents the total area (integration) of N-methyl protons of the octyl group, and I_{H2-H6} represents the peak area of protons C2–C6 on the CS backbone.

$$DS = \left(\frac{I_{Ar}/5}{I_{H2-H6}/6} \right) \quad (\text{Eq.7})$$

where I_{Ar} represents the total area (integration) of N-benzyl protons, and I_{H2-H6} represents the peak area of protons C2–C6 on the CS backbone.

It is important to note that DS value determined by ¹H-NMR method is less than elemental analysis method (Table 4.1), particularly in case of OCS. This difference was due to the limitation of solubility in ¹H-NMR solvent. Moreover, the methylene protons of the succinyl groups overlapped with the solvent, DMSO-d₆. Therefore, the DSS was determined using elemental analysis instead of ¹H-NMR spectroscopy.

These results from ATR-FTIR and $^1\text{H-NMR}$ spectra were discussed to indicate the successful introduction of both functionalities onto the CS backbone.

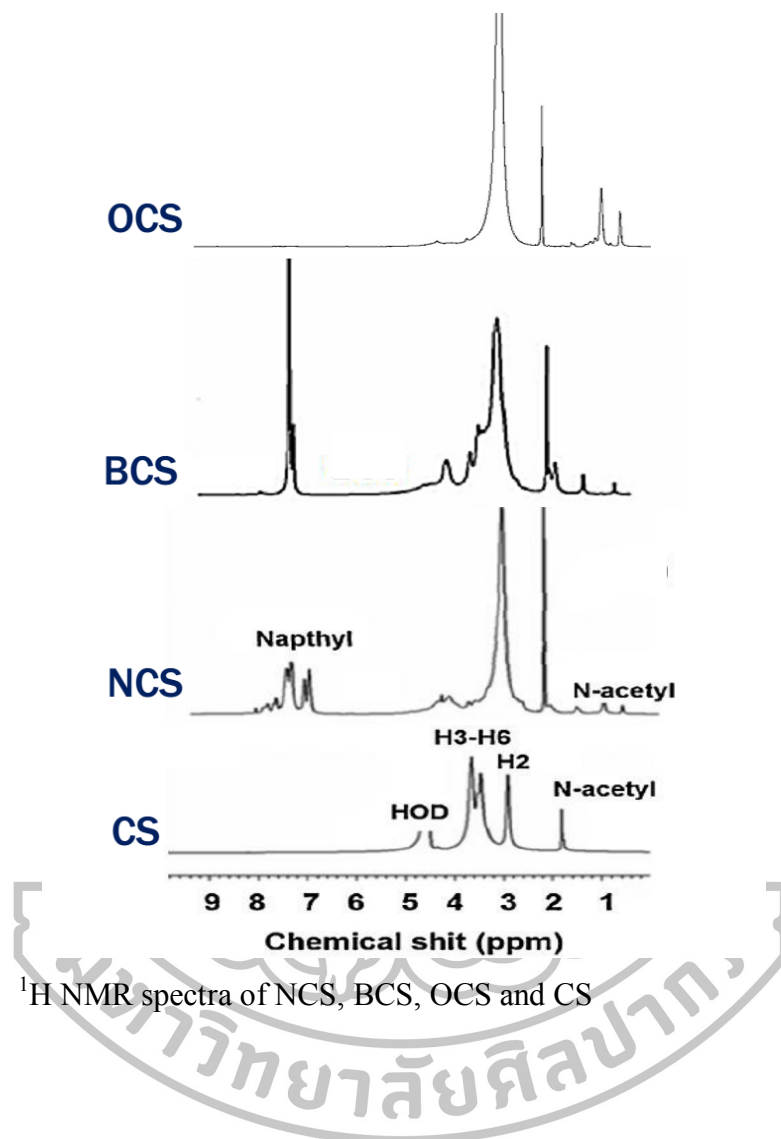


Figure 4.2 $^1\text{H-NMR}$ spectra of NCS, BCS, OCS and CS

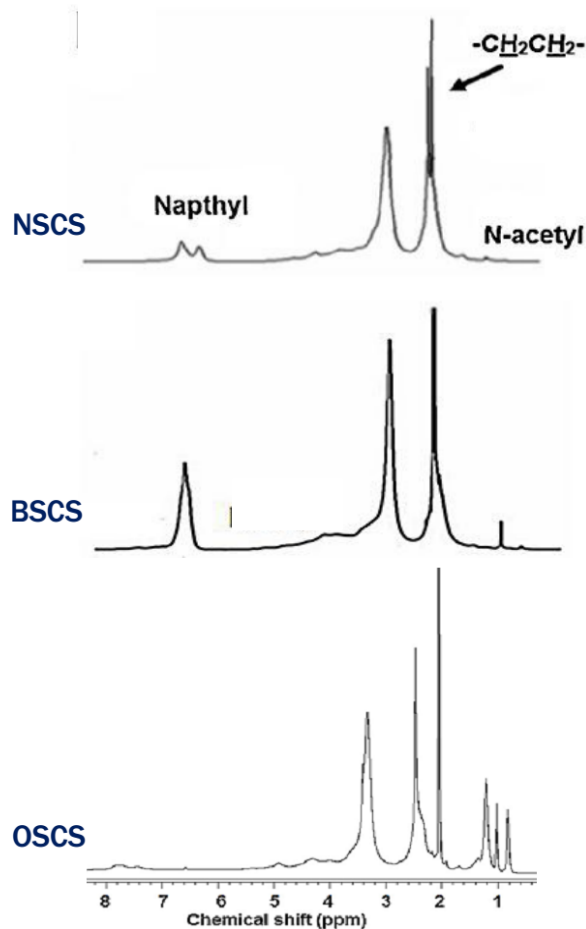


Figure 4.3 ^1H NMR spectra of NSCS, BSCS and OSCS

4.1.2 ATR-FTIR characteristics

The ATR-FTIR spectra of CS, NCS, OCS, BCS, NSCS, OSCS and BSCS are shown in Figure 4.4. The ATR-FTIR spectra of NCS, OCS and BCS were similar to that of CS and showed the additional absorption bands of functional groups (i.e., naphthyl, benzyl and octyl). The characteristic bands at 1632, 1490, 817 and 746 cm^{-1} (NCS spectrum) and at 1600, 1494, 743 and 695 cm^{-1} (BCS spectrum) were assigned to C=C stretching, C-H deformation (out of plane) for naphthyl and benzyl groups, respectively (Lim et al., 2013; Sajomsang et al., 2008) while the OCS spectrum had the strong absorption bands for C-H stretching of octyl groups at 2923 and 2856 cm^{-1} (Figure 4.4 (a)). After *N,O*-succinylation process, the NSCS, OSCS and BSCS spectra exhibited the characteristic bands for C=O stretching of the succinic acid moiety at 1704 cm^{-1} (NSCS spectrum), 1714 cm^{-1} (OSCS spectrum) and 1715 cm^{-1} (BSCS spectrum) (Figure 4.4 (b)).

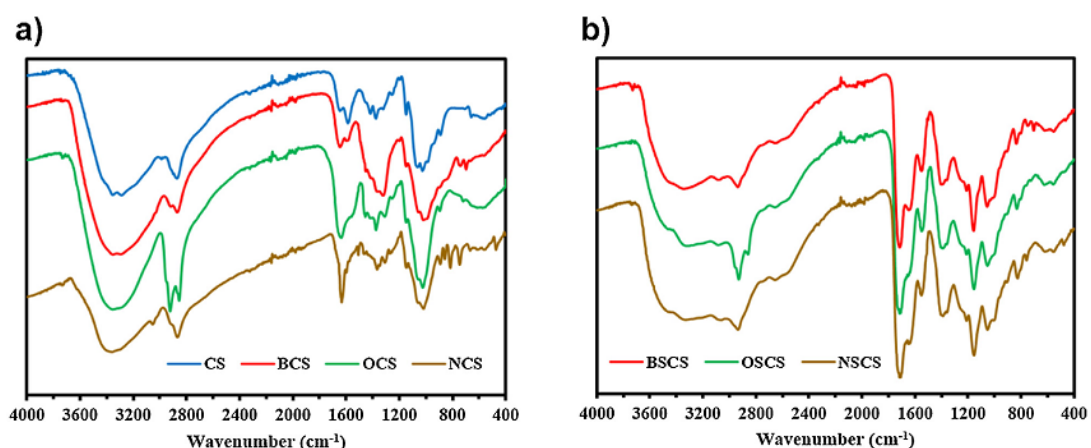


Figure 4.4 (a) ATR-FTIR spectra of CS, BCS, OCS and NCS; (b) BSCS, OSCS and NSCS

4.2 Blank polymeric micelles

4.2.1 Critical micelle concentration (CMC)

The fluorescence assay was conducted to determine the concentration of NSCS, OSCS and BSCS polymer for micellization at the first taken place. Briefly, the hydrophobic pyrene probe was added to aqueous polymer solutions of increasing concentration and pyrene fluorescence spectra were recorded for all solutions. The change in the intensity ratio of the first and third vibration bands (I_1/I_3) at 373 nm (I_1) and 382 nm (I_3) in the emission spectra was used to investigate the shift in graft copolymer hydrophobic microdomains. The plots of the intensity ratio I_1/I_3 versus the concentration of polymer solutions of NSCS, OSCS and BSCS are shown in Figure 4.5 and the CMC value was determined for each copolymer solution from the intersection of two straight lines. When the concentration reached the CMC, the I_1/I_3 ratio dramatically decreased. The CMC for NSCS, OSCS and BSCS was 0.0678, 0.0855 and 0.0575 mg/mL, respectively, and was lower than the CMC value of low molecular weight surfactants (Jiang et al., 2006). There is a covalent linkage in individual molecules within the hydrophobic core in polymeric micelles. This linkage prevents dynamic exchange of monomers between free solution and the micellar pseudo-phase which confers rigidity and stability to the polymeric micelles (Murthy, 2015).

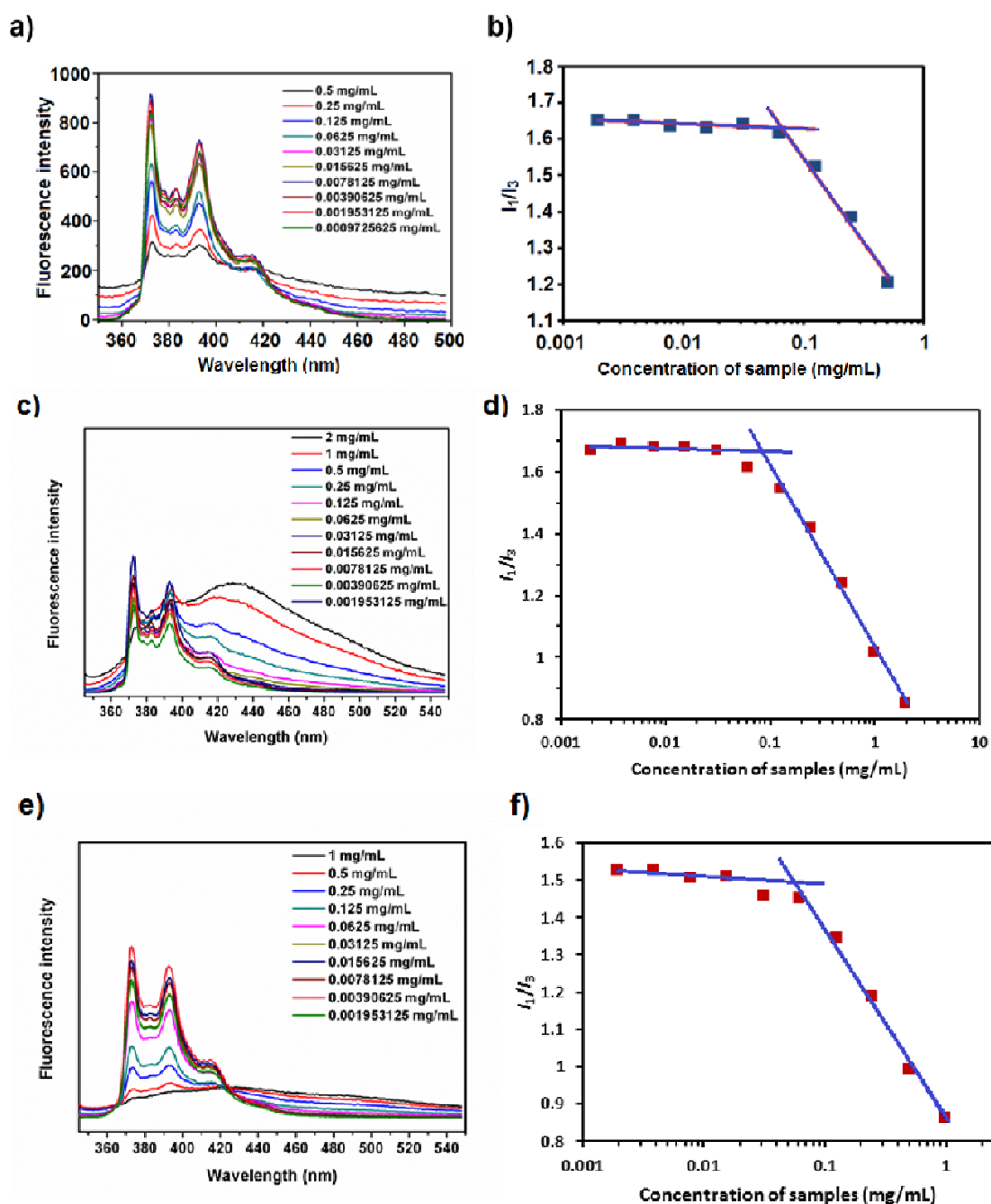


Figure 4.5 Fluorescence emission spectra of pyrene in water in the presence of NSCS (a), BSCS (c), and OSCS (e) polymeric micelles; a plot of the change in the intensity ratio (I_1/I_3) from excitation spectra of pyrene in water at various concentrations of NSCS (b), BSCS (d), and OSCS (f).

4.2.2 *In vitro* cytotoxicity

As a major requirement, the polymer used to prepare the polymeric micelles should be non-toxic. Although chitosan is generally considered as a biodegradable and safe polymer, some case studies identified the toxic effects of chitosan derivatives (Ngawhirunpat et al., 2009). The Caco-2 cells, represented functional similarities to intestinal epithelium, are commonly used *in vitro* model for studies cytotoxicity or prediction of intestinal drug absorption (Bu et al., 2016; Tu et al., 2016). HT-29 cells, originally derived from a human colon cancer, were selected as model for the study of colon cancer. Thus, the cytotoxicity of blank NSCS, OSCS and BSCS micelles was determined using MTT assay, which is based on the reduction of MTT by the mitochondrial dehydrogenase of intact cells to a purple formazan product (Calvello et al., 2016), performed with Caco-2 cells and HT-29 cells. The viability of Caco-2 cells treated with the various concentrations of all blank polymeric micelles is shown in Figure 4.6. The half maximal inhibitory concentration (IC_{50}) value of the NSCS, OSCS and BSCS polymeric micelles for Caco-2 cells was 3.08 ± 0.15 , 2.95 ± 0.06 and 3.23 ± 0.08 mg/mL, respectively. No significant differences in the cytotoxicity were observed among the polymeric micelles in the Caco-2 cells. In a previous research, Chae et al. (2005) described low molecular weight chitosan (3.8–13 kDa; DDA 87–92%) at concentrations lower than 5 mg/mL revealed cell viability of Caco-2 cell > 80% after treating sample for 2 h. These results showed that all self-assembled polymeric micelles had low cytotoxicity in Caco-2 cells, indicating the excellent biocompatibility of the constituent polymers. As shown in Figure 4.7, blank NSCS, OSCS and BSCS micelles showed minimal cytotoxicity under concentration up to 0.5 mg/mL. The result indicated that blank micelles may be regarded as a safe drug carrier.

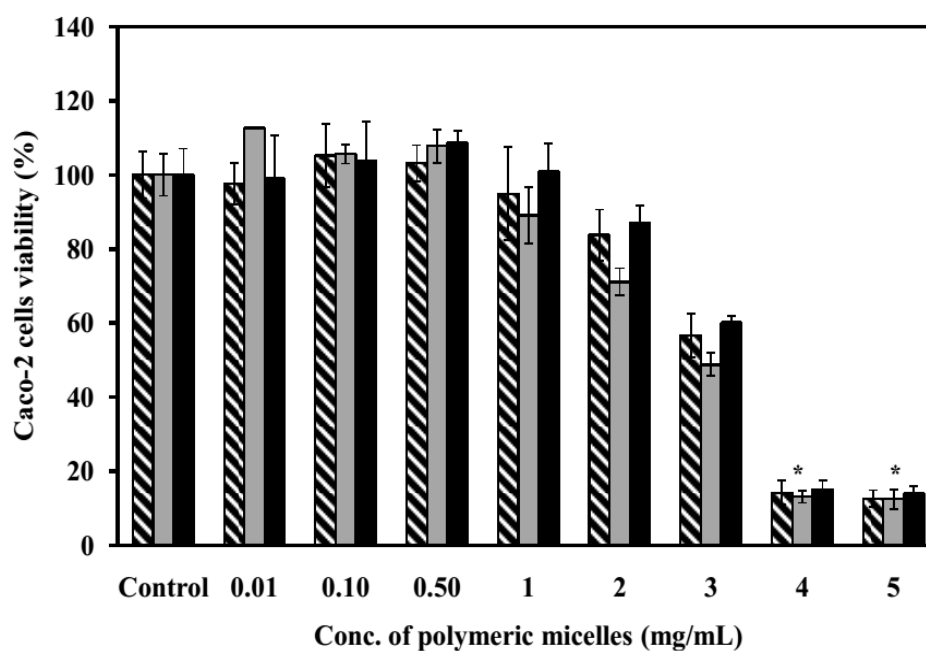


Figure 4.6 The percent cell viability in Caco-2 cells at varying concentrations of polymeric micelles; (▨) NSCS, (■) OSCS, (■) BSCS. Each value represents the mean \pm SD of five wells. * Statistically significant ($p < 0.05$).

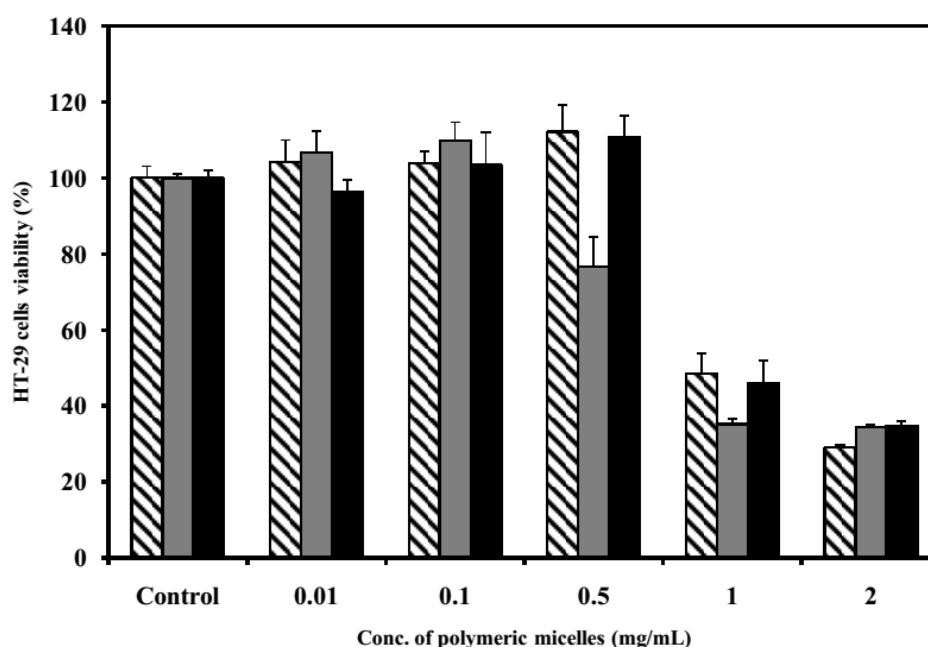


Figure 4.7 The present cell viability in HT-29 cells at varying concentrations of polymeric micelles; (▨) NSCS, (■) OSCS, (■) BSCS. Each value represents the mean \pm SD of five wells.

4.3 MX-loaded polymeric micelles

The physical entrapment method which is the simplest and most convenient has been employed to encapsulate MX model drug into NSCS polymeric micelles. Polymeric micelle formation and drug incorporation into the micelles were expected to occur simultaneously. The drug loading efficiency and capacity of polymeric micelles depend on the hydrophobic interactions between hydrophobic polymer blocks and drugs, the miscibility between polymers and drugs, and also influence of preparation methods (Miller et al., 2013; Murthy, 2015). Thus, the effect of physical entrapment methods (dialysis, O/W emulsion, dropping, evaporation) and weight ratio of drugs to polymer (5-40% to polymer) of MX-loaded NSCS polymeric micelles on entrapment efficiency (EE) and loading capacity (LC) was studied and the results are shown in Figure 4.8. The x-axis represents the initial amount of drug used in the preparation (ranging from 5% to 40%), and the y-axis represents the percentage of MX incorporated into the polymeric micelles (% MX-loaded) (Figure 4.8 (a)) and the polymeric micelles loading capacity (Figure 4.8 (b)). The results of MX-loaded NSCS polymeric micelles by evaporation method had a great effect on the EE and LC (Klaikherd et al., 2009; Yang et al., 2012; Zhang, C.Y. et al., 2012). The MX-loaded NSCS micelles showed the highest entrapment efficiency (22–52%) and loading capacity (25–75 $\mu\text{g}/\text{mg}$). The loading capacity increased from 25 to 75 $\mu\text{g}/\text{mg}$ with an increase in the initial MX loading from 5% to 40%. The result revealed that the self-aggregated micelles could improve drug solubility with high incorporation efficiency. This enhancement of drug solubility in water is derived from hydrophobic interaction between drugs and hydrophobic copolymer. Thus, the hydrophobic interactions among the hydrophobic of N-naphthyl chain, MX, and solvent may be an important key to control this incorporation process. This result was similar to the previous studies reporting that the entrapment efficiency of stearyl gemcitabine-loaded poly(ethylene glycol)–poly(d,l lactide) (PEG–PLA) polymeric micelles and dexamethasone-loaded PEGylated poly-4-(vinylpyridine) polymeric micelles were also dependent on the entrapment methods (Daman et al., 2014; Miller et al., 2013). The co-solvent evaporation method had a higher drug loading percentage than direct dialysis, O/W emulsion and the dropping method; therefore, the entrapment method affected the drug-loading efficiency.

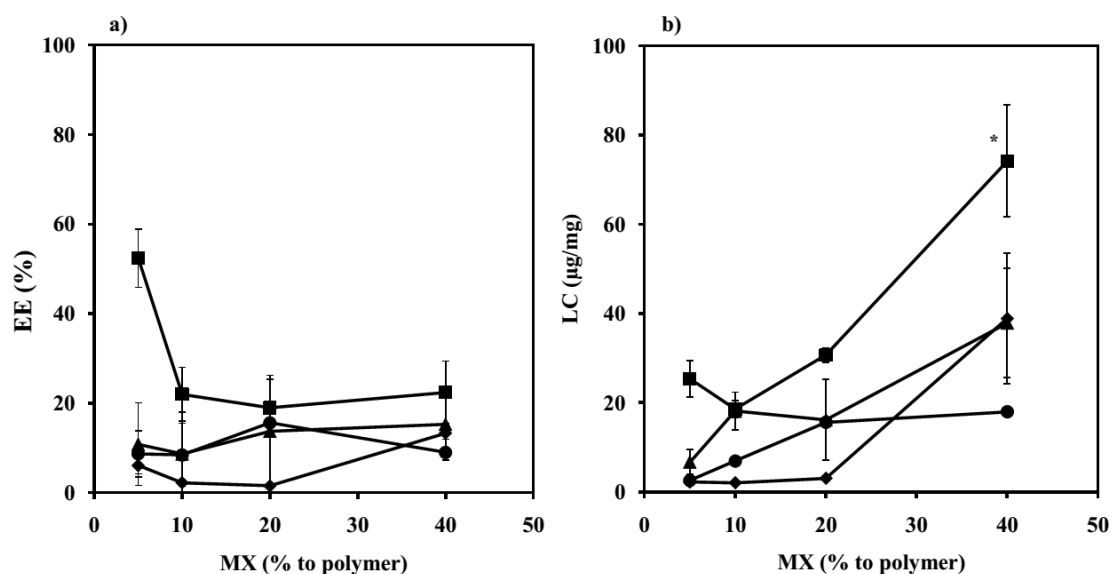


Figure 4.8 Effect of entrapment method and initial drug concentration (5–40% to polymer) on (a) the entrapment efficiency, (b) loading capacity of MX-loaded NSCS micelles (◆) dialysis method; (●) dropping method; (■) evaporation method; (▲) emulsion method. Data are plotted as the mean \pm S.D. of three measurements.

After the different physical entrapment methods were studied for the effect on the entrapment efficiency and loading capacity, the evaporation method which gave the highest entrapment efficiency of MX was selected to study the effect of the hydrophobic moieties (naphthyl, octyl and benzyl) and weight ratios of drug to polymer on entrapment efficiency. Figure 4.9 shows the EE and LC of MX-loaded PMs with different grafted hydrophobic moieties. The MX-loaded OSCS PMs showed the highest entrapment efficiency (33–46%) and loading capacity (22–158 µg/mg) values, followed by NSCS (EE 22–52%; LC 18–74 µg/mg) and BSCS (EE 11–32%; LC 11–40 µg/mg), respectively. The results revealed that the optimum MX-loading ratio were 40%. These results suggested the presence of hydrophobic interactions between the loaded drugs and the hydrophobic moieties of the PMs (Ding et al., 2014; Xiangyang et al., 2007). Interestingly, the alkyl groups (octyl) on the chitosan backbone had stronger interaction with the hydrophobic domain of the drugs than the aryl groups (naphthyl and benzyl). These results were in agreement with the previously investigated incorporation behaviors of camptothecin by varying degree of

hydrophobicity and rigidity of the micelle inner core. The results indicated that not only hydrophobicity but also other factors (hydrogen bonding and steric factor) influenced the incorporation behaviors (Yamamoto et al., 2007). Thus, the chemical structure of hydrophobic moieties in the inner core of the PMs was a key factor in controlling the loading efficiency.

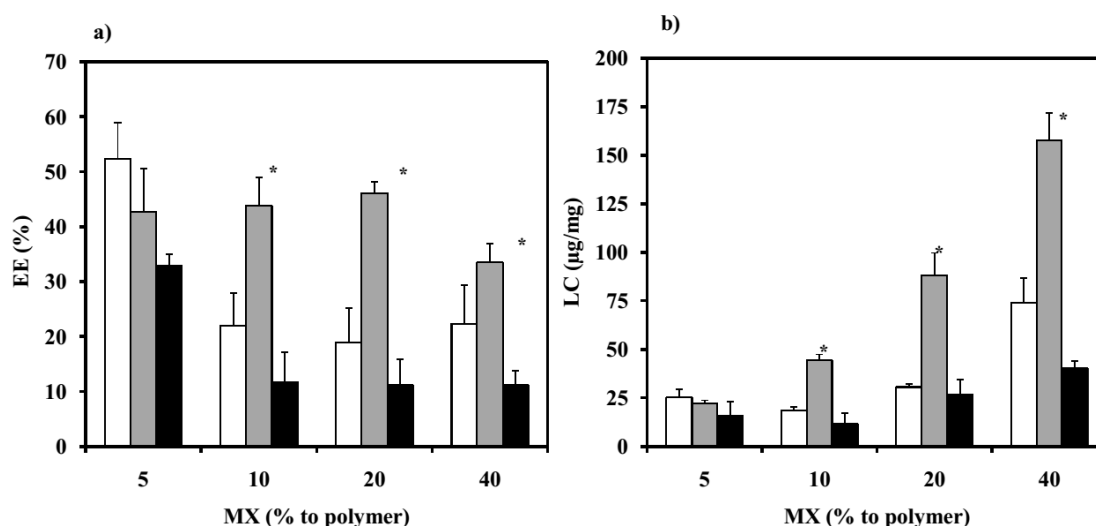


Figure 4.9 Effect of hydrophobic moieties and initial drug loading (5-40% to polymer) on (a) the entrapment efficiency, (b) loading capacity of MX-loaded polymeric micelles; (□) MX-loaded NSCS, (■) MX-loaded OSCS, (■) MX-loaded BSCS. Data are plotted as the mean \pm SD of three measurements. * Statistically significant ($p < 0.05$).

4.3.1 Particle size

The mean particle sizes and PDI of NSCS micelles with and without MX prepared using multiple methods (dialysis, dropping, O/W emulsion and evaporation) were studied. After the preparation, the particle sizes of NSCS micelles with and without MX of solutions were measured by the DLS method and the results are listed in Table 4.2. The particle sizes of blank polymeric micelles ranged from 84 to 233 nm. The different entrapment methods influenced the particle size of the micelles. The blank micelles prepared via the dropping method had the smallest mean particle sizes (84.31 nm), followed those prepared by dialysis (196.20 nm) and evaporation (233.50), respectively. The type of solvents was also an important factor affecting the micelle particle size. After the incorporation of MX into NSCS, OSCS and BSCS polymeric

micelles, the particle sizes became larger, compared to the blank micelles (Table 4.2 and Table 4.3). The particle sizes of the MX-loaded micelles had a tendency to increase with an increase in the weight ratio of MX to polymer (Kumar et al., 2012). The larger particle size of the MX loaded into the polymeric micelles might be due to the increase of MX in the micelles and the aggregation of the micelles (Ngawhirunpat et al., 2009).

Table 4.2 The particle sizes and PDI of NSCS micelles with and without MX. Each value represents the mean \pm SD from three independent measurements.

MX to polymer	Dialysis		Dropping		O/W emulsion		Evaporation	
	Particle size	PDI	Particle size	PDI	Particle size	PDI	Particle size	PDI
0	196.20 \pm 1.51	0.061	84.31 \pm 0.88	0.198	-	-	233.50 \pm 7.07	0.384
5	275.03 \pm 6.12	0.169	108.77 \pm 4.03	0.217	192.93 \pm 0.85	0.070	291.77 \pm 6.35	0.383
10	266.17 \pm 6.91	0.223	113.87 \pm 1.32	0.156	192.13 \pm 2.54	0.100	382.17 \pm 12.02	0.523
20	311.80 \pm 11.39	0.215	127.07 \pm 0.29	0.153	192.13 \pm 2.54	0.076	312.17 \pm 12.00	0.381
40	310.30 \pm 0.78	0.166	142.73 \pm 0.57	0.174	195.37 \pm 2.17	0.120	293.80 \pm 6.84	0.310

Table 4.3 The particle sizes and polydispersity index (PDI) of polymeric micelles with and without MX. Each value represents the mean \pm SD of three independent measurements.

MX to polymer (%)	NSCS		OSCS		BSCS	
	Particle size (nm)	PDI	Particle size (nm)	PDI	Particle size (nm)	PDI
0	233.50 \pm 7.07	0.384	213.13 \pm 8.13	0.309	226.63 \pm 9.57	0.304
5	291.77 \pm 6.35	0.383	257.50 \pm 3.41	0.318	246.67 \pm 4.52	0.312
10	382.17 \pm 12.02	0.523	275.03 \pm 6.12	0.299	269.67 \pm 4.58	0.279
20	312.17 \pm 12.00	0.381	331.30 \pm 3.68	0.331	337.77 \pm 16.13	0.349
40	293.80 \pm 6.84	0.310	309.83 \pm 4.14	0.320	312.63 \pm 11.75	0.386

4.3.2 Morphology characteristics

The morphologies of the self-assembled PMs in different pH medium (pH 1.2, 5.0 and 6.8) were characterized by AFM, and are shown in Figure 4.10.

Moreover, the particle sizes of micelles with and without MX in different pH were investigated using DLS to gain an insight in understanding the function of pH sensitive PMs and the results are shown in Table 4.4. When the self-assemblies were performed at pH 1.2, which is lower than the pK_{a1} (4.21 at 25°C) of succinic acid, the AFM images of micelles before and after MX loading revealed aggregates with the particle sizes ranging from 850.80 ± 99.35 to 7000.00 ± 680.24 nm due to unionized carboxyl groups of the succinic acid and effect of intermolecular hydrogen bond between hydroxyl in the outer shell. The AFM images of all PMs at pH 5.0 exhibited the formation of spherical PMs, and the particle sizes decreased in the range of 240.50 ± 3.12 to 451.53 ± 5.41 nm as a result of partial ionization of succinic acid on the micelle surface (Figure 4.10). At pH 6.8, the particle sizes of the micelles were in the range from 455.33 ± 26.22 to 575.20 ± 10.70 nm may be due to dissociation and swelling from the effect of deprotonation, while AFM images indicated that the micelles had a spherical morphology and dissociate partially of copolymers.

Table 4.4 The particle sizes and polydispersity index (PDI) of polymeric micelles with 20% MX to polymer and without MX by the evaporation method. Each value represents the mean \pm SD from three independent measurements.

Formulations	pH 1.2		pH 5.0		pH 6.8	
	Particle size (nm)	PDI	Particle size (nm)	PDI	Particle size (nm)	PDI
Blank NSCS	3622.00 \pm 315.23	0.990	433.43 \pm 38.42	0.495	551.63 \pm 7.09	0.482
Blank OSCS	850.80 \pm 99.35	0.172	240.50 \pm 3.12	0.243	466.67 \pm 22.16	0.480
Blank BSCS	1595.00 \pm 70.15	0.351	250.83 \pm 1.97	0.242	457.77 \pm 1.36	0.196
MX-loaded NSCS	7000.00 \pm 680.24	0.594	352.13 \pm 30.37	0.448	506.13 \pm 20.87	0.377
MX-loaded OSCS	1071.00 \pm 13.23	0.295	451.53 \pm 5.41	0.336	455.33 \pm 26.22	0.334
MX-loaded BSCS	880.20 \pm 81.30	0.259	315.03 \pm 2.61	0.274	575.20 \pm 10.70	0.317

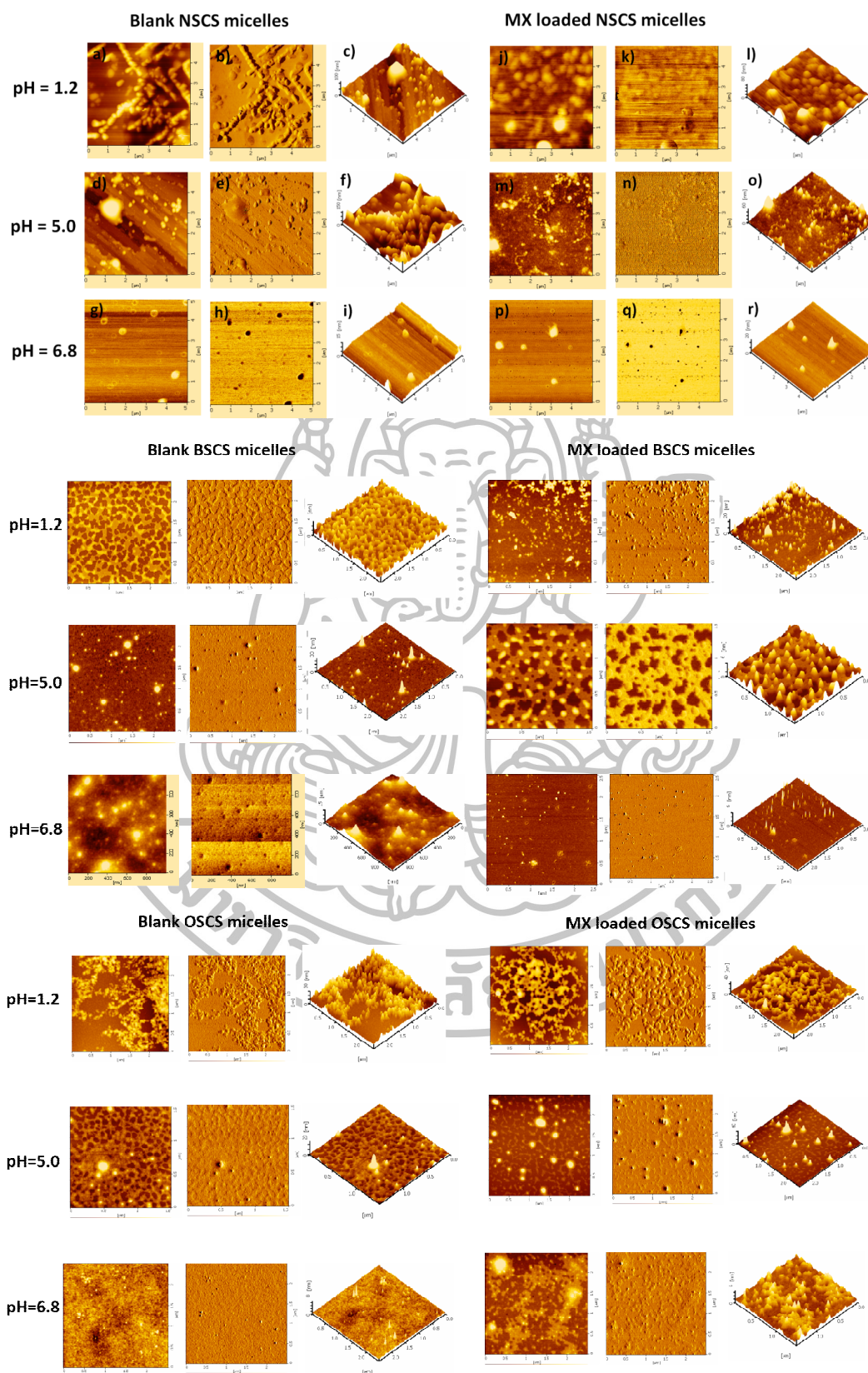


Figure 4.10 AFM images of NSCS, BSCS and OSCS micelles, and MX-loaded NSCS, BSCS and OSCS micelles at different pH.

4.3.3 Stability by GPC

The stability of all PMs with MX at various concentrations was characterized by GPC. It was observed from micelles formation that the peaks of micelle detected by RI detector (for polymer) showed the same retention time as detected by UV absorption at 365 nm (for MX). Therefore, the peak area of peak detected by UV absorption at 365 nm representing the amount of MX-loaded PMs was used to study stability of PMs. The ratios of the peak area of PMs/MX concentration; [MX], are shown in Figure 4.11. The smallest of peak area/[MX] explained that the most of MX was adsorbed to the GPC column by hydrophobic interactions due to the unstable packaging of MX in the PMs. Thus, If the ratio of peak area/drug concentration is large, represents to more stable incorporation of drug in the micelles (Opanasopit et al., 2007). The PMs formed from OSCS with initial MX contents of 5% showed the highest MX-loaded PMs stability, the result revealed that the values of peak area/[MX] were higher than those formed from NSCS and BSCS. Moreover, the values of the peak area/[MX] of all MX-loaded PMs decreased with the increasing initial MX to polymer, indicating that drug content in process of drug incorporation affected the formation of stable MX-loaded PMs.

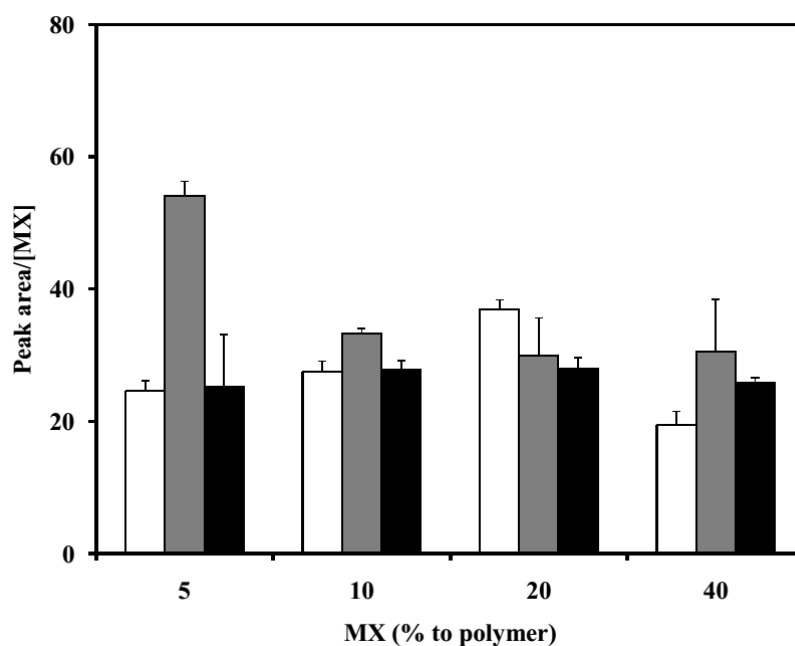


Figure 4.11 Polymeric micelles stability by ratio of peak area/[MX]; (□) MX-loaded NSCS, (■) MX-loaded OSCS, (■) MX-loaded BSCS. Data are plotted as the mean \pm SD of three measurements.

4.3.4 *In vitro* releases study

In vitro MX release studies were carried out on MX-loaded pH-sensitive PMs and MX free drug. A 40% initial MX concentration in the MX-loaded PMs with different grafted copolymers was selected due to high entrapment. As shown in Figure 4.12, the release studies were conducted for 8 h to mimic the conditions of the GI tract. A 0.1 N HCl (pH 1.2) medium was selected as the release medium to simulate the gastric fluid (SGF) medium of the stomach for the initial 2 h. Afterward, the pH was adjusted to 6.8 to simulate the intestinal fluid (SIF) medium of the small intestine. In the SGF medium between 0 and 2 h, the amount of drug released from the MX-loaded OSCS PMs was less than 10%, which was slightly lower than those of the MX-loaded PMs prepared from NSCS and BSCS and the MX free drug suspension (approximately 20%). However, the amount of drug released from all MX-loaded PMs was not statistically significant different from MX free drug ($p > 0.05$). In comparison, the amount of drug release decreased as follows: MX loaded BSCS PMs > MX-loaded NSCS PMs > MX-loaded OSCS PMs. Not only hydrophobicity but also other factors (i.e., mobility/rigidity, hydrogen bonding, steric factor, π - π interaction) of the core restricts water penetration influence the drug release from the different inner core structures (Yamamoto et al., 2007; Yokoyama, 2014). This indicated that the pH-sensitive PMs prepared from OSCS could retain MX within the inner core of the PMs or protect MX better than the PMs prepared from NSCS and BSCS under strong acidic condition. It is important to note that the lower MX release in the SGF medium might be due to the poor solubility of MX at acidic pH. This result was in accordance with a previous study revealing that less than 20% of the loaded MX in MX tablets was released in SGF due to its poor solubility at acidic pH. When the pH was increased to 6.8, the MX release dramatically increased (Samprasit et al., 2015). This is attributed to the two dissociation constants (pK_a) of MX, 1.09 and 4.18. The isoelectric point (pI) of MX, which was computed from $(pK_{a1} + pK_{a2})/2$, was 2.63. Therefore, for pH above 2.63, the solubility and ionization levels increase (Luger et al., 1996). When the pH was increased to 6.8, the MX release from MX free drug dramatically increased due to its greater solubility and ionization. However, the release of MX from the MX-loaded PMs in SIF (approximately 100%) was higher than that in SGF and that from the free drug (approximately 60%). These results can be described as follows,

the pendant carboxyl groups in the succinic acid moiety of the self-assembled PMs were protonated at low pH, resulting in a tight and compact structure. The hydrophobic interactions between the alkyl moieties (octyl) in the chain and aryl groups of MX increased as the acidity increased. These also resulted in a decreased MX release rate from MX-loaded OSCS PMs (Bissantz, Kuhn, and Stahl, 2010). These results may be attributed to three factors. First, the ionization of the succinic acid moiety with a pH above the pK_a of succinic acid induces the swelling and dissociation of PMs. Second, the electrostatic repulsion force increases between the succinic segments and succinic segment drug. Third, MX is an acidic drug that exhibits high solubility in alkali medium (Altememy, D.R. and Altememy, J.J., 2014; Samprasit et al., 2013). Moreover, each individual MX molecule was bound to a functional site of the PMs, reducing the crystal lattice energy. The state of MX in the PMs changed from crystalline to amorphous which might enhance the rate of MX release. These also resulted in higher MX release from all MX-loaded micelles than that from the free drug. Therefore, the self-assembled PMs based on pH responsive CS completely released MX within the 8 h period. Moreover, no significant differences were observed in the release profiles in SIF among the different PMs. Our results have led us to the assumption that the MX-loaded OSCS PMs were the most suitable formulation for improving the bioavailability of MX.

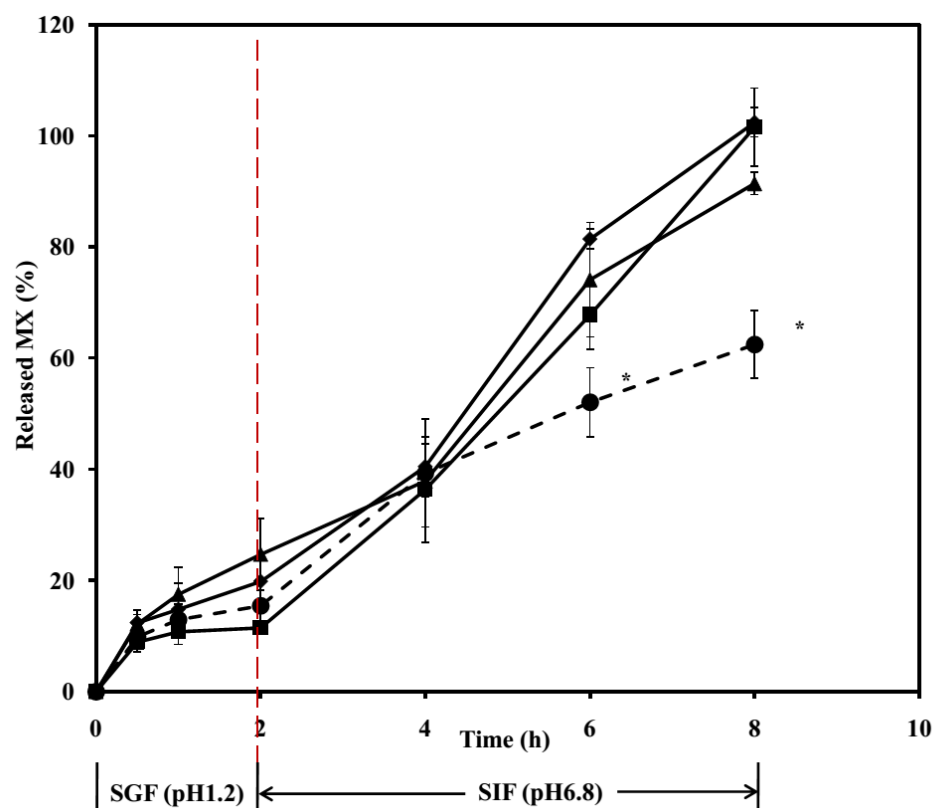


Figure 4.12 MX release profiles from the (◆) MX-loaded NSCS; (■) MX-loaded OSCS; (▲) MX-loaded BSCS; and (●) MX suspension in 0.1 N HCl, pH 1.2 (0-2 h), then in PBS pH 6.8 (2-8 h). Data are plotted as the mean \pm SD of three measurements. * Statistically significant ($p < 0.05$).

4.3.5 *In vitro* intestinal permeation study

The permeation profiles and the flux of all MX-loaded PMs and MX suspensions are illustrated in Figure 4.13. The steady-state flux across porcine intestine was used to determine the effect of MX permeation between different MX-loaded micelles and free MX. The results indicated no significant differences in the intestinal permeation of MX from MX-loaded PMs (OSCS, NSCS and BSCS) and MX free drug. MX is classified in the Biopharmaceutics Classification System (BCS) as a class II chemical with high permeability and low solubility (Ahad et al., 2014). Because of the high permeability of MX, we could not observe the differences in intestinal permeation of MX from MX-loaded PMs and MX free drug. This result

suggested that the pH-sensitive polymeric micelles from chitosan-based could be used as an oral carrier for protection the gastric environment and improving the solubility.

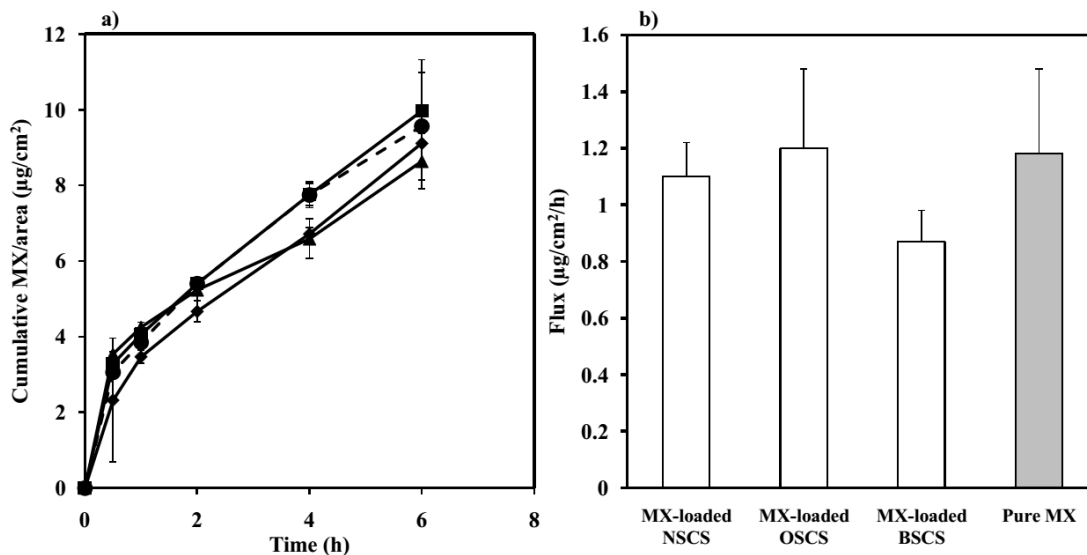


Figure 4.13 (a) The permeation profiles of (◆) MX-loaded NSCS; (■) MX-loaded OSCS; (▲) MX-loaded BSCS; and (●) MX suspension. (b) The fluxes of MX through porcine small intestinal for NSCS, OSCS and BSCS micelles (white bar graph); MX suspension (shaded bar graph). Data are plotted as the mean \pm SD of three measurements.

4.4 Curcumin-loaded polymeric micelles

Figure 4.14 shows EE and LC of CUR-loaded into NSCS PMs by physical entrapment methods (dialysis, O/W emulsion, dropping and evaporation). The x-axis represents the initial amount of CUR used in the preparation (ranging from 5% to 40%), and the y-axis represents the percentage of CUR incorporated into the polymeric micelles (% CUR-loaded) (Figure 4.14 (a)) and the polymeric micelles loading capacity (Figure 4.14 (b)). It can be seen that the physical methods and weight ratios of drugs to polymer (5-40% to polymer) had an influence on the EE and LC. The CUR-loaded NSCS by dialysis method showed the highest EE (24-30%) and LC (14-105 µg/mg), followed by evaporation (EE 16-25%; LC 12-67 µg/mg), dropping (EE 2-24%; LC 16-49 µg/mg and O/W emulsion (EE 3-20%; LC 20-29 µg/mg). It was found that various factors in drug incorporation process are important key factor in controlling incorporation efficiency (Miller et al., 2013). An increasing initial amount

of CUR in each method that had tendency to decrease EE (Yang et al., 2012). At the same initial CUR to polymer, the dialysis method had a higher drug loading percentage than co-solvent evaporation, O/W emulsion and the dropping method; therefore, it was selected for the subsequent studies to prepare CUR-loaded OSCS and CUR-loaded BSCS.

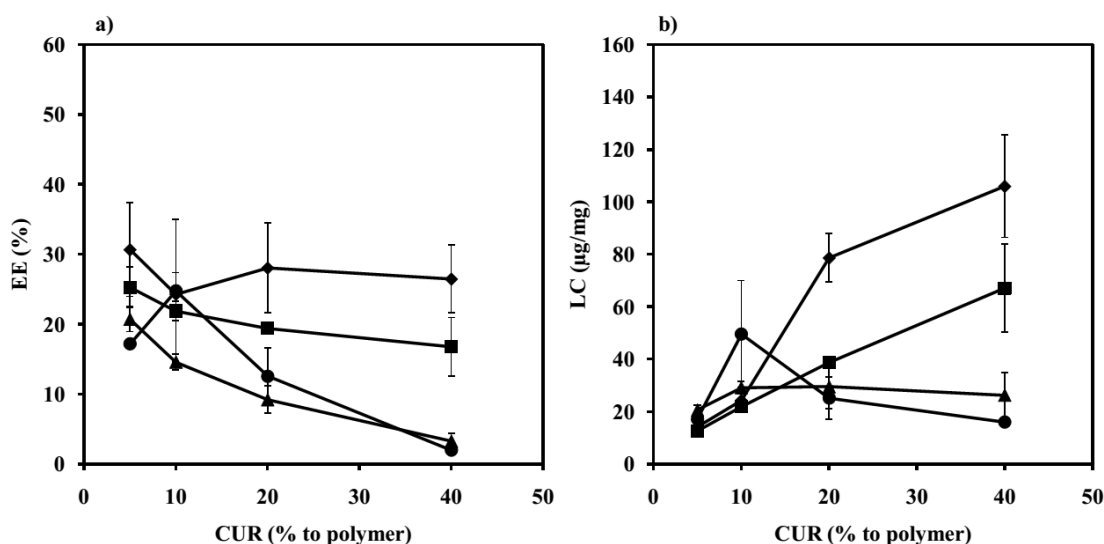


Figure 4.14 Effect of entrapment method and initial drug concentration (5–40% to polymer) on (a) the entrapment efficiency, (b) loading capacity of MX-loaded NSCS micelles (◆) dialysis method; (●) dropping method; (■) evaporation method; (▲) emulsion method. Data are plotted as the mean \pm S.D. of three measurements.

The EE and LC values of CUR-loaded into NSCS, OSCS and BSCS, which were prepared by dialysis method, are illustrated in Figure 4.15. The results revealed that curcumin-loaded PMs with different grafted hydrophobic moieties at the same weight ratio drug to polymer showed no significantly different EE of curcumin in self-assembly micelles which comprised of various hydrophobic moieties. This was probably due to the hydrophobic interactions strength between hydrophobic moieties of copolymers and CUR and the miscibility between copolymers and drugs (Murthy, 2015; Qiu et al., 2014).

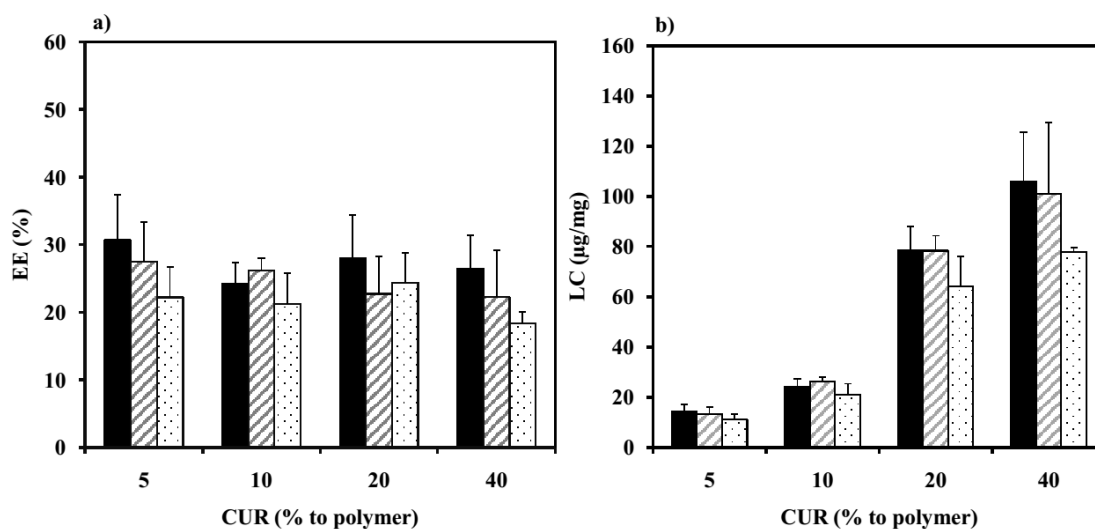


Figure 4.15 Effect of hydrophobic moieties and initial drug loading (5-40% to polymer) on (a) the entrapment efficiency, (b) loading capacity of MX-loaded polymeric micelles; (■) MX-loaded NSCS, (▨) MX-loaded OSCS, (▤) MX-loaded BSCS. Data are plotted as the mean \pm SD of three measurements. * Statistically significant ($p < 0.05$).

4.4.1 Particle size

The results of particle sizes and PDI of CUR-loaded NSCS PMs and blank NSCS PMs by physical entrapment methods are shown in Table 4.5. As described in section 4.3.1, the different physical methods influenced the particle size of the PMs. The mean particle size of CUR-loaded NSCS PMs by dropping method ranged from 120-181 nm, followed by O/W emulsion (148-166 nm), dialysis (201-321 nm) and evaporation (289-338 nm). The results showed that the mean particle sizes of drug-loaded micelles were larger than that of blank micelles, because the CUR was entrapped in the copolymer micelles. Moreover, the particle sizes of CUR-loaded PMs with different hydrophobic moieties by dialysis method, are listed in Table 4.6. An increasing initial weight ratio of CUR to polymer exhibited a trend to increase the particle sizes of the CUR-loaded micelles. The results of mean particle sizes of the CUR-loaded NSCS, OSCS and BSCS were different, that might be dependent on the copolymer composition (Zhang, X. et al., 2014).

Table 4.5 The particle sizes and PDI of NSCS micelles with and without CUR. Each value represents the mean \pm SD from three independent measurements.

CUR to polymer	Dialysis		Dropping		O/W emulsion		Evaporation	
	Particle size	PDI	Particle size	PDI	Particle size	PDI	Particle size	PDI
0	196.20 \pm 1.51	0.061	84.31 \pm 0.88	0.198	-	-	233.50 \pm 7.07	0.384
5	201.17 \pm 1.90	0.239	129.97 \pm 3.79	0.297	148.37 \pm 2.93	0.239	289.13 \pm 27.71	0.453
10	224.53 \pm 2.54	0.237	181.47 \pm 18.69	0.451	150.73 \pm 2.24	0.214	326.47 \pm 21.66	0.402
20	274.43 \pm 3.20	0.353	120.20 \pm 6.46	0.452	156.50 \pm 1.99	0.230	317.40 \pm 23.61	0.374
40	321.13 \pm 2.41	0.239	124.30 \pm 5.68	0.455	166.93 \pm 0.59	0.215	338.47 \pm 6.36	0.358

Table 4.6 The particle sizes and PDI of polymeric micelles with and without MX. Each value represents the mean \pm SD of three independent measurements.

CUR to polymer (%)	NSCS		OSCS		BSCS	
	Particle size (nm)	PDI	Particle size (nm)	PDI	Particle size (nm)	PDI
0	196.20 \pm 1.51	0.061	163.67 \pm 4.18	0.414	171.47 \pm 0.99	0.251
5	201.17 \pm 1.90	0.239	180.57 \pm 2.62	0.264	171.10 \pm 4.75	0.484
10	224.53 \pm 2.54	0.237	192.60 \pm 3.50	0.471	200.40 \pm 17.05	0.323
20	274.43 \pm 3.20	0.353	259.70 \pm 5.51	0.404	216.40 \pm 1.55	0.169
40	321.13 \pm 2.41	0.239	255.50 \pm 6.56	0.295	219.80 \pm 2.63	0.202

4.4.2 Morphology characteristics

Morphology of resulting pH sensitive PMs was observed under different pH conditions (pH 1.2, 5.0 and 6.8) by AFM and DLS techniques. In this case, the CUR-loaded OSCS was selected to represent as shown in Figure 4.16. In pH 1.2 medium, the CUR-loaded OSCS micelles showed the aggregation of micelles with particle sizes of about 1072 nm by DLS because of unionized carboxyl groups and intermolecular hydrogen bond formation of succinic acid. AFM image, self-assembled micelles at pH 5.0 appeared as the spherical shape and the size of around 237 nm. As the pH increased to 6.8, the mean particle size of CUR-loaded OSCS was about 285 nm due to the effect of deprotonation as explained in part 4.3.2.

However, AFM image still showed spherical morphology. These results illustrated the pH-sensitivity property of CUR-loaded PMs.

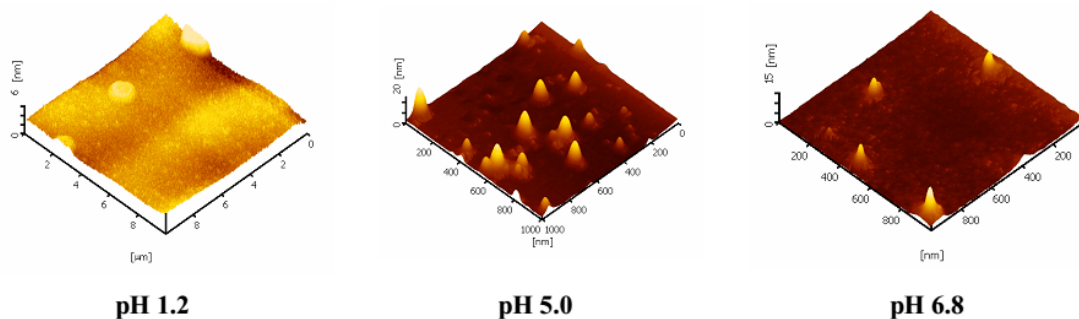


Figure 4.16 AFM images of CUR-loaded OSCS micelles at different pH.

4.4.3 Stability by GPC

The stability of CUR-loaded PMs was determined by GPC equipped with RI and UV detector. Figure 4.17 shows the ratios of the peak area of PMs/CUR concentration; [CUR]. At large ratios, the drug was more stable incorporated into the PMs as described in section 4.3.3. The ratios of the peak area/[CUR] of all CUR-loaded PMs decreased with increasing the initial CUR to polymer. At 5% CUR initial drug-loaded, the NSCS micelles showed the highest values of peak area/[CUR], followed by BSCS and OSCS, respectively. This results indicated that not only the drug content but also hydrophobic part were necessary to form stable CUR-loaded PMs formation.

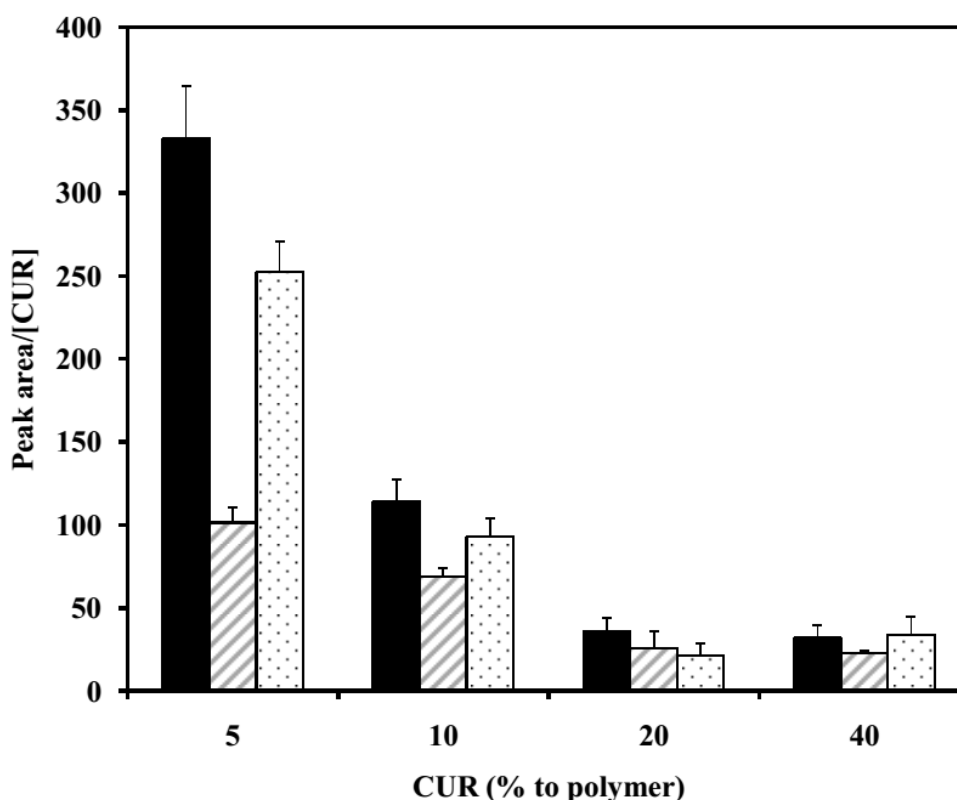


Figure 4.17 Polymeric micelles stability by ratio of peak area/[CUR]; (■) CUR-loaded NSCS; (▨) CUR-loaded OSCS; (▤) CUR-loaded BSCS. Data are plotted as the mean \pm SD of three measurements.

4.4.4 *In vitro* releases study

Although, several studies have shown that CUR may possess as a potential preventive or therapeutic agent for colorectal cancer, its poor bioavailability is the problem to limit its efficacy (Cen et al., 2009; Wang et al., 2009; Guo et al., 2013). To overcome this issue, pH sensitive PMs carriers were developed for colon-cancer tissue-targeted CUR delivery. It has been reported that in the stomach the pH is 1-2; in the small intestine the pH is 5.1-7.5 and in the colon the pH is 7-7.5 (Li et al., 2009; Yang et al., 2012). Hence, the release behavior of CUR at the fixed amount of drug from the pH-sensitive PMs with different grafted copolymers and CUR free drug was evaluated at 37°C in three-different pH media (SGF; pH 1.2, SIF; pH 6.8 and Simulated colonic fluid (SCF); pH7.4) in order to mimic the GI tract, as shown in Figure 4.18. The time interval for three different stages was at 1-2 h in SGF, then 3-5 h in SIF and

6-8 h in SCF. The results showed that the release rate of CUR from all pH sensitive CUR-loaded PMs was relatively low at acidic pH 1.2 (SGF), with about 20% of amount of CUR released after 2 h. This may be due to the poor solubility of drug. Afterward, the amount of CUR released increased in SIF (approximately 50-55%; 5 h) and SCF (approximately 60-70%; 8 h) due to the swelling and dissociation of PMs structure caused by the ionization of the succinic acid moiety with a pH above the pK_a of succinic acid at the higher pH conditions. The accumulative release of CUR from the all CUR-loaded PMs in SCF was significant higher than that of CUR from free drug (approximately 20%). This results indicated that all pH sensitive PMs may be a prospective candidate as colon delivery carrier for the efficient administration of CUR drug.

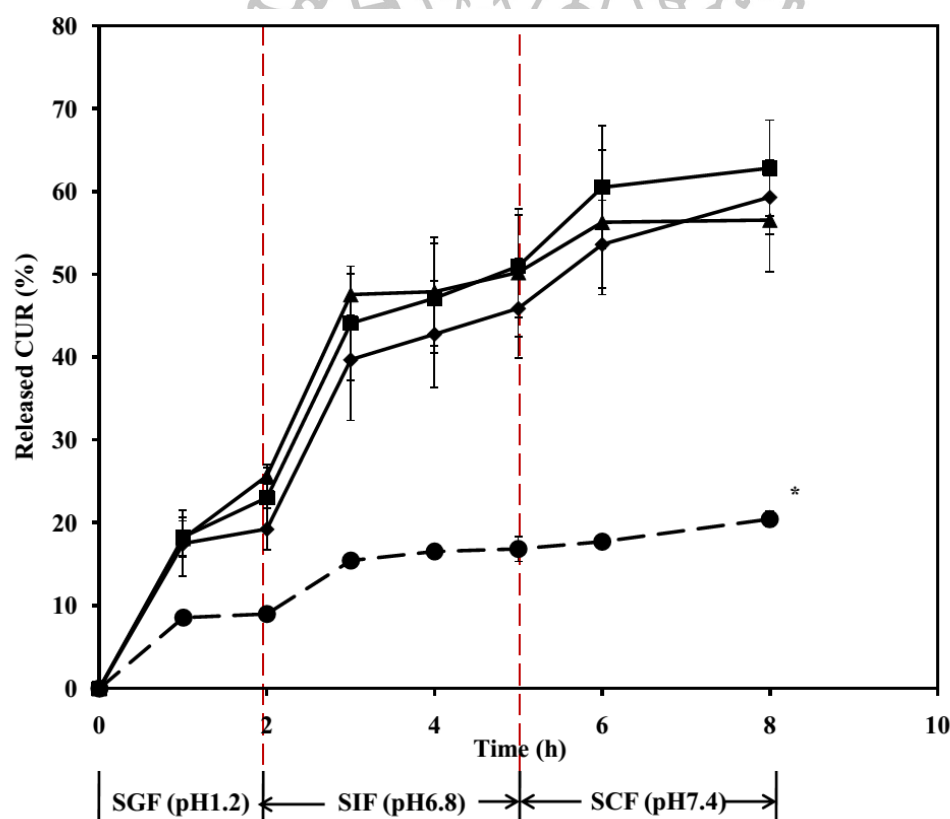


Figure 4.18 CUR release profiles from the (◆) CUR-loaded NSCS; (■) CUR-loaded OSCS; (▲) CUR-loaded BSCS; and (●) CUR suspension in 0.1 N HCl, pH 1.2 (0–2 h), then in PBS pH 6.8 (2–5 h) and then, in PBS pH 7.4 (5–8 h). Data are plotted as the mean \pm SD of three measurements. * Statistically significant ($p < 0.05$).

4.4.5 Anti-cancer activity

The CUR-loaded NSCS, OSCS and BSCS and CUR free drug were evaluated for the anti-cancer activity in HT-29 cells using the MTT assay. As shown in Figure 4.19, the different concentration of all CUR-loaded PMs and CUR free drug (0.1-20 $\mu\text{g/mL}$) had cytotoxicity on HT-29 cells in dose-dependent manner. After treatment, the IC_{50} values of all the self-assembled PMs and free drug were calculated. The CUR-loaded NSCS exhibited greater level of inhibition of cell viability (IC_{50} 6.18 ± 0.18 $\mu\text{g/mL}$) than CUR free drug (IC_{50} 11.38 ± 3.07 $\mu\text{g/mL}$), while CUR-loaded OSCS (IC_{50} 9.29 ± 0.44 $\mu\text{g/mL}$) and CUR-loaded BSCS (IC_{50} 9.79 ± 0.57 $\mu\text{g/mL}$) showed level of inhibition to a similar extent as free CUR. This result indicated that the CUR-loaded NSCS was more potent than CUR free drug in the growth suppression of the HT-29 cell lines studied.

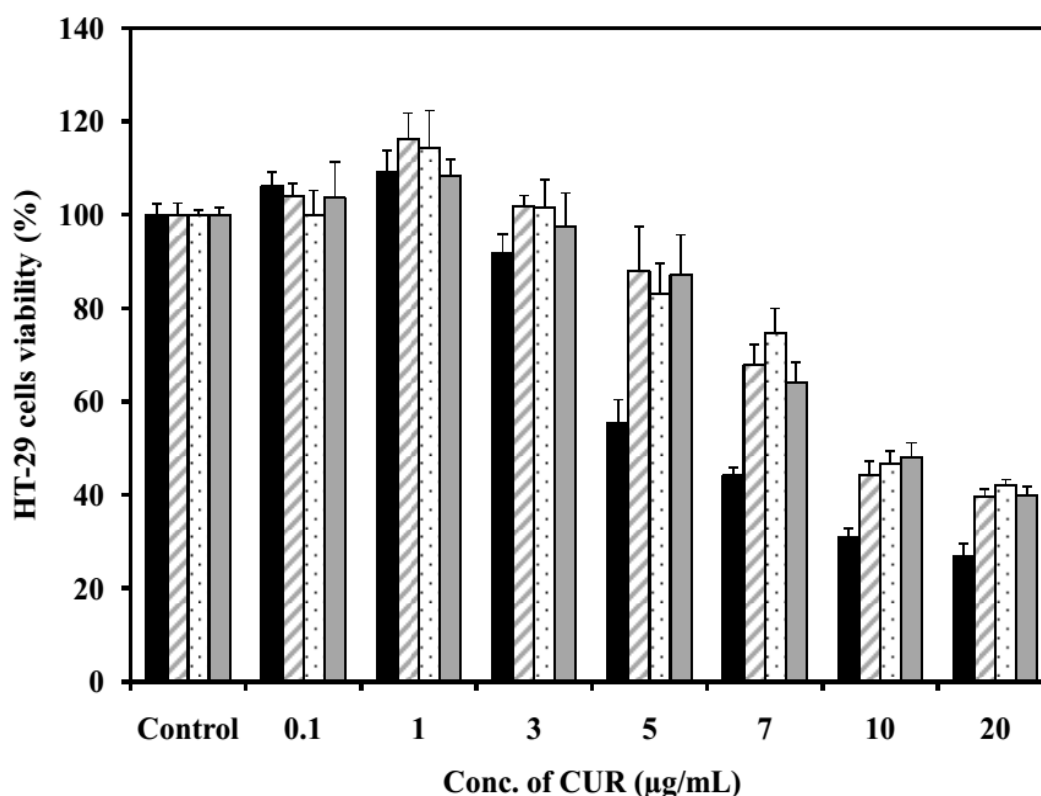


Figure 4.19 Anticancer activity of (■) CUR-loaded NSCS, (▨) CUR-loaded OSCS, (▤) CUR-loaded BSCS and (■) CUR free drug against HT-29 cells by MTT assay. Each value represents the mean \pm SD of five wells.

4.4.6 Stability test

The stability of CUR-loaded NSCS, OSCS and BSCS, and CUR free drug was evaluated under the accelerated conditions (at 25°C) compared with the long term conditions (at 4°C) for 90 days. Figure 4.20 shows that the percentage of an amount of CUR from all CUR-loaded polymeric micelles under both conditions was higher than 80%. There was no significant difference in the amount of in micelles and CUR free drug under this storage drug condition. This indicated that CUR-loaded polymeric micelles exhibited high stability.

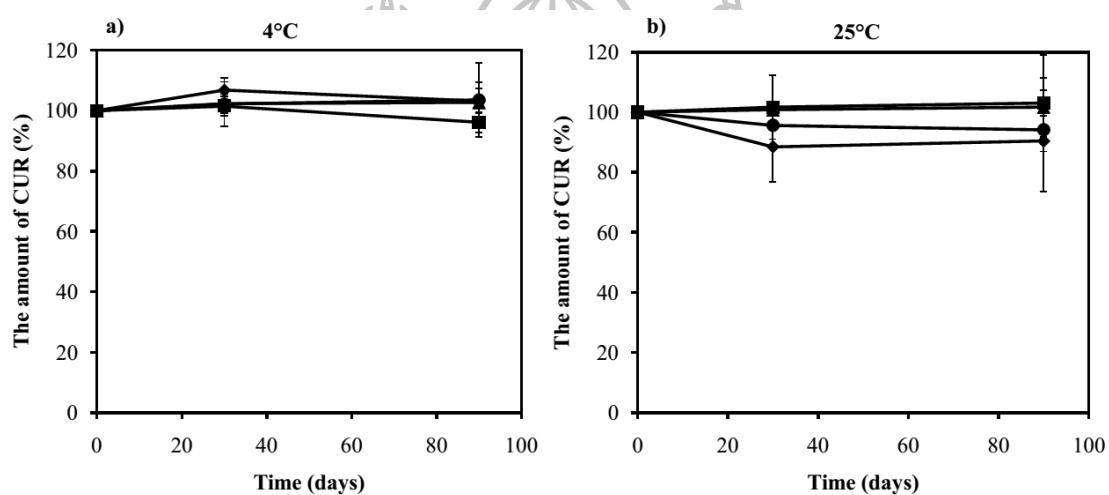


Figure 4.20 The stability of (◆) CUR-loaded NSCS; (■) CUR-loaded OSCS; (▲) CUR-loaded BSCS; and (●) free CUR drug under the accelerated conditions (at 25°C) compared with the long term conditions (at 4°C) for 90days. Data are plotted as the mean \pm SD of three measurements.

CHAPTER 5

CONCLUSIONS

In the present study, pH sensitive amphiphilic chitosan derivatives, i.e. *N*-naphthyl-*N,O*-succinyl chitosan (NSCS), *N*-octyl-*N,O*-succinyl chitosan (OSCS) and *N*-benzyl-*N,O*-succinyl chitosan (BSCS) were synthesized and prepared as polymeric micelles to improve the solubility of poorly water soluble drug and to control the drug release. Two drugs, namely meloxicam (MX) and curcumin (CUR), were selected as a hydrophobic drug for intestinal absorption and colorectal cancer treatment, respectively. The influence of the physical entrapment methods, type of amphiphilic chitosan derivatives, amount of drugs on entrapment efficiency, loading capacity, particle size and stability of drugs-loaded polymeric micelles were evaluated. In addition, the *in vitro* cytotoxicity and their release behavior were investigated. It can be concluded as follows:

5.1 Development of MX-loaded pH sensitive polymeric micelles

All amphiphilic chitosan derivatives could be formed as polymeric micelles with low CMC in aqueous solution, and showed the low cytotoxicity in Caco-2 cells. They successfully entrapped MX and increased the solubility through the solubilization of the drug in the hydrophobic core. The loading capacity increased with the increasing initial MX loading from 5% to 40%. Among the preparation methods, the evaporation method showed higher loading percentage than other methods. The MX-loaded OSCS which were prepared by evaporation method had the highest entrapment efficiency (33-46%) and loading capacity (22-158 $\mu\text{g}/\text{mg}$), followed by the MX-loaded NSCS (22-52%, 18-74 $\mu\text{g}/\text{mg}$) and MX-loaded BSCS (11-32%, 11-40 $\mu\text{g}/\text{mg}$). All polymeric micelles had the particle sizes in the range of nanometric scale and showed spherical shape. The AFM images of micelles presented the morphological changes under different pH, indicating the pH sensitive characteristics of the polymeric micelles. The structure stability of polymeric micelles depended on the initial concentration of the drug. The OSCS micelles with initial MX contents of 5% showed

the highest stability. The release profiles of all MX-loaded polymeric micelles presented pH sensitive property. In an acidic medium as simulated gastric fluid (SGF) at 0–2 h, low cumulative MX release was obtained in the MX-loaded OSCS micelles compared to MX-loaded NSCS micelles and MX-loaded BSCS micelles as well as MX free drug. However, when the pH medium was increased from 1.2 to 6.8 as simulated intestinal fluid (SIF), the MX release from all formulations significantly increased (approximately 100%), compared with free MX (approximately 60%) due to the fact that the high pH above the pK_a of succinic acid attached to the chitosan backbone induced the swelling and dissociation of polymeric micelles. Moreover, there were no significant differences in the porcine intestinal permeation of MX from MX-loaded PMs and MX free drug. This indicated that the amphiphilic chitosan derivatives could be used for oral MX delivery.

5.2 Development of CUR-loaded pH sensitive polymeric micelles

pH sensitive polymeric micelles carriers were developed to incorporate curcumin (CUR) for oral colon-targeted drug delivery. The physical entrapment methods (dialysis, O/W emulsion, dropping method and evaporation method) were applied. All formulations were able to load CUR in the inner core. The CUR-loaded polymeric micelles prepared by the dialysis method showed the highest entrapment efficiency (24-30%) and loading capacity (14-105 $\mu\text{g}/\text{mg}$) followed by evaporation (16-25%, 12-67 $\mu\text{g}/\text{mg}$), dropping (2-24%, 16-49 $\mu\text{g}/\text{mg}$) and O/W emulsion (3-20%, 20-29 $\mu\text{g}/\text{mg}$). However, at the same initial drug to polymer, the CUR-loaded polymeric micelles with different grafted hydrophobic moieties by the dialysis method exhibited no different drug loading content. The particle sizes of polymeric micelles were in range of 120-338 nm. The change of morphology under various pH confirmed the pH sensitivity of the polymeric micelles. The cumulative release of CUR from all micelles in SGF was about 20%. When pH medium was changed to pH 6.8 (SIF) and pH 7.4 (simulated colonic fluid; SCF), the curcumin release was significantly increased (SIF; 50-55%) and (SCF; 60-70%), compared to the free drug (20%) ($p < 0.05$). In addition, the CUR-loaded NSCS micelles exhibited the highest anti-cancer activity against HT-29 colorectal cancer cells with IC_{50} of $6.18 \pm 0.18 \mu\text{g}/\text{mL}$. The CUR-loaded NSCS, OSCS and BSCS and CUR free drug were stable under accelerated

conditions as well as long term conditions for 3 months. These findings support the potential of these pH-sensitive polymeric micelles to improve the solubility of CUR, control the drug release at a colon targeted site by oral administration and give the great anti-colorectal cancer activity against HT-29 cells, especially NSCS.



REFERENCES

- Aggrawal, B.B. et al (2007). "Curcumin induces the degradation of cyclin E expression through ubiquitin-dependent pathway and up-regulates cyclin-dependent kinase inhibitors p21 and p27 in multiple human tumor cell lines." **Biochemical Pharmacology** 73, 7 (April): 1024-1032.
- Ahad, A. et al. (2014). "Enhanced anti-inflammatory activity of carbopol loaded meloxicam nanoethosomes gel." **International Journal of Biological Macromolecules** 67 (June): 99-104.
- Akl, M.A. et al. (2016). "Factorial design formulation optimization and in vitro characterization of curcumin-loaded PLGA nanoparticles for colon delivery." **Journal of Drug Delivery Science and Technology** 32 (April): 10-20.
- Aliabadi H.M. et al. (2007). "Encapsulation of hydrophobic drugs in polymeric micelles through co-solvent evaporation: The effect of solvent composition on micellar properties and drug loading." **International of Pharmaceutics** 329, 1-2 (February): 158-165.
- Altememy, D.R. and Altememy, J.J. (2014). "Formulation and evaluation of meloxicam liquisolid compact." **International Journal of Pharmacy and Pharmaceutical Sciences** 6, 10: 453-463.
- Bashir, S. et al. (2015). "N-succinyl chitosan preparation, characterization, properties and biomedical applications: a state of the art review." **Reviews in Chemical Engineering** 31, 6: 563-597.
- Batrakova, E.V. et al. (2006). "Polymer micelles as drug carriers." In **Nanoparticulates as drug carriers**, 57-93. Edited by Vladimir P Torchilin. Singapore: World Scientific Publishing Co, Inc.
- Bernkop-Schnürch, A. (2013). "Nanocarrier systems for oral drug delivery: Do we really need them?." **European Journal of Pharmaceutical Sciences** 49, 2 (May): 272-277.
- Bissantz, C., Kuhn, B., and Stahl, M. (2010). "A medicinal chemist's guide to molecular interactions." **Journal of Medicinal Chemistry** 53, 14 (March): 5061-5084.

- Biswas, S. (2013). "Polymeric micelles for the delivery of poorly soluble drugs." In **Drug delivery strategies for poorly water-soluble drugs**, 411-476. Edited by Dennis Douroumis and Alfred Fahr. New York: John Wiley & Sons, Inc.
- Bonferoni, M.C. et al. (2014). "Ionic polymeric micelles based on chitosan and fatty acids and intended for wound healing. Comparison of linoleic and oleic acid." **European Journal of Pharmaceutics and Biopharmaceutics** 87, 1 (May): 101-106.
- Bromberg, L. (2008). "Polymeric micelles in oral chemotherapy." **Journal of Controlled Release** 128, 2 (June): 99-112.
- Bu, P. et al. (2016). "Cytotoxicity assessment of lipid-based self-emulsifying drug delivery system with Caco-2 cell model: Cremophor EL as the surfactant." **European Journal of Pharmaceutical Sciences** 91 (August): 162-171.
- Calvello, R. et al. (2016). "Bovine and soybean milk bioactive compounds: Effects on inflammatory response of human intestinal Caco-2 cells." **Food Chemistry** 210 (November): 276-285.
- Cen, L. et al. (2009). "New structural analogues of curcumin exhibit potent growth suppressive activity in human colorectal carcinoma cells." **BMC Cancer**, doi:10.1186/1471-2407-9-99.
- Chae, S.Y., Jang, M., and Nah, J. (2005). "Influence of molecular weight on oral absorption of water soluble chitosans." **Journal of Controlled Release** 102, 2 (February): 383-394.
- Chan, F. K., Moriwaki, K., and Rosa, M.J.D. (2013). "Detection of Necrosis by Release of Lactate Dehydrogenase (LDH) Activity." **Methods in Molecular Biology** 979 (January): 65-70.
- Chaurasia, S. et al. (2015). "Lipopolysaccharide based oral nanocarriers for the improvement of bioavailability and anticancer efficacy of curcumin." **Carbohydrate Polymers** 130 (October): 9-17.
- Chiappetta, D.A. et al. (2011). "Oral pharmacokinetics of the anti-HIV efavirenz encapsulated within polymeric micelles." **Biomaterials** 32, 9 (March): 2379-2387.
- Cho, Y.W. et al. (2004). "Hydrotropic agents for study of in vitro paclitaxel release from polymeric micelles." **Journal of Controlled Release** 97, 2 (June): 249-257.

- Chuah, L.H. et al. (2014). "Cellular uptake and anticancer effects of mucoadhesive curcumin-containing chitosan nanoparticles." **Colloids and Surfaces B: Biointerfaces** 116 (April): 228–236.
- Daman, Z. et al. (2014). "Preparation, optimization and in vitro characterization of stearyl-gemcitabine polymeric micelles: a comparison with its self-assembled nanoparticles." **International Journal of Pharmaceutics** 468, 1-2 (July): 142-151.
- Daugherty, A.L. and MRSNY, R.J. (1999). "Transcellular uptake mechanisms of the intestinal epithelial barrier Part one." **Pharmaceutical Science & Technology Today** 2, 4 (April): 144-151.
- Ding, H. et al. (2012). "Applications of polymeric micelles with tumor targeted in chemotherapy." **Journal of Nanoparticle Research** 14, 11 (November). doi:10.1007/s11051-012-1254-1.
- Ding, J. et al. (2014). "Noncovalent interaction-assisted polymeric micelles for controlled drug delivery." **Chemical Communications** 50 (June): 11274-11290.
- Duan, Y. et al. (2016). "Evaluation in vitro and in vivo of curcumin-loaded mPEG-PLA/TPGS mixed micelles for oral administration." **Colloids and Surfaces B: Biointerfaces** 141 (May): 345-354.
- Duangjit, S. et al (2013). "Evaluation of meloxicam-loaded cationic transfersomes as transdermal drug delivery carriers." **American Association of Pharmaceutical Sciences Technology** 14, 1: 133-140.
- Engelhardt, G. et al. (1996). "Meloxicam: influence on arachidonic acid metabolism - Part II - in vivo findings." **Biochemical Pharmacology** 51, 1 (January): 29-38.
- Jain, K.K. (2008). **Drug Delivery Systems**. Basel: Humana Press.
- Felber, A.E., Dufresne, M-H., and Leroux, J-C.(2012). "pH-sensitive vesicles polymeric micelles, and nanospheres prepared with polycarboxylates." **Advanced Drug Delivery Reviews** 64, 11 (August): 979-992.

- Fotakis, G. and Timbrell, J.A. (2006). "In vitro cytotoxicity assays: Comparison of LDH, neutral red, MTT and protein assay in hepatoma cell lines following exposure to cadmium chloride." **Toxicology Letters** 160, 2 (January): 171-177.
- Francis, M.F., Cristea, M., and Winnik, F.M. (2004). "Polymeric micelles for oral drug delivery: Why and how." **Pure and Applied Chemistry** 76, 7-8: 1321-1335.
- Fu, et al. (2013). "Application of chitosan and its derivatives in analytical chemistry: A mini-review." **Journal of Carbohydrate Chemistry** 32, 8-9 (December): 463-474.
- Gaucher, G. et al. (2010). "Polymeric micelles for oral drug delivery." **European Journal of Pharmaceutics and Biopharmaceutics** 76, 2 (October): 147-158.
- Ghaemy, M., Ziaei, S., and Alizadeh, R. (2014). "Synthesis of pH-sensitive amphiphilic pentablock copolymers via combination of ring-opening and atom transfer radical polymerization for drug delivery." **European Polymer Journal** 58 (September): 103-114.
- Godfroy, I. (2009). "Polymeric micelles-The future of oral drug delivery." **Journal of Biomaterials Applications Reviews** 3: 216-232.
- Guo, L. et al (2013). "Curcumin inhibits proliferation and induces apoptosis of human colorectal cancer cells by activating the mitochondria apoptotic pathway." **Phytotherapy Research** 27, 3: 422-430.
- Huang, L. et al. (2016). "Preparation of pH-sensitive micelles from miktoarm star block copolymers by ATRP and their application as drug nanocarriers." **Reactive and Functional Polymers** 107 (October): 28-34.
- Huo, M. et al. (2012). "Somatostatin receptor-mediated tumor-targeting drug delivery using octreotide-PEG-deoxycholic acid conjugate-modified N-deoxycholic acid-O,N-hydroxyethylation chitosan micelles." **Biomaterials** 33, 27 (September): 6393-6407.
- Jani, P. et al. (1989). "The uptake and translocation of latex nanospheres and microspheres after oral administration to rats." **Journal of Pharmacy and Pharmacology** 41, 12 (December): 809-812.

- Jani, P. et al. (1990). "Nanoparticle uptake by the rat gastrointestinal mucosa: quantitation and particle size dependency." **Journal of Pharmacy and Pharmacology** 42, 12 (December): 821-826.
- Jette, K.K. et al. (2004). "Preparation and drug loading of poly(ethylene glycol)-block-poly(ϵ -caprolactone) micelles through the evaporation of a cosolvent azeotrope." **Pharmaceutical Research** 21, 7 (July): 1184-1191.
- Jiang, G.B. et al. (2006). "Novel polymer micelles prepared from chitosan grafted hydrophobic palmitoyl groups for drug delivery." **Molecular Pharmaceutics** 3, 2 (January): 152-160.
- Jones, M-C. and Leroux, J-C. (1999). "Polymeric micelles - a new generation of colloidal drug carriers." **European Journal of Pharmaceutics and Biopharmaceutics** 48, 2 (September): 101-111.
- Kalepu S., Manthina M., and Padavala V. (2013). "Oral lipid-based drug delivery systems—an overview." **Acta Pharmaceutica Sinica B** 3, 6 (December): 361-372.
- Kawamori, T. et al. (1999). "Chemopreventive effect of curcumin, a naturally occurring anti-inflammatory agent, during the promotion/progression stages of colon." **Cancer Research** 59, 3 (February): 597-601.
- Kedar, U. et al. (2010). "Advances in polymeric micelles for drug delivery and tumor targeting-review article." **Nanomedicine: Nanotechnology, Biology and Medicine** 6, 6 (December): 714-729.
- Kim H., Lee I. (2007). "A novel drug delivery system design for meloxicam." **Journal of Pharmacy and Pharmaceutical Sciences** 10, 3: 288–298.
- Kim, S. et al. (2010). "Overcoming the barriers in micellar drug delivery: loading efficiency, in vivo stability, and micelle-cell interaction." **Expert Opinion on Drug Delivery** 7, 1 (December): 49–62.
- Kim, S. et al. (2008). "Hydrotropic polymer micelles containing acrylic acid moieties for oral delivery of paclitaxel." **Journal of Controlled Release** 132, 3 (December): 222-229.
- Klaikherd, A., Nagamani, C., and Thanyumanavan, S. (2009). "Multi-stimuli sensitive amphiphilic block copolymer assemblies." **Journal of the American Chemical Society** 131, 13 (March): 4830-4838.

- Koh, J-Y. and Choi, D.W. (1987). "Quantitative determination of glutamate mediated cortical neuronal injury in cell culture by lactate dehydrogenase efflux assay." **Journal of Neuroscience Methods** 20, 1 (May): 83-90.
- Koh, J-Y. and Cotman, C.W. (1992). "Programmed cell death: its possible role in calcium channel antagonist neurotoxicity." **Brain Research** 587, 2: 233-240.
- Kumar A. et al (2011). "Review on solubility enhancement techniques for hydrophobic drugs." **International Journal of Comprehensive Pharmacy** 2, 3: 1-7.
- Kumar P., Singh C. (2013). "A study on solubility enhancement methods for poorly water soluble drugs." **American Journal of Pharmacological Sciences** 1, 4: 67-73.
- Kumar, R. et al. (2012). "*In vitro* evaluation of theranostic polymeric micelles for imaging and drug delivery in cancer." **Theranostics** 2, 7: 714-722.
- Kwon, G.S and Okano, T. (1996). "Polymeric micelles as new drug carriers." **Advanced Drug Delivery Reviews** 21, 2 (September): 107-116.
- Lavasanifar, A., Samuel, J., and Kwon, G.S. (2002). "Poly(ethylene oxide)-block-poly(L-amino acid) micelles for drug delivery." **Advanced Drug Delivery Reviews** 54, 2 (February): 169-190.
- Lee, I. et al. (2013). "Ketal containing amphiphilic block copolymer micelles as pH-sensitive drug carriers." **International Journal of Pharmaceutics** 448, 1 (May): 259-266.
- Letchford, K., Liggins, R., and Burt, H. (2008). "Solubilization of hydrophobic drugs by methoxy poly(ethylene glycol)-block-polycaprolactone diblock copolymer micelles: Theoretical and experimental data and correlations." **Journal of Pharmaceutical Sciences** 97, 3 (March): 1179-1190.
- Li, Y. et al. (2009). "pH-Responsive composite based on prednisone-block copolymer micelle intercalated inorganic layered matrix: Structure and in vitro drug release." **Chemical Engineering Journal** 151, 1-3 (August): 359-366.
- Lia W. et al. (2014). "Amphiphilic chitosan derivative-based core-shell micelles: Synthesis, characterisation and properties for sustained release of Vitamin D₃." **Food Chemistry** 152, (June): 307-315.

- Lim, E. et al. (2013). "Chitosan based intelligent theragnosis nanocomposites enable pH-sensitive drug release with MR-guided imaging for cancer therapy." **Nanoscale Research Letters** 8, 467 (November): 1-12.
- Liu, Y. et al. (2013). "pH-sensitive polymeric micelles triggered drug release for extracellular and intercellular drug targeting delivery." **Asian Journal of Pharmaceutical Sciences** 8, 3 (June): 159-167.
- Lobner, D. "Comparison of the LDH and MTT assays for quantifying cell death: validity for neuronal apoptosis?." **Journal of Neuroscience Methods** 96, 2 (March): 147-152.
- Long, L. et al. (2016). "Synthesis of star-branched PLA-b-PMPC copolymer micelles as long blood circulation vectors to enhance tumor-targeted delivery of hydrophobic drugs in vivo." **Materials Chemistry and Physics** 180 (September): 184-194.
- Lopez-Garcia, J.A. and Laird, J.M. (1998). "Central antinociceptive effects of meloxicam on rat spinal cord in vitro." **Neuroreport** 9, 4 (March): 647-651.
- Lu, Y., Park, K. (2013). "Polymeric micelles and alternative nanonized delivery vehicles for poorly soluble drugs." **International Journal of Pharmaceutics** 453, 1 (August): 198-214.
- Luger, P. et al. (1996). "Structure and physicochemical properties of meloxicam, a new NSAID." **European Journal of Pharmaceutical Sciences** 4, 3 (May): 175-187.
- Mehanny, M. et al (2016). "Exploring the use of nanocarrier systems to deliver the magical molecule; Curcumin and its derivatives." **Journal of Controlled Release** 225 (March): 1-30.
- Miller, T. et al. (2013). "Drug loading of polymeric micelles." **Pharmaceutical Research** 30, 2: 584-595.
- Mitchell, J.A. et al. (1993). "Selectivity of nonsteroidal anti-inflammatory drugs as inhibitors of constitutive and inducible cyclooxygenase." **Proceedings of the National Academy of Sciences of the United States of America** 90, 24 (December): 11693-11697.
- Miwa, A. et al. (1998). "Development of novel chitosan derivatives as micellar carriers of taxol." **Pharmaceutical Research** 15, 12 (December): 1844-1850.

- Mondon, K., Gurny, R., and Moller, M. (2008). "Colloidal drug delivery systems - recent advances with polymeric micelles." **CHIMIA** 62, 10: 832-840.
- Mosmann, T. (1983). "Rapid colorimetric assay for cellular growth and survival: Application to proliferation and cyto-toxicity assays." **Journal of Immunological Methods** 65, 1-2 (December): 55-63.
- Movassaghian, S., Merkel, O.M., and Torchilin, V.P. (2015). "Applications of polymer micelles for imaging and drug delivery." **WIREs Nanomedicine and Nanobiotechnology** 7 (September/October): 691-707.
- Murthy, R.S.R. (2015). "Polymeric micelles in targeted drug delivery." In **Targeted drug delivery: Concepts and design**, 501-540. Edited by Padma V. Devarajan and Sanyog Jain. USA: Springer.
- Muzzarelli, C. et al. (2003). "Alkaline chitosan solutions." **Carbohydrate Research** 338, 21 (October): 2247-2255.
- Muzzarelli, R.A.A. et al (2012). "Current views on fungal chitin/chitosan, human chitinases, food preservation, glucans, pectins and inulin: A tribute to Henri Braconnot, precursor of the carbohydrate polymers science, on the chitin bicentennial." **Carbohydrate Polymers** 87, 2 (January): 995-1012.
- Nakayama, M., Akimoto, J., and Okano, T. (2014). "Polymeric micelles with stimuli-triggering systems for advanced cancer drug targeting." **Journal of Drug Targeting** 22,7 (August): 584-599.
- Ngawhirunpat, T. et al. (2009). "Incorporation methods for cholic acid chitosan-g-mPEG self-assembly micellar system containing camptothecin." **Colloids and Surfaces B: Biointerfaces** 74, 1 (November): 253-259.
- Nishiyama, N and Kataoka, K. (2001). "Preparation and characterization of size-controlled polymeric micelle containing cis-dichlorodiammineplatinum (II) in the core." **Journal of Controlled Release** 74, 1-3 (July): 83-94.
- Oberoi, HS. et al. (2011). "Core cross-linked block ionomer micelles as pH-responsive carriers for cis-diamminedichloroplatinum(II)." **Journal of Controlled Release** 153, 1 (July): 64-72.
- Opanasopit, P. et al. (2004). "Block copolymer design for camptothecin incorporation into polymeric micelles for passive tumor targeting." **Pharmaceutical Research** 21, 10: 2001-2008.

- Opanasopit, O. et al. (2007). "Camptothecin-incorporating N-phthaloylchitosan-g-mPEG self-assembly micellar system: Effect of degree of deacetylation." **Colloids and Surfaces B: Biointerfaces** 60, 1 (October): 117-124.
- Owen, S.C., Chan, D.P.Y., and Shoichet M.S. (2012). "Polymeric micelle stability." **Nano Today** 7, 1 (February): 53-65.
- Patel B.P., Patel D.M., Patel J.K., Patel J.D. (2012). "A review on techniques which are useful for solubility enhancement of poorly water soluble drugs." **International Journal for Research in Management and Pharmacy** 1, 1: 56-70.
- Pu, X. et al. (2012). "Study progression in polymeric micelles for the targeting delivery of poorly soluble anticancer agents to tumor." **Asian Journal of Pharmaceutical Sciences** 7, 1: 1-17.
- Qiu, L. et al. (2014). "Self-assembled pH-responsive hyaluronic acid-g-poly(L-histidine) copolymer micelles for targeted intracellular delivery of doxorubicin." **Acta Biomaterialia** 10, 5 (May): 2024-2035.
- Qui L.Y., Wu X.L., and Jin Y. (2009). "Doxorubicin-Loaded Polymeric Micelles Based on Amphiphilic Polyphosphazenes with Poly(N-isopropylacrylamide-co-N,N-dimethylacrylamide) and Ethyl Glycinate as Side Groups: Synthesis, Preparation and In Vitro Evaluation." **Pharmaceutical Research** 26, 4: 946-957.
- Ramasamy, T.S. et al. (2015). "Targeting colorectal cancer stem cells using curcumin and curcumin analogues: insights into the mechanism of the therapeutic efficacy." **Cancer Cell International** doi 10.1186/s12935-015-0241-x.
- Rao, C.V. et al. (1995). "Chemoprevention of colon carcinogenesis by dietary curcumin, a naturally occurring plant phenolic compound." **Cancer Research** 55, 2 (January): 259-266.
- Sajomsang, W. et al. (2008). "Synthesis and characterization of N-aryl chitosan derivatives." **International Journal of Biological Macromolecules** 43, 2 (August): 79-87.
- Sajomsang, W. et al (2014). "Synthesis and anticervical cancer activity of novel pH responsive micelles for oral curcumin delivery." **International of Journal Pharmaceutics**, 477, 1-2 (December): 261-272.

- Samprasit, W. et al. (2015). "Formulation and evaluation of meloxicam oral disintegrating tablet with dissolution enhanced by combination of cyclodextrin and ion exchange resins." **Drug Development and Industrial Pharmacy** 41, 6 (May): 1006-1016.
- Samprasit, W., et al. (2013). "Improvement of drug loading onto ion exchange resin by cyclodextrin inclusion complex." **Drug Development and Industrial Pharmacy** 39, 11 (October): 1672-1680.
- Sandur, SK. et al. (2009). "Curcumin modulates the radiosensitivity of colorectal cancer cells by suppressing constitutive and inducible NF-B activity." **International Journal Radiation Oncology Biology Physics** 75, 2 (October): 534-42.
- Sant, V.P., Smith, D., and Leroux, J-C. (2004). "Novel pH-sensitive supramolecular assemblies for oral delivery of poorly water soluble drugs: preparation and characterization." **Journal of Controlled Release** 97, 2 (June): 301-312.
- Satturwar, P. et al. (2007). "pH-responsive polymeric micelles of poly(ethylene glycol)-b-poly(alkyl(meth)acrylate-co-methacrylic acid): influence of the copolymer composition on self-assembling properties and release of candesartan cilexetil." **European Journal of Pharmaceutics and Biopharmaceutics** 65, 3 (March): 379-387.
- Savic, R. Eisenberg, A., and Maysinger, D. (2006). "Block copolymer micelles as delivery vehicles of hydrophobic drugs: micelle-cell interactions." **Journal of Drug Targeting** 14, 6 (October): 343-355.
- Savjani K.T., Gajjar A.K., Savjani J.K. (2012). "Drug solubility: Importance and enhancement techniques." **International Scholarly Research Network Pharmaceutics**. doi:10.5402/2012/195727.
- Sezgin, Z., Yuksel, N., and Baykara, T. (2006). "Preparation and characterization of polymeric micelles for solubilization of poorly soluble anticancer drugs." **European Journal of Pharmaceutics and Biopharmaceutics** 64, 3 (November): 261-268.
- Sharma, D. et al. (2009). "Solubility enhancement-eminent role in poorly soluble drugs." **Research Journal of Pharmacy and Technology** 2, 2: 220-224.

- Shemesh, N. and Arber, N. (2014). "Curcumin alone and combination for prevention of colorectal cancer." **Current Colorectal Cancer Reports** 10, 1 (March): 62-67.
- Shen, L. and Ji, H-F.(2007). "Theoretical study on physicochemical properties of curcumin." **Spectrochimica Acta Part A** 67, 3-4 (July) : 619-623.
- Sinha, V.R. and Kumria, R. (2002). "Binders for colon specific drug delivery: an in vitro evaluation." **International Journal of Pharmaceutics** 249, 1-2 (December): 23-31.
- Sinko, P.J. (2011). **Martin's Physical Pharmacy and Pharmaceutical Sciences**. 6th ed. Falls Church: Aptara, Inc.
- Soppimath, K.S., Tan, D.C-W., and Yang, Y-Y.(2005). "pH-triggered thermally responsive polymer core-shell nanoparticles for drug delivery." **Advances Materials** 17 (February): 318-323.
- Su, CC. et al. (2006). "Curcumin inhibits cell migration of human colon cancer Colo 205 cells through the inhibition of nuclear factor kappa B/p65 and down-regulates cyclooxygenase-2 and matrix metalloproteinase-2 expression." **Anticancer Research** 26, 2A (March-April): 1281-1288.
- Sun, Y. et al. (2010). "Preparation and characterization of 5-Fluorouracil loaded chitosan microspheres by a two-step solidification method. " **Chemical and Pharmaceutical Bulletin** 58, 7 (July): 891-895.
- Tan, C., Wang, Y., and Fan, W. (2013). "Exploring polymeric micelles for improved delivery of anticancer agents: recent developments in preclinical studies." **Pharmaceutics** 5, 1 (March): 201-219.
- Tran, D.L. et al. (2011). "Some biomedical applications of chitosan-based hybrid nanomaterials." **Advances in Natural Sciences: Nanoscience and Nanotechnology** 2, 4 (December): 1-6.
- Tu, J. et al. (2016). "Chitosan nanoparticles reduce LPS-induced inflammatory reaction via inhibition of NF- κ B pathway in Caco-2 cells." **International Journal of Biological Macromolecules** 86 (May): 848-856.
- Villalba, B.T. et al (2016). "Polymeric nanocapsules as a technological alternative to reduce the toxicity caused by meloxicam in mice." **Regulatory Toxicology and Pharmacology** 81 (November): 316-321.

- Wang, G. et al. (2012). "Understanding and correcting for carbon nanotube interferences with a commercial LDH cytotoxicity assay." **Toxicology** 299, 2-3 (September): 99-111.
- Wang, Jin-bo.et al. (2009). "Curcumin induces apoptosis through the mitochondria-mediated apoptotic pathway in HT-29 cells." **Journal of Zhejiang University SCIENCE B** 10, 2 (February): 93-102.
- Wang, J. et al. (2016). "Recent progress on synthesis, property and application of modified chitosan: An overview." **International Journal of Biological Macromolecules** 88 (July): 333-344.
- Wang J., Ma W., and Tu P. (2015). "The mechanism of self-assembled mixed micelles in improving curcumin oral absorption: In vitro and in vivo." **Colloids and Surfaces B: Biointerfaces** 133 (September): 198-119.
- Xiangyang, X. et al. (2007). "Preparation and characterization of N-succinyl-N-octyl chitosan micelles as doxorubicin carriers for effective anti-tumor activity." **Colloids and Surfaces B: Biointerfaces** 55, 2 (April): 222-228.
- Xu, W., Ling, P., Zhang, T. (2013). "Polymeric micelles, a promising drug delivery system to enhance bioavailability of poorly water-soluble drugs." **Journal of Drug Delivery**. <http://dx.doi.org/10.1155/2013/340315>.
- Xue, Y-N.et al. (2009). "Synthesis and self-assembly of amphiphilicpoly(acrylic acid-b-DL-lactide) to form micelles for pH-responsive drug delivery." **Polymer** 50, 15 (July): 3706-3713.
- Yamamoto, T. et al. (2007). "What are determining factors for stable drug incorporation into polymeric micelle carriers? Consideration on physical and chemical characters of the micelle inner core." **Journal of Controlled Release** 123, 1 (October): 11-18.
- Yang, Y.Q. et al. (2011). "pH-sensitive micelles self-assembled from amphiphilic copolymer brush for delivery of poorly water-soluble drugs." **Biomacromolecules** 12, 1: 116-122.
- Yang, Y.Q. et al. (2012). "Synthesis and physicochemical characterization of amphiphilictriblock copolymer brush containing pH-sensitive linkage for oral drug delivery." **Langmuir** 28, 21: 8251-8259.

- Yang, Y.Q. et al. (2013). "pH-sensitive micelles self-assembled from multi-arm star triblock co-polymers poly(ϵ -caprolactone)-*b*-poly(2-(diethylamino)ethyl methacrylate)-*b*-poly(poly(ethylene glycol) methyl ether methacrylate) for controlled anticancer drug delivery." **Acta Biomaterialia** 9, 8 (August): 7679-7690.
- Yokoyama, M. (2011). "Clinical application of polymeric micelle carrier systems in chemotherapy and image diagnosis of solid tumors." **Journal of Experimental and Clinical Medicine** 3, 4 (August): 151-158.
- Yokoyama, M. (2014). "Polymeric micelles as drug carriers: Their lights and shadows." **Journal of Drug Targeting** 22, 7: 576-583.
- Yoo, H.S., Lee, E.A, and Park, T.G. (2002). "Doxorubicin-conjugated biodegradable polymeric micelles having acid-cleavable linkages." **Journal of Controlled Release** 82, 1 (July): 17-27.
- Yuan, Z. et al. (2013). "Chitosan-Graft- β -Cyclodextrin Nanoparticles as a Carrier for Controlled Drug Release." **International Journal of Pharmaceutics** 446, 1-2 (February): 191-198.
- Zhang, C.Y. et al. (2012). "Self-assembled pH-responsive MPEG-*b*-(PLA-co-PAE) block copolymer micelles for anticancer drug delivery." **Biomaterials** 33, 26 (September): 6273-6283.
- Zhang, Y., et al. (2012). "Sustained release of ibuprofen from polymeric micelles with a high loading capacity of ibuprofen in media simulating gastrointestinal tract fluids." **Reactive and Functional Polymers**, 72, 6 (June): 359-364.
- Zhang, C., Qineng, P., and Zhang, H. (2004). "Self-assembly and characterization of paclitaxel-loaded N-octyl-O-sulfate chitosan micellar system." **Colloids and Surfaces B: Biointerface** 39, 1-2 (November): 69-75.
- Zhang, X. et al. (2014). "Micelles of enzymatically synthesized PEG-poly(amine-co-ester) block copolymers as pH-responsive nanocarriers for docetaxel delivery." **Colloids and Surfaces B: Biointerfaces** 115, (March): 349-358.

- Zhang, Y. et al. (2010). "Cyclosporin A-loaded poly(ethylene glycol)-b-poly(D,L-lactic acid) Micelles: Preparation, in vitro and in vivo characterization and transport mechanism across the intestinal barrier." **Molecular Pharmaceutics** 7, 4 (August): 1169-1182.
- Zhiang, J. et al. (2009). "Anionic poly(lactic acid)-polyurethane micelles as potential biodegradable drug delivery carriers." **Colloids and Surfaces A** 337, 1-3 (April): 200-204.







1. Determination of MX content

Standard : Meloxicam

Method: HPLC method with UV detection at wavelength 365 nm

Concentration ($\mu\text{g/mL}$): 1, 3, 5, 10, 20, 30, 40, 50

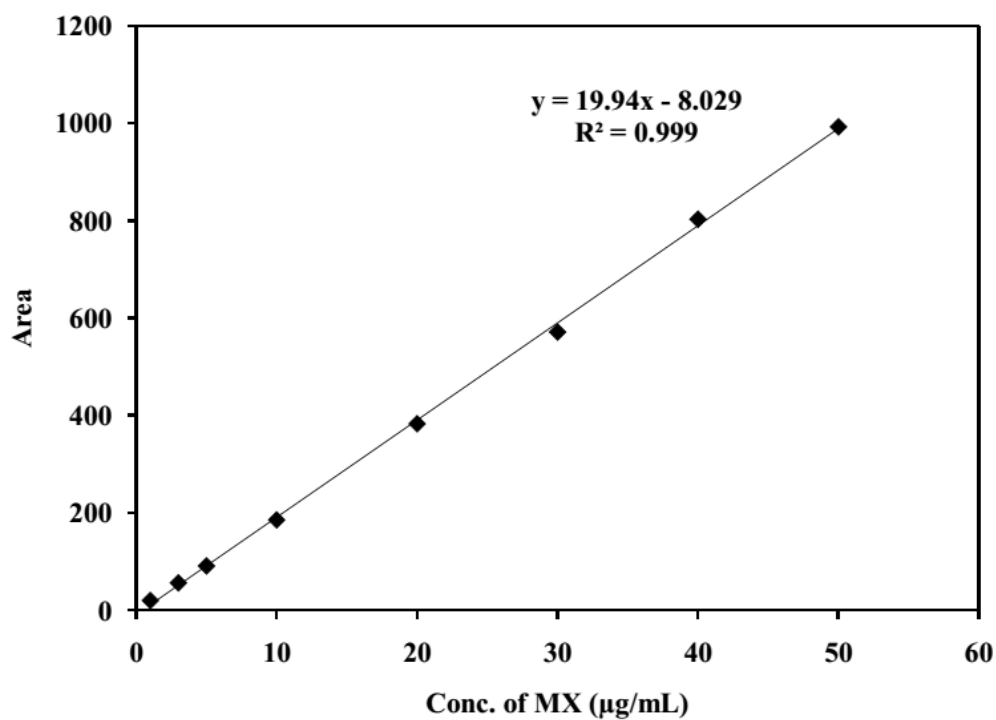


Figure A.1 Meloxicam standard curve



2. Determination of curcumin content

Standard : Curcumin

Method: HPLC method with UV detection at wavelength 428 nm

Concentration ($\mu\text{g/mL}$): 5, 10, 20, 30, 40, 50

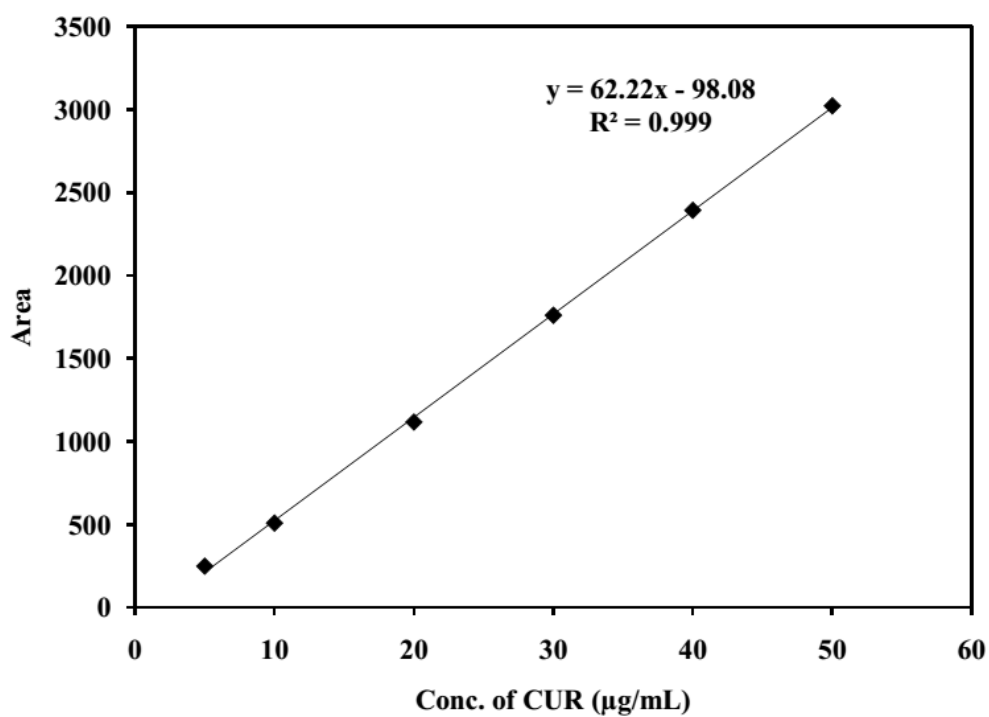


Figure A.2 Curcumin standard curve



3. Entrapment efficiency evaluation

Table A.1 Entrapment efficiency of MX into NSCS with initial drug to polymer (5-40%) by dialysis method

Concentration % weight to polymer	Entrapment efficiency (%)				
	1	2	3	Mean	SD
5	4.71	7.41	4.48	5.53	1.63
10	1.77	2.63	2.34	2.24	0.44
20	1.44	1.62	1.60	1.55	0.10
40	12.31	14.28	13.90	13.49	1.04

Table A.2 Loading capacity of MX into NSCS with initial drug to polymer (5-40%) by dialysis method

Concentration % weight to polymer	Loading capacity ($\mu\text{g}/\text{mg}$)				
	1	2	3	Mean	SD
5	2.09	2.35	2.11	2.19	0.15
10	2.33	1.77	2.23	2.11	0.30
20	2.88	3.24	3.18	3.10	0.19
40	49.23	28.55	29.20	35.66	11.76

Table A.3 Entrapment efficiency of MX into NSCS with initial drug to polymer (5-40%) by dropping method

Concentration % weight to polymer	Entrapment efficiency (%)				
	1	2	3	Mean	SD
5	12.33	7.89	5.03	8.42	3.68
10	13.39	8.46	3.44	8.43	4.97
20	16.10	14.69	15.09	15.29	0.73
40	8.89	8.63	9.05	8.86	0.21

Table A.4 Loading capacity of MX into NSCS with initial drug to polymer (5-40%) by dropping method

Concentration % weight to polymer	Loading capacity ($\mu\text{g}/\text{mg}$)				
	1	2	3	Mean	SD
5	2.09	3.08	2.24	2.47	0.54
10	7.19	6.70	7.05	6.98	0.26
20	15.09	16.10	16.65	15.95	0.79
40	18.11	17.79	18.30	18.07	0.26

Table A.5 Entrapment efficiency of MX into NSCS with initial drug to polymer (5-40%) by evaporation method

Concentration % weight to polymer	Entrapment efficiency (%)				
	1	2	3	Mean	SD
5	56.51	44.87	55.35	52.35	6.49
10	19.94	17.17	28.72	21.94	6.03
20	15.91	14.76	26.17	18.95	6.29
40	20.75	16.31	30.05	22.37	7.01

Table A.6 Loading capacity of MX into NSCS with initial drug to polymer (5-40%) by evaporation method

Concentration % weight to polymer	Loading capacity ($\mu\text{g}/\text{mg}$)				
	1	2	3	Mean	SD
5	28.26	22.43	20.25	23.65	4.14
10	19.94	17.17	25.29	20.80	4.13
20	31.81	29.52	43.27	34.87	7.37
40	82.99	65.25	75.47	74.57	8.90

Table A.7 Entrapment efficiency of MX into NSCS with initial drug to polymer (5-40%) by O/W emulsion method

Concentration % weight to polymer	Entrapment efficiency (%)				
	1	2	3	Mean	SD
5	4.26	4.50	17.32	8.70	7.47
10	2.10	15.18	3.45	6.91	7.19
20	22.54	4.91	5.18	10.87	10.10
40	23.26	15.28	7.29	15.28	7.98

Table A.8 Loading capacity of MX into NSCS with initial drug to polymer (5-40%) by O/W emulsion method

Concentration % weight to polymer	Loading capacity ($\mu\text{g}/\text{mg}$)				
	1	2	3	Mean	SD
5	8.66	4.75	7.27	6.89	1.98
10	15.18	21.10	19.88	18.72	3.13
20	9.81	22.54	9.75	14.03	7.36
40	29.18	46.52	28.22	34.64	10.30

Table A.9 Entrapment efficiency of MX into OSCS with initial drug to polymer (5-40%) by evaporation method

Concentration % weight to polymer	Entrapment efficiency (%)				
	1	2	3	Mean	SD
5	47.25	33.75	47.17	42.72	7.77
10	46.61	46.84	37.82	43.76	5.14
20	44.18	48.18	46.11	46.16	2.00
40	36.93	30.03	33.48	33.48	3.45

Table A.10 Loading capacity of MX into OSCS with initial drug to polymer (5-40%) by evaporation method

Concentration % weight to polymer	Loading capacity ($\mu\text{g}/\text{mg}$)				
	1	2	3	Mean	SD
5	22.5	23.62	20.25	22.12	1.72
10	42.37	46.61	45.8	44.93	2.25
20	80.3	96.36	89.54	88.73	8.06
40	167.78	147.73	159.9	158.47	10.10

Table A.11 Entrapment efficiency of MX into BSCS with initial drug to polymer (5-40%) by evaporation method

Concentration % weight to polymer	Entrapment efficiency (%)				
	1	2	3	Mean	SD
5	34.36	32.61	32.87	32.95	1.38
10	15.60	7.89	14.72	12.74	4.22
20	10.53	6.88	16.11	11.17	4.65
40	14.10	9.21	10.18	11.16	2.59

Table A.12 Loading capacity of MX into BSCS with initial drug to polymer (5-40%) by evaporation method

Concentration % weight to polymer	Loading capacity ($\mu\text{g}/\text{mg}$)				
	1	2	3	Mean	SD
5	8.59	15.8	23.25	15.88	7.33
10	7.89	15.6	14.55	12.68	4.18
20	32.21	21.06	32.17	28.48	6.43
40	36.84	40.7	43.76	40.43	3.47

Table A.13 Entrapment efficiency of CUR into NSCS with initial drug to polymer (5-40%) by dialysis method

Concentration % weight to polymer	Entrapment efficiency (%)				
	1	2	3	Mean	SD
5	35.43	32.99	25.96	31.46	4.92
10	21.78	27.77	23.32	24.29	3.11
20	21.3	28.9	34.01	28.07	6.40
40	30.5	27.93	21.06	26.50	4.88

Table A.14 Loading capacity of CUR into NSCS with initial drug to polymer (5-40%) by dialysis method

Concentration % weight to polymer	Loading capacity ($\mu\text{g}/\text{mg}$)				
	1	2	3	Mean	SD
5	17.72	12.01	12.98	14.24	3.06
10	21.78	27.77	23.32	24.29	3.11
20	68.43	86.62	81.12	78.72	9.33
40	121.99	111.74	84.23	105.99	19.53

Table A.15 Entrapment efficiency of CUR into NSCS with initial drug to polymer (5-40%) by dropping method

Concentration % weight to polymer	Entrapment efficiency (%)				
	1	2	3	Mean	SD
5	17.7	16.75	15.87	16.77	0.92
10	32.01	17.6	20.55	23.39	7.61
20	9.77	15.43	13.21	12.80	2.85
40	2.03	1.98	2.08	2.03	0.05

Table A.16 Loading capacity of CUR into NSCS with initial drug to polymer (5-40%) by dropping method

Concentration % weight to polymer	Loading capacity ($\mu\text{g}/\text{mg}$)				
	1	2	3	Mean	SD
5	17.70	16.75	16.39	16.95	0.68
10	64.03	35.20	44.08	47.77	14.76
20	19.53	30.86	29.14	26.51	6.11
40	16.25	15.84	15.26	15.78	0.50

Table A.17 Entrapment efficiency of CUR into NSCS with initial drug to polymer (5-40%) by evaporation method

Concentration % weight to polymer	Entrapment efficiency (%)				
	1	2	3	Mean	SD
5	23.2	27.32	22.64	24.39	2.56
10	20.91	22.9	20.75	21.52	1.20
20	19.57	19.27	18.91	19.25	0.33
40	13.84	19.75	16.52	16.70	2.96

Table A.18 Loading capacity of CUR into NSCS with initial drug to polymer (5-40%) by evaporation method

Concentration % weight to polymer	Loading capacity ($\mu\text{g}/\text{mg}$)				
	1	2	3	Mean	SD
5	11.60	13.66	12.36	12.54	1.04
10	20.91	22.9	22.56	22.12	1.06
20	39.13	38.55	37.15	38.28	1.02
40	55.35	78.98	70.78	68.37	12.00

Table A.19 Entrapment efficiency of CUR into NSCS with initial drug to polymer (5-40%) by O/W emulsion method

Concentration % weight to polymer	Entrapment efficiency (%)				
	1	2	3	Mean	SD
5	21.99	19.47	20.56	20.67	1.26
10	13.77	15.42	14.02	14.40	0.89
20	10.92	9.67	7.08	9.22	1.96
40	4.05	2.53	3.55	3.38	0.77

Table A.20 Loading capacity of CUR into NSCS with initial drug to polymer (5-40%) by O/W emulsion method

Concentration % weight to polymer	Loading capacity ($\mu\text{g}/\text{mg}$)				
	1	2	3	Mean	SD
5	21.99	19.47	19.02	20.16	1.60
10	27.54	30.85	28.67	29.02	1.68
20	21.84	38.68	28.31	29.61	8.49
40	32.37	20.25	28.22	26.95	6.16

Table A.21 Entrapment efficiency of CUR into OSCS with initial drug to polymer (5-40%) by dialysis method

Concentration % weight to polymer	Entrapment efficiency (%)				
	1	2	3	Mean	SD
5	20.71	31.25	30.53	27.50	5.89
10	24.34	26.31	27.97	26.21	1.82
20	18.83	25.04	26.66	23.51	4.13
40	17.36	27.21	27.02	23.86	5.63

Table A.22 Loading capacity of CUR into OSCS with initial drug to polymer (5-40%) by dialysis method

Concentration % weight to polymer	Loading capacity ($\mu\text{g}/\text{mg}$)				
	1	2	3	Mean	SD
5	10.35	15.63	14.30	13.43	2.75
10	26.31	27.97	24.34	26.21	1.82
20	85.28	75.12	74.86	78.42	5.94
40	124.53	69.45	108.82	100.94	28.37

Table A.23 Entrapment efficiency of CUR into BSCS with initial drug to polymer (5-40%) by dialysis method

Concentration % weight to polymer	Entrapment efficiency (%)				
	1	2	3	Mean	SD
5	18.72	20.68	27.32	22.24	4.51
10	24.07	23.69	15.84	21.20	4.65
20	27.34	26.54	19.27	24.38	4.45
40	16.49	19.71	18.88	18.36	1.67

Table A.24 Loading capacity of CUR into BSCS with initial drug to polymer (5-40%) by dialysis method

Concentration % weight to polymer	Loading capacity ($\mu\text{g}/\text{mg}$)				
	1	2	3	Mean	SD
5	13.66	9.32	10.34	11.11	2.27
10	24.07	15.84	22.90	20.94	4.45
20	53.08	62.24	76.82	64.05	11.97
40	78.98	78.83	75.53	77.78	1.95



APPENDIX B

1. Cytotoxicity of blank polymeric micelles

Table B.1 The percentage cell viability in Caco-2 cells of NSCS

Conc.(mg/mL)	% Cell viability						
	N1	N2	N3	N4	N5	mean	SD
Control	103.435	106.831	103.144	92.761	93.829	100.000	6.301
0.01	94.023	102.853	93.344	104.308	93.441	97.594	5.415
0.10	109.839	109.645	92.373	100.815	113.429	105.220	8.555
0.50	104.211	107.995	97.225	107.316	98.680	103.086	4.925
1.00	91.597	105.181	74.520	99.263	103.920	94.873	12.573
2.00	89.948	81.797	88.395	72.676	85.678	83.699	6.895
3.00	59.189	59.674	57.064	46.187	60.383	56.588	5.974
4.00	12.323	16.495	14.652	9.606	17.660	14.147	3.242
5.00	14.458	14.361	9.218	13.584	11.062	12.536	2.308

Table B.2 The percentage cell viability in Caco-2 cells of OSCS

Conc. (mg/mL)	% Cell viability						
	N1	N2	N3	N4	N5	mean	SD
Control	103.733	90.452	100.323	100.772	104.720	100.000	5.658
0.01	112.617	112.796	112.617	118.629	118.360	115.004	3.189
0.10	108.848	102.566	105.528	114.770	105.438	107.430	4.667
0.50	109.835	102.477	110.822	113.335	111.809	109.655	4.216
1.00	79.415	75.018	81.748	88.568	97.003	84.350	8.604
2.00	68.108	50.162	69.993	66.673	75.197	66.027	9.438
3.00	46.931	52.315	37.868	36.522	47.021	44.11	6.714
4.00	14.716	14.268	11.396	13.909	11.127	13.083	1.690
5.00	9.781	14.268	13.460	9.512	15.165	12.437	2.620

Table B.3 The percentage cell viability in Caco-2 cells of BSCS

Conc.(mg/mL)	% Cell viability						
	N1	N2	N3	N4	N5	mean	SD
Control	90.926	96.644	100.019	102.456	109.955	100.000	7.049
0.01	92.520	86.614	91.864	116.610	112.486	100.019	13.538
0.10	93.832	104.049	99.175	122.703	118.298	107.612	12.407
0.50	110.986	111.736	117.923	106.299	127.203	114.829	8.059
1.00	90.926	103.487	100.112	109.111	130.390	106.805	14.744
2.00	92.051	88.864	84.177	80.240	89.520	86.970	4.717
3.00	60.836	62.148	60.742	58.305	58.493	60.105	1.655
4.00	13.123	16.498	16.498	11.717	16.967	14.961	2.379
5.00	15.654	13.311	10.874	15.654	13.780	13.855	1.979

Table B.4 The percentage cell viability in HT-29 cells of NSCS

Conc.(mg/mL)	% Cell viability						
	N1	N2	N3	N4	N5	mean	SD
Control	104.345	97.564	96.457	101.162	100.471	100.000	3.120
0.01	104.484	111.126	107.667	101.301	95.765	104.069	5.906
0.1	100.332	101.301	104.069	106.421	107.528	103.930	3.124
0.5	107.944	111.957	104.761	112.926	123.166	112.151	6.970
1.0	56.186	43.454	51.481	44.838	46.776	48.547	5.239
2.0	29.062	28.370	29.062	29.338	29.754	29.117	0.505

Table B.5 The percentage cell viability in HT-29 cells of OSCS

	% Cell viability						
Conc.(mg/mL)	N1	N2	N3	N4	N5	Mean	SD
Control	100.059	99.032	100.646	98.738	101.526	100.000	1.149
0.01	113.116	100.205	106.367	111.649	102.259	106.719	5.650
0.1	105.487	110.182	109.888	117.518	106.954	110.006	4.642
0.5	75.851	78.932	63.527	81.573	83.187	76.614	7.826
1.0	36.532	34.478	33.744	34.331	36.825	35.182	1.397
2.0	34.771	33.744	34.478	33.744	35.358	34.419	0.693

Table B.6 The percentage cell viability in HT-29 cells of BSCS

	% Cell viability						
Conc.(mg/mL)	N1	N2	N3	N4	N5	Mean	SD
Control	99.857	102.292	96.705	100.143	101.003	100.000	2.071
0.01		98.997		97.135	92.693	96.275	3.239
0.1	95.702	108.309	94.842	102.722	115.473	103.410	8.701
0.5	105.731	116.619		110.172		110.840	5.475
1.0	41.834	43.410	42.980	46.132	56.160	46.103	5.839
2.0	35.100	35.673	34.957	32.951	35.673	34.871	1.122

2. Cytotoxicity of drug-loaded into polymeric micelles

Table B.7 The percentage cell viability in HT-29 cells of CUR-loaded NSCS

Conc.($\mu\text{g/mL}$)	% Cell viability						
	N1	N2	N3	N4	N5	Mean	SD
Control	101.33	97.95	103.62	98.07	99.03	100.00	2.44
0.1	111.58	103.86	104.70	105.07	105.31	106.10	3.11
1.0	105.07	113.99	112.42	103.02	110.98	109.10	4.79
3.0	86.13	96.38	95.05	91.44	90.23	91.85	4.07
5.0	48.01	55.61	61.52	57.78	54.04	55.39	4.99
7.0	45.84	45.72	43.79	44.27	41.86	44.29	1.63
10.0	32.33	32.81	29.19	28.59	31.60	30.90	1.90
20.0	30.28	27.02	26.66	23.16	27.86	27.00	2.57

Table B.8 The percentage cell viability in HT-29 cells of CUR-loaded OSCS

Conc.($\mu\text{g/mL}$)	% Cell viability						
	N1	N2	N3	N4	N5	Mean	SD
Control	96.92	97.87	102.32	100.57	102.32	100.00	2.51
0.1	107.32	100.84	102.05	103.67	105.97	103.97	2.68
1.0	112.72	114.07	120.28	110.69	123.79	116.31	5.50
3.0	102.86	104.62	102.86	99.49	99.22	101.81	2.36
5.0	91.93	80.59	90.98	76.67	100.30	88.09	9.47
7.0	74.38	63.31	68.98	64.52	67.90	67.82	4.35
10.0	44.01	44.01	46.57	40.50	47.65	44.30	2.88
20.0	41.85	40.36	37.66	38.07	39.96	39.58	1.72

Table B.9 The percentage cell viability in HT-29 cells of CUR-loaded BSCS

Conc.($\mu\text{g/mL}$)	% Cell viability						
	N1	N2	N3	N4	N5	Mean	SD
Control	99.75	98.37	101.14	99.91	100.83	100.00	1.09
0.1	91.13	102.22	101.14	105.14	100.06	99.94	5.27
1.0	108.07	110.53	110.22	127.77	115.46	114.41	7.94
3.0	100.37	99.60	95.60	111.76	100.68	101.60	6.03
5.0	88.36	81.59	73.12	82.97	89.29	83.07	6.48
7.0	76.97	74.51	75.58	66.19	80.36	74.72	5.25
10.0	44.64	48.95	46.49	43.26	49.72	46.61	2.75
20.0	40.49	42.49	41.10	43.72	42.18	42.00	1.26

Table B.10 The percentage cell viability in HT-29 cells of free CUR

Conc.($\mu\text{g/mL}$)	% Cell viability						
	N1	N2	N3	N4	N5	Mean	SD
Control	101.11	99.61	99.91	97.66	101.71	100.00	1.56
0.1	103.21	103.21	91.96	106.21	113.41	103.60	7.73
1.0	106.81	105.61	113.86	104.86	110.11	108.25	3.72
3.0	99.46	100.36	90.61	106.96	89.71	97.42	7.24
5.0	76.21	83.56	91.21	85.51	99.16	87.13	8.60
7.0	64.96	57.31	67.66	62.26	68.11	64.06	4.44
10.0	48.75	47.70	50.11	42.75	50.71	48.00	3.16
20.0	41.55	41.85	39.90	37.35	38.55	39.84	1.93



1. *In vitro* MX release study

Table C.1 % MX release in SGF (pH 1.2) 2 h then changed to SIF (pH 6.8) to 8 h.

Sample	Time (h)	% MX release				
		N1	N2	N3	Mean	SD
MX-loaded NSCS	0	0.00	0.00	0.00	0.00	0.00
	0.5	11.19	13.39	12.06	12.41	1.43
	1	15.30	19.27	9.87	14.81	4.72
	2	20.92	23.99	14.64	19.85	4.77
	4	38.81	46.43	37.26	40.48	4.07
	6	79.50	80.22	83.16	81.42	1.83
	8	101.94	100.05	105.24	102.41	2.63
MX-loaded OSCS	0	0.00	0.00	0.00	0.00	0.00
	0.5	10.89	7.81	7.97	8.89	1.73
	1	13.39	9.48	9.41	10.76	2.27
	2	11.36	12.14	11.03	11.51	0.57
	4	30.76	31.00	47.24	36.33	9.45
	6	60.62	71.09	71.57	67.76	6.19
	8	109.68	97.53	97.53	101.58	7.01
MX-loaded BSCS	0	0.00	0.00	0.00	0.00	0.00
	0.5	12.96	14.84	8.87	12.16	2.50
	1	21.57	18.85	12.15	17.52	4.85
	2	30.99	24.95	18.17	24.70	6.41
	4	36.43	41.09	36.09	37.87	2.79
	6	85.61	71.02	65.70	74.11	10.31
	8	90.77	89.23	94.06	91.42	2.02
Free MX	0	0.00	0.00	0.00	0.00	0.00
	0.5	12.84	7.52	9.31	9.89	2.71
	1	16.17	11.29	11.33	12.93	2.80
	2	19.43	13.72	13.64	15.47	2.72
	4	40.80	54.79	34.03	39.31	9.71
	6	50.32	58.95	46.92	52.06	6.20
	8	69.43	59.67	58.21	62.44	6.10

2. *In vitro* CUR release study

Table C.2 % CUR release in SGF (pH 1.2) 2 h then changed to SIF (pH 6.8) to 5 h and then changed to SCF (pH 7.4) to 8 h.

Sample	Time (h)	% MX release				
		N1	N2	N3	Mean	SD
CUR-loaded NSCS	0	0.00	0.00	0.00	0.00	0.00
	1	14.53	16.01	14.38	14.97	0.90
	2	16.89	19.01	21.83	19.25	2.48
	3	50.59	36.23	42.15	42.99	7.22
	4	51.35	39.61	46.94	45.97	5.93
	5	53.29	43.81	51.03	49.37	4.95
	6	60.18	53.30	57.66	57.05	3.48
	8	66.51	57.20	60.97	61.56	4.68
CUR-loaded OSCS	0	0.00	0.00	0.00	0.00	0.00
	1	20.74	16.01	18.08	18.28	2.37
	2	26.96	19.01	23.14	23.04	3.98
	3	49.18	36.23	46.86	44.09	6.90
	4	52.11	39.61	49.63	47.11	6.62
	5	55.02	43.81	54.10	50.98	6.22
	6	68.10	53.30	60.18	60.53	7.41
	8	68.75	57.20	62.55	62.83	5.78
CUR-loaded BSCS	0	0.00	0.00	0.00	0.00	0.00
	1	16.20	17.55	17.61	17.12	0.80
	2	26.76	25.22	25.00	25.66	0.96
	3	51.07	46.18	47.62	48.29	2.51
	4	53.26	47.52	51.99	50.93	3.02
	5	55.53	49.84	56.08	53.82	3.46
	6	53.00	63.61	63.61	59.92	6.00
	8	50.18	62.85	60.82	57.95	6.81
Free CUR	0	0.00	0.00	0.00	0.00	0.00
	1	8.55	8.55	8.55	8.55	0.00
	2	8.98	8.98	8.98	8.98	0.00
	3	15.61	15.23	14.56	15.42	0.27
	4	16.96	16.11	15.67	16.53	0.60
	5	17.88	15.77	16.65	16.82	1.50
	6	18.33	17.10	20.24	17.72	0.87
	8	21.11	19.77	21.26	20.44	0.95

BIOGRAPHY

Name	Thisirak Woraphatphadung, Miss
Date of Birth	February 14, 1988
Place of Birth	Surin, Thailand
Nationality/Religion	Thai/Buddhism
E-mail address	thisirak14@gmail.com
Education	
2006-2010	Bachelor of Pharmacy (2 nd Class Honours), Faculty of Pharmaceutical Sciences, Khon Kaen University, Thailand
2011-2013	Master of Pharmacy (M. Pharm), in Pharmaceutical Technology, Faculty of Pharmaceutical Sciences, Khon Kaen University, Thailand
2013-2017	Doctor of Philosophy, Ph.D. in Pharmaceutical Technology, Faculty of Pharmacy, Silpakorn University, Thailand
Oct 2015-May 2016	Research student, Medical Engineering Laboratory, The Jikei University School of Medicine, Japan
Scholarship	
2011-2013	Research Fund for Supporting Lecturer to Admit High Potential Student to Study and Research on His Expert Program Year 2011 from Graduate School Khon Kaen University
2013-2017	Thailand Research Funds through the golden Jubilee Ph.D. Program (Grant No. PHD/0027/2556)

Presentation

Oral

1. **Thisirak Woraphatphadung**, Warayuth Sajomsang, Theerasak Rojanarata, Tanasait Ngawhirunpat, Praneet Opanasopit “pH responsive meloxicam-incorporating amphiphilic chitosans micelles: Effect of hydrophobic graft copolymer” The 3rd Current Drug Development International Conference, 1st-3rd May 2014, Pavillion Queen's Bay Krabi, Ao Nang Beach Thailand.

2. **Thisirak Woraphatphadung**, Warayuth Sajomsang, Theerasak Rojanarata, Tanasait Ngawhirunpat, Praneet Opanasopit “N-naphthyl-N,O-succinyl chitosan Polymeric micelles Incorporating Meloxicam by Physical Entrapment” The 7th Annual Northeast Pharmacy Research Conference of 2015, 7-8th March, Faculty of Pharmaceutical Sciences, Khon Kaen University, Thailand.

Poster

1. **Thisirak Woraphatphadung**, Saengrawee Sutthiparinyanont, Padungkwan Chitropas “Physicochemical properties of tapioca starch modified by alcoholic-alkali treated technique” The 13th Graduate Research Conference Khon Kaen University, 17th February 2012, Khon Kaen University, Thailand.

2. **Thisirak Woraphatphadung**, Warayuth Sajomsang, Theerasak Rojanarata, Tanasait Ngawhirunpat, Praneet Opanasopit “Meloxicam-loaded pH sensitive polymeric micelles: Solvents and entrapment methods” The 30th Annual Research Conference in Pharmaceutical Sciences, 10th January 2014, Chulalongkorn University, Bangkok, Thailand.

3. **Thisirak Woraphatphadung**, Warayuth Sajomsang, Theerasak Rojanarata, Tanasait Ngawhirunpat, Praneet Opanasopit “Polymeric Micelles for Enhanced Solubility of Meloxicam in Oral Drug Delivery” The 3rd International Conference and Exhibition on Pharmaceutical - Nutraceutical and Cosmeceutical Technology 2014, 1st-2nd December 2014, The Queen Sirikit National Convention Center (QSNCC), Bangkok, Thailand.

4. **Thisirak Woraphatphadung**, Warayuth Sajomsang, Theerasak Rojanarata, Tanasait Ngawhirunpat, Praneet Opanasopit “N-arylsuccinyl chitosan polymeric micelles improve solubility of nsaid” The JSPS-NRCT Follow-Up Seminar 2015 and 31st International Annual Meeting in Pharmaceutical Sciences (JSPS-NRCT 2015 and 31st IAMPS), 22nd-23rd January 2015, Faculty of Pharmaceutical Sciences, Chulalongkorn University, Bangkok, Thailand.

5. **Thisirak Woraphatphadung**, Warayuth Sajomsang, Theerasak Rojanarata, Tanasait Ngawhirunpat, and Praneet Opanasopit “Development of chitosan base pH sensitive polymeric micelles for oral meloxicam delivery” 26th FAPA Congress 2016, 9-13th November 2016, Bangkok, Thailand.

6. **Thisirak Woraphatphadung**, Warayuth Sajomsang, Theerasak Rojanarata, Tanasait Ngawhirunpat, Prasert Akkaramongkolporn and Praneet Opanasopit “pH-sensitive chitosan-based polymeric micelles containing furosemide for oral drug delivery” Seoul International Conference on Engineering and Applied Science (SICEAS) 2017, 7-9th February 2017, Seoul, South Korea.

7. **Thisirak Woraphatphadung**, Warayuth Sajomsang, Tanasait Ngawhirunpat, Theerasak Rojanarata and Praneet Opanasopit “Development of pH sensitive polymeric micelles for enhancing solubility of curcumin” The 4th International Conference on Advanced Pharmaceutical Research (ICAPH 2017), 21st-22nd February 2017, Miracle Grand Convention Hotel, Bangkok, Thailand.

8. **Thisirak Woraphatphadung**, Warayuth Sajomsang, Theerasak Rojanarata, Tanasait Ngawhirunpat, Prasert Akkaramongkolporn and Praneet Opanasopit “Preparation of Curcumin-loaded Polymeric micelles for Oral Colon-Targeted Drug Delivery” 9th Annual Conference of Northeastern Pharmacy Research 2017, 11st-12nd March, Ubon Ratchathani University, Ubon Ratchathani, Thailand.

Scientific Publication:

1. **Thisirak Woraphatphadung**, Jariya Kowapradit, Tanasait Ngawhirunpat, Theerasak Rojanarata and Praneet Opanasopit. Effect of salt forms of chitosan on in vitro permeability enhancement in intestinal epithelial cells (Caco-2). Tropical Journal of Pharmaceutical Research. August 2013; 12 (4): 495-501.

2. **Thisirak Woraphatphadung**, Warayuth Sajomsang, Theerasak Rojanarata, Tanasait Ngawhirunpat, Praneet Opanasopit. Polymeric micelles for enhanced solubility of meloxicam in oral drug delivery. Advanced Materials Research. 2015; 1060:7-11.

3. **Thisirak Woraphatphadung**, Warayuth Sajomsang, Pattarapond Gonil, Somsak Saesoo and Praneet Opanasopit. Synthesis and characterization of pH-responsive N-naphthyl-N,O-succinyl chitosan micelles for oral meloxicam delivery. Carbohydrate Polymers. 2015; 121:99-106.

4. **Thisirak Woraphatphadung**, Warayuth Sajomsang, Pattarapond Gonil, Alongkot Treetong, Prasert Akkaramongkolporn, Tanasait Ngawhirunpat, Praneet Opanasopit. pH-Responsive polymeric micelles based on amphiphilic chitosan derivatives: Effect of hydrophobic cores on oral meloxicam delivery. *International Journal of Pharmaceutics*. 2016; 497:150-160.

5. Prasopchai Tonglairoum, **Thisirak Woraphatphadung**, Tanasait Ngawhirunpat, Theerasak Rojanarata, Prasert Akkaramongkolporn, Warayuth Sajomsang & Praneet Opanasopit. Development and evaluation of N-naphthyl-N,O-succinyl chitosan micelles containing clotrimazole for oral candidiasis treatment. *Pharmaceutical Development and Technology*. 2017; 22(2):184-190.

Article Publication:

1. Polymeric micelles for drug delivery: Drug loading by physical entrapment and factors affecting its efficiency. *Thai Bulletin of Pharmaceutical Sciences (TBPS)*, 2014; 9:46-61.
2. Solid dispersions: Technique to enhance solubility of poorly water soluble drug. *Isan Journal of Pharmaceutical Sciences (IJPS)*, 2015; 11(2):1-15.

Awards:

1. FAPA-PAT Best Poster Award: Gold Medal from 26th FAPA Congress 2016, 9-13th November 2016, Bangkok, Thailand.
2. Outstanding Award from The 4th International Conference on Advanced Pharmaceutical Research (ICAPH 2017), 21st-22nd February 2017, Miracle Grand Convention Hotel, Bangkok, Thailand.
3. Excellent Poster Award from 13th Graduate Research Conference Khon Kaen University, 17th February 2012, Khon Kaen University, Thailand.